

**Studies on the Genome-wide Localization of StpA and H-NS  
in *Escherichia coli* Using ChIP-chip Analysis**

ChIP-chip 法を用いた大腸菌核様体蛋白質 StpA 及び H-NS と  
ゲノム DNA との相互作用の研究

**By**

**Ebru UYAR**

**Laboratory of Functional Genomics**

**Graduate School of Bioscience**

**Nara Institute of Science and Technology**

**March, 2009**

An academic dissertation presented to the  
Graduate School of Bioscience  
Nara Institute of Science and Technology  
In a partial fulfilment of the requirements for the degree of  
DOCTOR OF SCIENCE

Ebru UYAR

Dissertation Committee

Prof. Naotake OGASAWARA	(Supervisor)
Prof. Hisaji MAKI	(Member)
Prof. Hirotada MORI	(Member)
Prof. Hiroshi TAKAGI	(Member)

所属 (主指導教員)	Graduate School of Biological Science, Functional Genomics Lab		
氏名	Ebru Uyar	提出	平成 2008 年 12 月 22 日
題目	Studies on the genome-wide localization of StpA and H-NS in <i>Escherichia coli</i> using ChIP-chip analysis		
<p>                     Nucleoid-associated proteins (NAP) of prokaryotic cells (e.g., FIS, IHF, HU, H-NS, and StpA) have versatile functions through their extensive interaction with the chromosome. They participate in various DNA transactions such as transcription, replication, and recombination. Furthermore, they have significant contribution to the organization and dynamic structure of chromosome DNA. One of the major member of NAPs, heat-stable nucleoid structuring protein (H-NS), has been extensively studied in <i>Escherichia coli</i> and related bacteria. StpA (Suppressor of <i>td</i><sup>-</sup> phenotype A), is another NAP and shares 58% sequence identity with H-NS at the amino acid level. Although StpA resembles H-NS structurally and biochemically, the inactivation of <i>stpA</i> does not result in the marked growth impairment observed by <i>hns</i> inactivation. To investigate the difference in function between StpA and H-NS, we performed ChIP-chip analysis of StpA and H-NS in <i>E. coli</i> cells. Our results revealed that the StpA binding regions overlap with those of H-NS in wild-type cells and that StpA/H-NS protein complex covers approximately 4% of the genome. Scatter plot analysis of the binding signals of StpA versus that of H-NS also represented high correlation between StpA and H-NS distribution in wild type cells. Furthermore, the H-NS binding profile in the <i>stpA</i> mutant is similar to that in wild-type cells which proposed that StpA deficiency can be compensated by H-NS. Thus, loss of StpA does not show a distinct phenotype.                 </p> <p>                     By comparison, the distribution of StpA binding regions is reduced to less than half in the <i>hns</i> mutant compared with wild-type cells. 66 % of the StpA binding regions covering about 2.5% of                 </p>			

the genome were lost in the absence of H-NS. The differential distribution of StpA in the presence or absence of H-NS indicates that about one-third of the StpA binding sites are recognized by StpA, independent of H-NS, while the remaining two-thirds are recognized by StpA interacting with H-NS.

It has been reported that StpA is subjected to proteolysis. In the absence of H-NS, more than half of the StpA molecules form oligomers which is sensitive to Lon-protease. Therefore, remaining StpA dimers (~20%) may not be sufficient to restore H-NS-like distribution profile. StpA(F21C), an StpA mutant resistant against Lon digestion, has been identified. Using this mutant protein, we attempted to evaluate the effectiveness of dimerization ability on StpA distribution profile. We first monitored the homodimer formation of StpA and H-NS *in vitro*. StpA(F21C) showed increased dimerization comparable to that of H-NS. In contrast to enhanced dimerization, however, the binding profile of StpA(F21C) protein in *hns* mutant strain does not change dramatically and only 16% of the lost binding regions could be restored by induced dimerization ability. This finding implied the probability of an intrinsic DNA binding property of StpA dimers which is different from that of H-NS dimers.

In conclusion, the overlapping profile of StpA and H-NS binding sites in wild type cells suggested a cooperative association of H-NS and StpA through the interaction between StpA and H-NS homodimers and/or StpA/H-NS heterodimer formation. The difference in the binding profiles of H-NS and StpA in *stpA* and *hns* mutants respectively, explains the growth impairment observed by the *hns* mutation. Based on these observations, a role as a molecular backup of H-NS is attributed to StpA during H-NS mediated-transcriptional regulation and higher order organization of the genomic DNA.

## ACHIEVEMENT

### **Publication:**

Differential binding profiles of StpA in wild-type and *hns* mutant cells: a comparative analysis of cooperative partners by ChIP-chip analysis (2009). Ebru Uyar, Ken Kurokawa, Mika Yoshimura, Shu Ishikawa, Naotake Ogasawara, and Taku Oshima.

Journal of Bacteriology.

## ACKNOWLEDGEMENTS

I owe my thanks to everyone who contributed directly or indirectly to make this thesis possible. First of all, I would like to express my deepest gratitude to my supervisor, Prof. Naotake Ogasawara, for welcoming me into his group and providing an excellent working atmosphere. I truly appreciate his continuous mentorship and constructive criticism throughout the last years, and am proud to have him as my thesis supervisor. He helped me not only in my study but also in many other aspects of life in Japan. I would like to extend my gratitude to Dr. Oshima for his invaluable discussion and guidance during the course of this work. The majority of this work would not be otherwise possible without his help. Additionally, I thank to my thesis committee: Prof. Maki, Prof. Mori and Prof. Takagi for their insightful discussions and valuable time.

I am especially thankful to Dr. Yoshimura, Dr. Ishikawa, Dr. Kobayashi and Dr. Morimoto for sharing their experience and knowledge. I also thank all past and present members of the Functional Genomics Lab. for their cooperation and warm friendship. Some of them and other lab's members, such as Loh, Kusuya, Onuma, Eun-cho, Okumura, Yekti and Meiw, whom I shared my sadness and happiness through my PhD, are of particular importance.

I also would like to thank to Prof. Kawamoto and her wife for providing me financial support via Kawamoto Hirohisa, Yasuko Scholarship, and Soroptimist International of Japan (Nara) for the grant.

I am highly indebted to my family for their unconditional love and never-ending support throughout my life. Last but not the least, I wish to express my greatest appreciation to my husband, Zafer, for his love, support, and constant encouragement.

## CONTENTS

List of figure	1
List of tables	2
<b>1. INTRODUCTION</b>	<b>3</b>
1.1. Organization of bacterial chromosome	3
1.1.1. Macromolecular crowding	5
1.1.2. DNA supercoiling	5
1.1.3. Nucleoid-associated proteins (NAP)	7
1.2. H-NS ( <u>H</u> eat-stable <u>n</u> ucleoid <u>s</u> tructuring protein)	12
1.2.1. H-NS-like proteins	17
1.2.2. StpA ( <u>S</u> uppressor of <u>t</u> d <sup>-</sup> phenotype <u>A</u> )	22
1.3. Basis and motivation of this work	26
<b>2. MATERIALS AND METHODS</b>	<b>27</b>
2.1. Bacterial strains and plasmids	27
2.2. Construction of <i>hns</i> mutant strain expressing StpA(F21C)-3xFLAG	30
2.3. Materials, media and buffers	32
2.3.1. Enzymes	32
2.3.2. Growth media	32
2.3.3. Buffers	32
2.3.4. Antibodies	34
2.4. SDS-PAGE analysis of cellular proteins	35
2.5. In vitro analysis of StpA and H-NS homodimer formation	36
2.6. ChIP-on-chip analysis	36

2.6.1. ChIP-on-chip analysis using anti-FLAG antibody	36
2.6.2. ChIP-on-chip analysis using StpA peptide antibody	38
2.7. Data assessment and quantitative analysis of the number of the StpA and H-NS binding sites	40
<b>3. RESULTS</b>	41
3.1. Confirmation of the FLAG-tagged StpA and H-NS expression levels	41
3.2. The genome-wide StpA binding profile overlaps with the H-NS binding profile	44
3.3. StpA binding regions are reduced in the absence of H-NS	48
3.4. Confirmation of biological activity of FLAG-tagged StpA	50
3.5. Distribution analysis of native StpA in the <i>hns</i> mutant using anti-StpA antibody	53
3.6. Quantitative analysis of the number of StpA binding regions in <i>hns</i> mutant verified the reduction of StpA distribution in <i>hns</i> mutant strain	56
3.7. StpA(F21C) mutant shows H-NS-like dimerization activity	57
3.8. Reduction of StpA binding in the <i>hns</i> mutant reflects the difference in intrinsic DNA binding properties between the StpA dimer and H-NS dimer	60
<b>4. DISCUSSION</b>	64
<b>5. REFERENCES</b>	70



## LIST OF FIGURES

Figure 1. Organization of dynamically supercoiled domains in genome DNA	4
Figure 2. Opposite effect of TopoI and DNA gyrase on transition of the DNA supercoiling in prokaryotes	7
Figure 3. Architectural properties of the nucleoid-associated proteins	8
Figure 4. Architectural properties of H-NS protein.	13
Figure 5. H-NS-mediated transcriptional silencing	16
Figure 6. Domain organization and multiple alignment of amino acid sequence of H-NS and StpA.	22
Figure 7. DNA bridging ability of H-NS and StpA	23
Figure 8. Strategy used for the construction of <i>hns</i> mutant strain expressing StpA(F21C)-3xFLAG	31
Figure 9. Basic steps of the protocol used for ChIP-chip analysis	39
Figure 10. The effect of FLAG tagging on the expression levels of StpA and H-NS	43
Figure 11. Genome-wide distribution of H-NS and StpA in exponential-phase <i>E. coli</i> cells	46
Figure 12. Scatter plot of StpA signals versus H-NS signals in wild type cells	47
Figure 13. Comparison of H-NS and StpA distribution in wild type and single mutants of <i>stpA</i> and <i>hns</i>	49
Figure 14. Growth curve of the strains used in ChIP-on-chip analysis	50
Figure 15. Western blot analysis of MalE expression level	52
Figure 16. Consistency between distribution profile of FLAG-tagged StpA and that of native StpA in the <i>hns</i> mutant	54

Figure 17. Scatter plot of StpA signals in wild type versus <i>hns</i> mutant cells	55
Figure 18. Homodimerization proficiency of H-NS and StpA	59
Figure 19. Distribution of StpA(F21C) in the <i>hns</i> mutant	61

### LIST OF SUPPLEMENTARY FIGURES

Supplementary Figure 1. Whole genome binding profiles of FLAG-tagged H-NS and StpA	87
Supplementary Figure 2. Comparison of native and FLAG-tagged StpA distribution in <i>hns</i> mutant cells	103

### LIST OF TABLES

Table 1. List of species carrying <i>hns</i> and <i>hns</i> -related genes.	21
Table 2. Bacterial strains and plasmids used in this study.	28
Table 3. PCR primers used in this study	29
Table 4. Quantitative analysis of the number of the StpA and H-NS binding sites	56

### LIST OF SUPPLEMENTARY TABLES

Supplementary Table. Functional classification of the genes bound by StpA homodimers	111
--	-----

## 1. INTRODUCTION

### 1.1. Organization of bacterial chromosome

Unlike eukaryotic chromosome, which is enclosed in a membrane thereby making a compartment known as nucleus, bacterial genome DNA is located in a special ribosome-free area called nucleoid (Robinow and Kellenberger, 1994). Bacterial chromosome compaction is performed by a complex process including DNA supercoiling, macromolecular crowding and nucleoid associated proteins (Dame, 2005; Stavans and Oppenheim, 2006). As a result of this compaction, ~500 negatively supercoiled DNA loops, known as microdomains, are shaped (Figure 1) and approximately 1600  $\mu\text{m}$  DNA in length is contained in a bacterial cell (~1  $\mu\text{m}$  in diameter and ~3–5  $\mu\text{m}$  in length). These topologically independent domains are around 10 kb in size and stochastically distributed throughout the genome, *in vivo* (Postow *et al.*, 2004). Half of the supercoiling is provided by NAPs, while the other half is introduced by DNA topoisomerases (Wang, 1996; Zechiedrich *et al.*, 2000). Introduction of a single or double stranded break by various endogenous and exogenous mechanisms, as well as active DNA metabolism cause a relaxation in a supercoiled domain. However, overall superhelicity for the rest of the chromosome remains unaffected (Travers and Muskhelishvili, 2005), since the supercoiled domains are isolated from each other by the formation of domain barriers that are maintained by the NAPs, such as H-NS and Fis.

Preserving this structure has a unique biological importance because the energy stored in the supercoiled DNA is the main source of power that is necessary for melting DNA to make it accessible for the other proteins. Therefore, through the extensive interaction with DNA, NAPs are also able to fulfill important roles in cellular process (e.g, transcription, replication, and recombination). However, our present knowledge of the NAPs and their global interaction with genome is still limited.

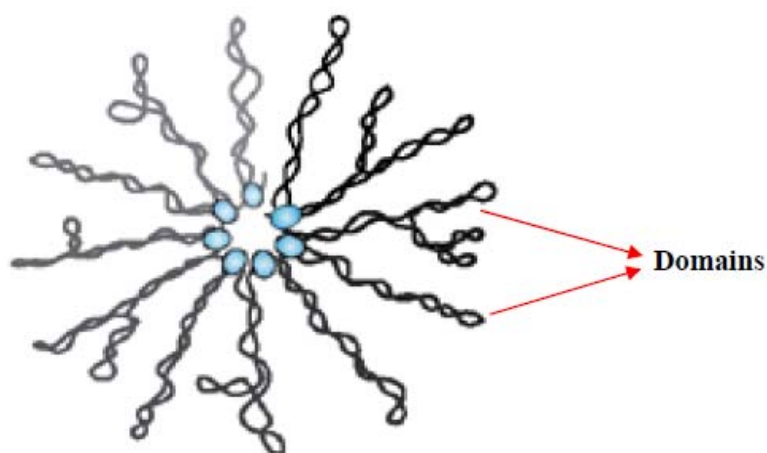


**Figure 1.** Organization of dynamically supercoiled domains in genome DNA (Thanbichler and Shapiro, 2008)

### **1.1.1. Macromolecular crowding**

Bacterial DNA occupies 1/8-1/5 of the volume within the cell envelope and has a direct contact with the surrounding cytoplasm which is crowded with a variety of macromolecules such as proteins and RNA at a total concentration of several hundred grams per liter (e.g 300-400 mg/ml of proteins) (Zimmerman and Trach, 1991). Since the concentration of these molecules occupy significant part of the total volume (around 20-40%), this phenomenon is termed as “macromolecular crowding”. The effects of macromolecular crowding on DNA condensation can be either directly by forcing chromosome DNA into thermodynamically favorable compact form or indirectly by influencing biochemical and physiological reactions through increasing the binding and activity of the enzymes (Schnell and Turner, 2004; Miyoshi and Sugimoto, 2008).

### **1.1.2. DNA supercoiling**

Naturally, chromosomal DNA is maintained in negatively supercoiled state in the cell (Worcel and Burgi, 1972). Negative supercoils serve as storage for free energy which aids in processes that require strand separation, such as DNA replication and transcription. Thus, strand separation can be accomplished more easily in negatively supercoiled DNA than in relaxed DNA. DNA supercoils are constrained by the NAPs such as H-NS and StpA,

hence influence the topology (Tupper *et al.*, 1994; Zhang *et al.*, 1996). However, negative supercoiling is only provided by DNA topoisomerases (Boles *et al.*, 1990). Four distinct topoisomerases have been characterized in *E. coli*; TopoI, TopoII (DNA gyrase), TopoIII and TopoIV (Wang, 1996). Mainly, two types of topoisomerases participate the modulation of supercoiling; TopoI and gyrase (TopoII). DNA gyrase introduces negative supercoils into positive and negative supercoiled DNA substrates by making a double stranded break and rejoining through an ATP-dependent mechanism, whereas TopoI relaxes negative supercoils by introducing single stranded break in an ATP independent reaction (Menzel and Gellert, 1983; Rui and Tse-Dinh, 2003) (Figure 2). Indeed, the expression level of DNA gyrase and TopoI are coupled with the supercoiling level and transcriptionally regulated by one of the NAPs, Fis (factor for inversion stimulation). Fis induces TopoI expression and reduces DNA gyrase expression if the DNA is highly supercoiled. TopoI activity causes a lowered level of supercoiling. If reduction in the supercoiling level is too low, transcription is accelerated again at the *gyrA* and *gyrB* promoters to balance superhelicity (Schneider *et al.*, 2001; Travers *et al.*, 2001). Thus, Fis-mediated complex regulation mechanism is functioning between DNA gyrase and TopoI to maintain overall superhelicity of the genome DNA.

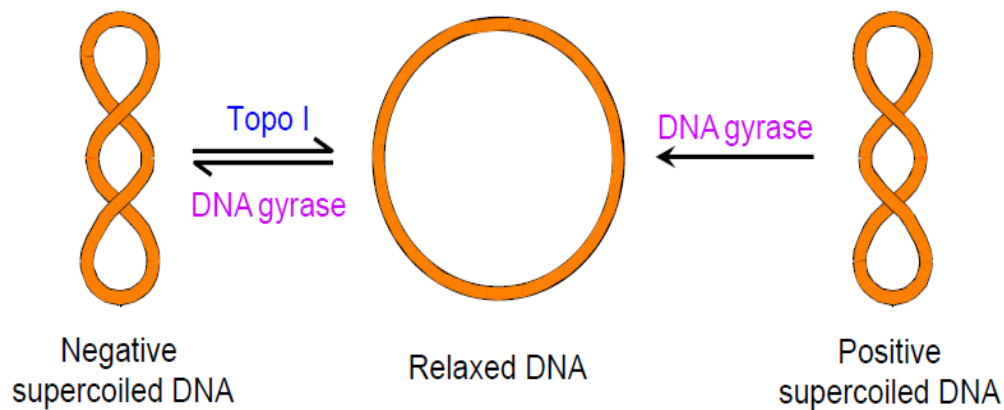


**Figure 2.** Opposite effect of TopoI and DNA gyrase on transition of the DNA supercoiling in prokaryotes.

### 1.1.3. Nucleoid associated proteins (NAP)

Twelve different species of NAPs have been isolated in *E. coli* (Azam and Ishihama, 1999) and classified as DNA bridging proteins or DNA bending proteins according to their effect on DNA structure (Luijsterburg *et al.*, 2006). Due to their abundance, low molecular weight, basicity, and function, NAPs resemble to the eukaryotic histone proteins. Expression of most of NAPs is regulated by environmental factors. For instance, as a member of cold-shock regulon, H-NS transcription is elevated upon cold-shock (La Teana *et al.*, 1991). Dramatic increase in Fis level can be observed upon nutrient up-shift (Ball *et al.*, 1992). Therefore, the protein composition of the nucleoid is highly flexible. Some of NAPs are well-characterized in terms of their structure and action on DNA conformation as seen in Figure 3 and they will be described below in details.

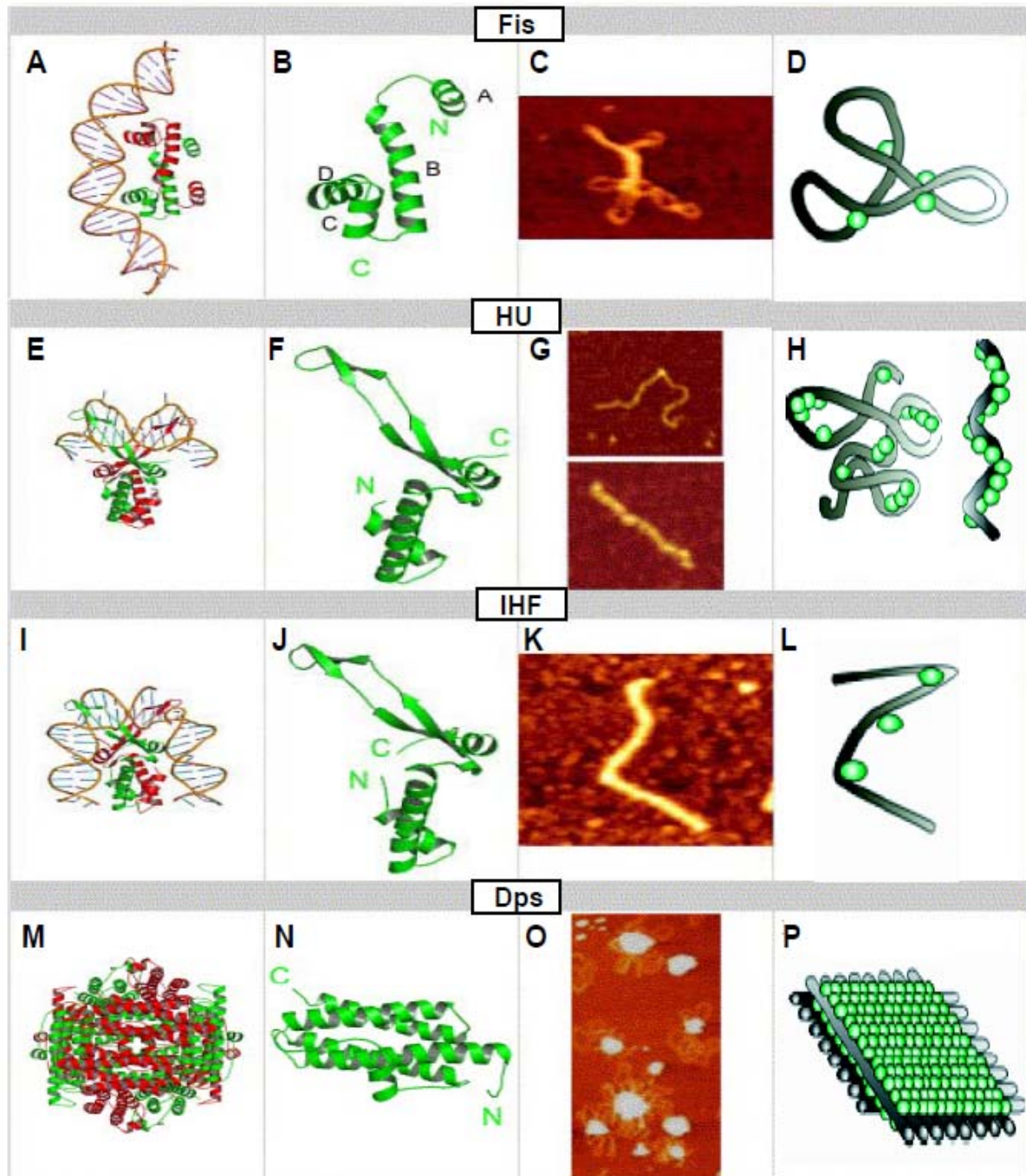


**Figure 3.** Architectural properties of the nucleoid-associated proteins. Structure of DNA bound by Fis (A), HU (E), IHF (I). Structure of dodecameric Dps of *E. coli* (M). Close-up of a monomeric subunits of Fis (B), HU (F), IHF (J), and Dps (N). Scanning Force Microscopy images of DNA complexed with Fis (C), HU (G), IHF (K), and Dps (O). Low resolution models for DNA compaction by Fis (D), HU (H), IHF (L), and Dps (P) (Luijsterburg *et al.*, 2006).



**Fis (factor for inversion stimulation)** is a homodimeric protein (22 kDa) which influences DNA topology directly or indirectly in a growth-phase dependent manner. In direct action, Fis constrains negative supercoils in DNA by bending it between  $50^{\circ}$  and  $90^{\circ}$  upon binding to highly degenerate consensus sequence through its helix-turn-helix motif located on the C-termini (Pan *et al.*, 1996) (Figure 3A-D). However, indirect modulation of DNA topology by Fis is achieved through DNA topoisomerases, namely TopoI and DNA gyrase. Fis is working as a sensor for DNA supercoiling, and thus, it regulates the transcription of gyrase subunits (*gyr A* and *gyr B*) and TopoI (*topA*) depends on the DNA topology to maintain the overall superhelicity of chromosome DNA (Schneider *et al.*, 2001). By monitoring the reporter genes that are sensitive to the changes in DNA supercoiling, Cozzarelli *et al.*, proved that Fis and H-NS are involved in the in the maintenance of domain barriers (2005). Recently, genome-wide identification of Fis and H-NS binding sites indicated both proteins occupy the similar regions on the *E. coli* genome (Grainger *et al.*, 2006).

**HU (heat-unstable nucleoid protein)** is characterized as a prokaryotic homologue of eukaryotic histones (Drlica and Rouviere-Yaniv, 1987). However, with respect to its function, it is similar to HMG (high morbidity group) proteins of eukaryotes (Megraw and

Chae, 1993); Bianchi, 1994). HU exists in solution as a 20 kDa heterodimer composed of two similar subunits, HU $\alpha$  and HU $\beta$ , encoded by the *hupA* and *hupB* genes respectively. Highest level of HU expression (approximately 30,000 to 55,000) is observed in exponential cells and decreased to less than one-third in stationary phase (Azam and Ishihama, 1999). The non-specific binding of HU dimers introduce flexible bends with an angle of up to 180<sup>0</sup> into DNA and result in reduction in DNA length (van Noort *et al.*, 2004) (Figure. 3E-H).

**IHF (integration host factor)** was originally discovered as a host factor required for the integration of phage  $\lambda$  DNA into host DNA (Nash and Robertson, 1981). It is a sequence-specific DNA-binding protein which consists of two subunits ( $\alpha$ - subunit ~ 11 kDa and  $\beta$ - subunit ~ 9.5 kDa) (Craig and Nash, 1984; Azam and Ishihama, 1999). Although it exists 12,000 copy per cell in exponential phase, the number increases around 5-fold in early stationary phase (Ditto *et al.*, 1994). After Dps, IHF is expressed as the second most abundant protein in the transition state and mainly found in DNA bound form *in vivo* (Engelhorn *et al.*, 1995; Yang and Nash, 1995). Through the interaction of the IHF heterodimers, the DNA is bent with a magnitude of 140<sup>0</sup> to 160<sup>0</sup> (Rice *et al.*, 1996) (Figure. 3I-L). Thus, it plays an important role with Dps to further compact nucleoid structure which is more relaxed in exponential phase. Localization analysis of IHF across the *E. coli* genome using ChIP-chip

technique indicated that 30% of the IHF binding sites are co-occupied by Fis and H-NS (Grainger *et al.*, 2006).

**Dps (DNA-binding protein from starved cells)** is a stress inducible (such as nutrition limitation and oxidative stress) non-specific DNA-binding protein of *E. coli* (Almiron *et al.*, 1992; Martinez and Kolter, 1997; Grant *et al.*, 1998). In exponential phase, its transcription is selectively repressed by Fis and H-NS in different mechanisms directed against RNA polymerase containing the house-keeping sigma factor (sigma 70), but not the stationary-phase sigma factor (sigma 38). Fis traps RNA polymerase including  $\sigma^{70}$  at the promoter and inhibits open complex formation, whereas H-NS prevent promoter binding by RNA polymerase including  $\sigma^{70}$ . When the culture enters into stationary phase, Dps suddenly becomes the most abundant nucleoid protein (180,000 molecules per cell) since its promoter is relieved from both Fis and H-NS-mediated repressions (Grainger *et al.*, 2008). As dodecameric complexes, it forms stable and super-compact nucleoprotein structures by decreasing superhelicity and thereby protects DNA from oxidative damage (Wolf *et al.*, 1999) (Frenkiel-Krispin *et al.*, 2004), nuclease cleavage, UV light, and thermal shock (Nair and Finkel, 2004) and acid (Choi *et al.*, 2000) (Figure 3M-P)

## 1.2. H-NS (Heat-stable nucleoid structuring protein)

H-NS is a small (~15 kDa) but major component of the *E. coli* nucleoid which has been initially identified in 1977 (Varshavsky *et al.*) and characterized biochemically in 1984 (Spassky *et al.*). Several lines of evidence regarding the H-NS effect on DNA topology have been provided early in the 1990s. In one of those reports, H-NS mediated transcriptional regulation of *proU* has been studied in details (Owen-Hughes *et al.*, 1992; Tupper *et al.*, 1994). Curved DNA sequences located at the downstream of the *proU* promoter was found to be the target for preferential binding of H-NS. Moreover, *in vivo* plasmid linking number was affected by the interaction between H-NS and curved DNA inserted into the plasmid, raising the idea that the H-NS influence on *proU* promoter might be executed indirectly, through the changes in DNA topology. To prove this hypothesis, Tupper *et al.* demonstrated that H-NS constrains negative supercoiling *in vitro*, presenting the first evidence for H-NS involvement in bacterial chromosome (Tupper *et al.*, 1994).

Structurally, H-NS consists of three domains; N-terminal protein interaction domain (extending up to residue 65), C-terminal DNA binding domain beginning at residue 90, and a flexible linker domain that attaches two domains (Dorman *et al.*, 1999) (Figure 4 and Figure 6). Although it exists in different combination (dimer, tetramer and oligomer) in solution, H-NS dimers are known to be the basic building block of the nucleoprotein

complex. Minimal dimerization domain stretches from residues 1-64 and contains 3  $\alpha$ -helices (H1, H2, and H3) (Renzoni *et al.*, 2001). The longest helix H3 is predicted to form the core of the coiled-coil structure, while the other helices have stabilizing functions. However, higher order oligomerization requires the linker domain, which is very divergent among H-NS like proteins (Stella *et al.*, 2005).

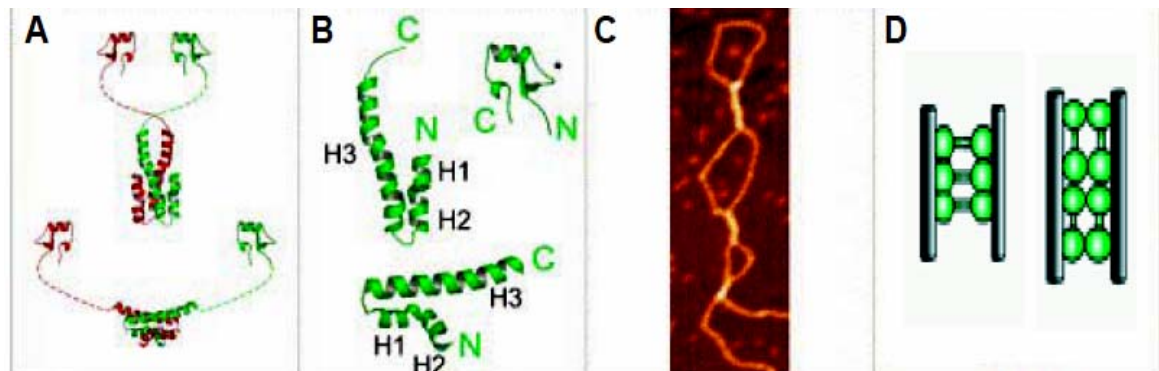


**Figure 4.** Architectural properties of H-NS protein. Structure of dimeric H-NS of *E. coli* (A), Close-up of a monomeric subunits of H-NS (B), Scanning Force Microscopy images of DNA-H-NS complex (C), Low resolution models for DNA compaction by H-NS (D).

H-NS dimers bind to DNA with non-sequence specific fashion, though they show preference for phased A-tract which cause an intrinsic curvature (Tolstorukov *et al.*, 2005). Biochemical analysis of its DNA binding feature around supercoiling sensitive *proU* promoter revealed that the dimers initially binds to two identical high-affinity binding sites located in negative regulator element (NRE) (Bouffartigues *et al.*, 2007). Subsequent to binding to these nucleation sites, oligomerization is triggered and results in the lateral

extension of the nucleoprotein complex toward low affinity binding sites. Then, through the interaction with either individual DNA molecules or different parts of the same DNA molecule, it forms DNA-protein-DNA bridges (Figure 4C and D).

The transcriptional level of H-NS is under tight control of several transcriptional regulators such as StpA, Fis, Lrp, and CspA (La Teana *et al.*, 1991; Falconi *et al.*, 1996; Dorman *et al.*, 1999; Dorman, 2004). Furthermore, autoregulation is coupled with DNA synthesis, resulting in a constant ratio of H-NS to DNA in *E. coli* cell (Free and Dorman, 1995). Therefore, optimal levels of H-NS should be maintained in bacterial cells for healthy growth. In support of this notion, an excess of H-NS induced drastic structural changes leading to further condensation of the DNA and lethality (Spurio *et al.*, 1992). Conversely, H-NS depletion led to diverse phenotypes including loss of mobility, formation of mucoid colonies and production of anucleate cells (Kaidow *et al.*, 1995; Sledjeski and Gottesman, 1995; Soutourina *et al.*, 1999).

H-NS is also specified as a global regulator which senses the environmental stimuli such as osmotic shock and temperature. Transcriptome analysis of *hns*-inactivated *E. coli* cells demonstrated that H-NS-regulated genes are mainly repressed disregarding a few particular cases (e.g., *mal* and *flhDC* operons) (Hommais *et al.*, 2001; Oshima *et al.*, 2006). Transcriptional silencing is executed by several ways through influencing the DNA

topology (Dorman, 2004). Distribution of the high-affinity binding sites in the vicinity of the promoter regions let H-NS to form DNA-H-NS-DNA bridges that traps RNA polymerase in DNA loop structure as in the case of P1 promoter of *rnnB*, *proU* and *hdeAB* promoters (Figure 5A) and prevents transcriptional elongation (Dame *et al.*, 2002; Shin *et al.*, 2005; Dame *et al.*, 2006). Thus, this mechanism is termed as RNA entrapment and has been generalized in *E. coli* by two independent studies, in which H-NS and RNA polymerase are co-precipitated at more than half of the H-NS binding sites (Grainger *et al.*, 2006; Oshima *et al.*, 2006).

Promoter occlusion is another silencing mechanism which is studied in detail in temperature sensitive *virF* promoter of *Shigella flexneri* (Prosseda *et al.*, 2004). The promoter region involves an intrinsic curvature that works as a thermosensor for H-NS-mediated transcriptional regulation. At low temperature, this curvature keeps two H-NS binding sites (-1, -250) in close proximity. The binding of H-NS results in DNA bending which forms a loop, thereby hindering RNA polymerase from binding to the promoter region. Repressive effect of this complex can be removed by temperature shift and Fis. Temperature increase contributes to derepression by displacing the centre of the curvature that results in the changes in local DNA topology (Figure 5B). Sliding of the

centre of curvature towards downstream region makes the promoter accessible for Fis binding at position +55, -1, -130, and -200 and weakens H-NS binding (Figure 5C).

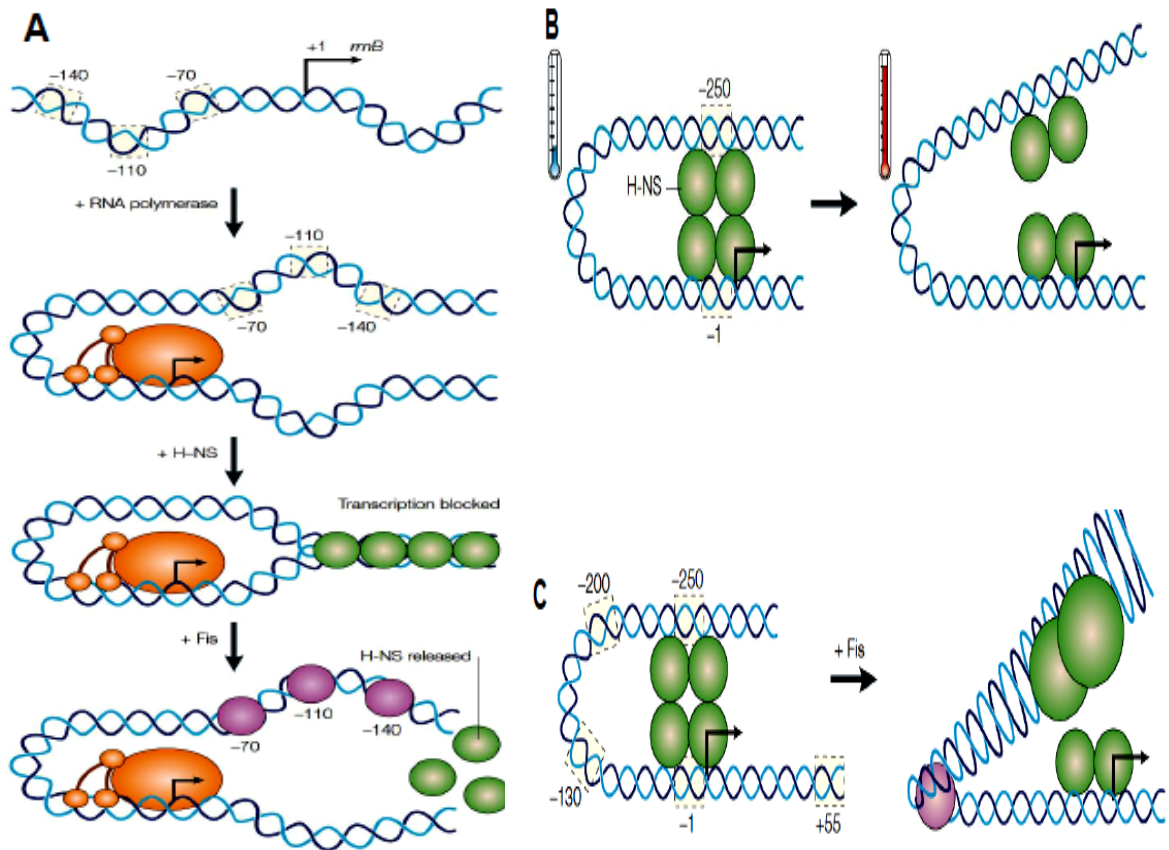


**Figure 5:** H-NS-mediated transcriptional silencing. RNA polymerase entrapment at P1 promoter of the *rmB* ribosomal RNA gene and its release by Fis (A), Temperature mediated transcriptional regulation of *virF* promoter (Dorman, 2004).

The innovation of the ChIP-chip (Chromatin immunoprecipitation couple with chip) technique has allowed deciphering of the precise binding sites of H-NS on the genomic DNA of *E. coli* and *Salmonella* (Navarre et al., 2006; Oshima et al., 2006). Genome-wide evaluation of H-NS distribution revealed that most of the genes repressed by H-NS are



horizontally acquired, thus, this phenomenon is called xenogeneic silencing (Navarre *et al.*, 2007). Through silencing of the foreign genes, H-NS can protect the host cell from the adverse effect. Integration of the new genes into functional regulatory network is mainly achieved by sequence-specific transcriptional activators such as GadW and GadX which are capable of upregulating acid resistance *gad* system repressed by H-NS in *E. coli* (Stoebel *et al.*, 2008). However, it is also possible to see that desilencing requires opposing activity of H-NS related proteins, such as Ler (It will be described below in details). Thus, xenogeneic silencing and the role of H-NS-like proteins in this process seems to be of special interest because it plays an important role in microbial evolution and generally requires activity of specific transcriptional factors

### **1.2.1. H-NS-like proteins**

Although H-NS-related information has been gathered from the studies generally performed with *E. coli* and *Salmonella*, H-NS-like proteins are wide-spread among  $\alpha$ -,  $\beta$ -, and  $\gamma$ -proteobacteria (Tendeng and Bertin, 2003). What's more, most of those species possess more than one H-NS-like protein (Table 1) (Bertin *et al.*, 2001; Tendeng and Bertin, 2003) probably resulted from gene duplication or horizontal transfer. For instance, members of *Enterobacteriaceae* such as *E. coli* and *Salmonella typhimurium* express an

H-NS paralogue called StpA (Suppressor of *td*<sup>-</sup> phenotype A) (Zhang *et al.*, 1996) which will be described below in details.

Three H-NS-related proteins has been identified in *Shigella flexneri*. Apart from chromosomally encoded H-NS and its paralogue StpA, the third protein, Sfh (*Shigella flexneri* H-NS-like protein), has been characterized as a plasmid encoded protein. Although the *stpA sfh* double mutation has wild type like doubling time, disruption of *hns* in combination with either *stpA* or *sfh* cause severe effect on the cellular growth rate (Beloin *et al.*, 2003). Three way interaction has been shown among these proteins suggesting a presence of complex regulation in controlling virulence gene expression (Deighan *et al.*, 2003).

Another H-NS-like protein is MvaT expressing in *Pseudomonas putida*, an opportunistic pathogen in cystic fibrosis patients. It controls the expression of more than 150 genes including virulence and biofilm formation genes (Vallet *et al.*, 2004; Westfall *et al.*, 2006). Scanning force microscopy analysis of plasmid DNA incubated with MvaT demonstrated that DNA binding property of MvaT is very similar to that of H-NS (Dame *et al.*, 2005), since both proteins can form DNA bridges. MvaT has also a paralogue known as MvaU *P. putida* and protein-protein interaction has been reported for these proteins (Vallet-Gely *et al.*, 2005). More recently, ChIP-chip analysis of MvaT and MvaU has been

performed to shed a light on their functional relationship. The results revealed that both proteins occupy the same regions on the chromosome proposing a functional coordination between MvaT and MvaU for expressional regulation of the identical set of genes (Castang *et al.*, 2008). Furthermore, loss of both MvaT and MvaU result in lethality indicating that at least one of these proteins is essential in the absence of the other and, cells can tolerate loss of either protein by means of functional redundancy between them.

In contrast to above mentioned cooperative interaction, an antagonism between H-NS and its partial paralogue Ler, which is encoded by the LEE (locus of enterocyte effacement) pathogenicity island of enteropathogenic (EPEC) and enterohaemorrhagic (EHEC) *E. coli* strains, has been observed (Mellies *et al.*, 2007). Ler acts as a counter-silencer at 37 °C and accelerate the transcription of not only major virulence operons in this island (Umanski *et al.*, 2002; Barba *et al.*, 2005) but also other operons (such as polar fimbriae (*lpf*) operon) located outside (Elliott *et al.*, 2000; Torres *et al.*, 2007) by disrupting H-NS-dependent nucleoprotein complex. In a recent study, the details of this opposing mechanism have been elucidated by the construction of different H-NS/Ler chimeras and found that flexible linker domain, which is widely degenerate among H-NS like proteins, is necessary to overcome H-NS-mediated silencing proposing a functional distinction between the linker domain of H-NS and Ler (Mellies *et al.*, 2008).

In addition to these full length H-NS-like proteins, several polypeptides which share homology with oligomerization domain of H-NS (such as Hha and YmoA) have been also defined in *E. coli*, *Salmonella*, *Yersinia*, and *Shigella* (Madrid *et al.*, 2007a; Madrid *et al.*, 2007b). Heterodimer formation between these proteins and H-NS (or StpA) (Nieto *et al.*, 2002; Paytubi *et al.*, 2004) proposed an existence of complex functional regulatory mechanism among H-NS like protein for the modulation of virulence genes. Absence of H-NS and Hha do not threaten the cell viability as both proteins have a paralogue (StpA and YdgT, respectively) in *E. coli*, *Salmonella* and *Shigella*. However, *hns* deletion and some *ymoA* mutations (e.g. insertional mutation and frame shift deletion) result in lethality in *Yersinia enterocolitica*. (Ellison *et al.*, 2003; Ellison and Miller, 2006) indicating the importance of those proteins for cellular physiology. Thus, again, it can be deduced that expression of many H-NS-like proteins is required for fine-tuning of the transcriptional regulation, even they have functional similarity.

In general, most of these proteins are involved in the regulatory network of bacterial virulence genes. Furthermore, there is a strong correlation between the regulations of horizontally acquired genes and H-NS-like proteins although they are also effective on house-keeping genes. Therefore, the studies on the functional analysis of the H-NS-like proteins are necessary to get a better understanding of their functional network.

$\alpha$ -proteobacteria	<i>Rhodobacter capsulatus</i> <i>Rhodobacter sphaeroides</i> (3) <i>Silicibacter pomeroyi</i> (2)
$\beta$ -proteobacteria	<b><i>Bordetella bronchiseptica</i></b> (1) <i>Bordetella pertussis</i> (1) <i>Burkholderia fungorum</i> (3) <i>Janthinobacterium</i> spp. <i>Nitrosomonas europaea</i> <i>Ralstonia metallidurans</i> (4) <i>Ralstonia solanacearum</i> (4)
$\gamma$ -proteobacteria	<b><i>Acinetobacter</i> spp.</b> (1) <i>Aeromonas hydrophila</i> <i>Azotobacter vinelandii</i> <i>Buchnera aphidicola</i> (1) <i>Dichelobacter nodosus</i> <b><i>Enterobacter</i> spp.</b> (2) <i>Escherichia coli</i> (3) <i>Erwinia chrysanthemi</i> <i>Haemophilus influenzae</i> (1) <i>Methylococcus capsulatus</i> <i>Pasteurella multocida</i> (1) <b><i>Photorhabdus luminescens</i></b> (2) <i>Proteus vulgaris</i> <i>Pseudomonas aeruginosa</i> (2) <i>Pseudomonas fluorescens</i> (3) <i>Pseudomonas putida</i> (5) <b><i>Pseudomonas</i> spp.</b> (1) <i>Pseudomonas syringae</i> (4) <i>Pseudomonas mevalonii</i> <b><i>Psychrobacter</i> spp.</b> (1) <i>Salmonella typhimurium</i> (2) <i>Serratia marcescens</i> <i>Shewanella putrefaciens</i> <i>Shigella flexneri</i> (3) <b><i>Vibrio cholerae</i></b> (1) <i>Vibrio parahaemolyticus</i> <i>Vibrio vulnificus</i> <i>Wigglesworthia glossinidia</i> (1) <i>Xanthomonas axonopodis</i> (4) <i>Xylella fastidiosa</i> (3) <i>Yersinia pestis</i> (1) <b><i>Yersinia enterocolitica</i></b> (1)

**Table 1.** The list of species carrying *hns* and *hns*-related genes. The numbers in the brackets indicate the number of *hns* and *hns*-related genes identified in each species (Tendeng and Bertin, 2003).

### 1.2.2. StpA (Suppressor of *td*<sup>-</sup> phenotype A)

StpA was initially identified by its suppressor activity in the *td* (thymidylate synthase) T4 phage mutant (Zhang and Belfort, 1992). It was subsequently identified as a multicopy suppressor of desilencing of arginine decarboxylase gene (*adi*) expression in the *hns* mutant strain (Shi and Bennett, 1994). StpA homology with H-NS is much higher (71%) at C-terminus (Figure 6).

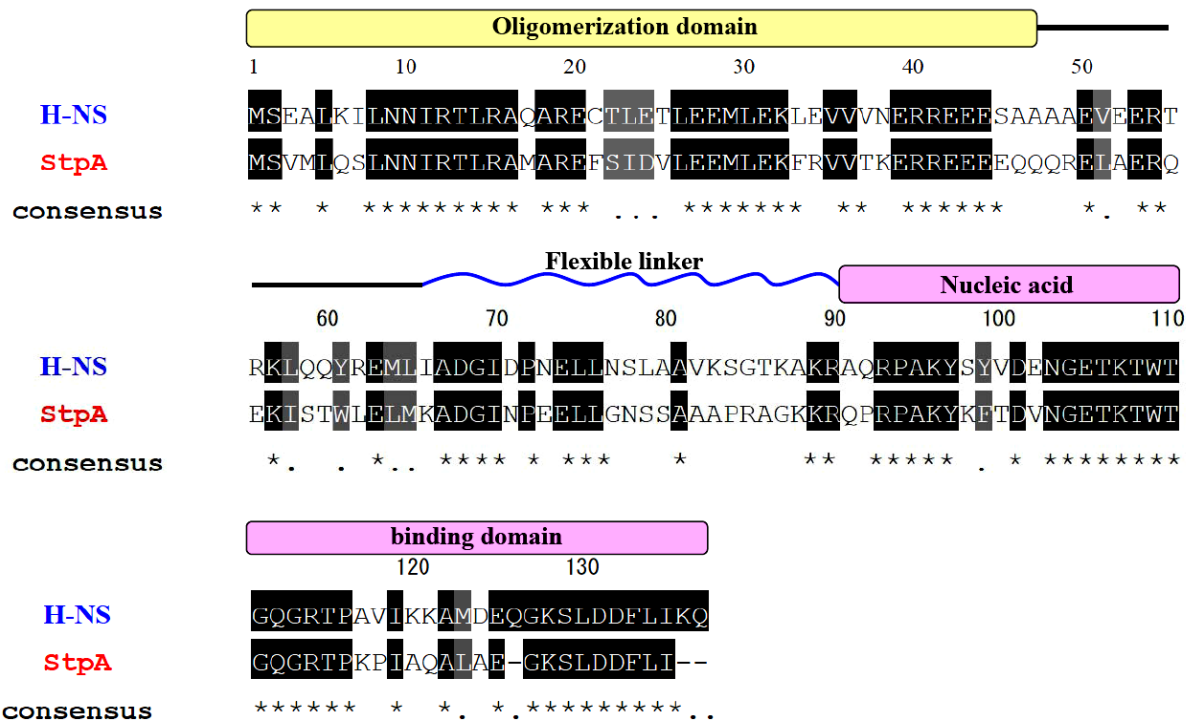


**Figure 6.** Domain organization and multiple alignment of amino acid sequence of H-NS and StpA. Multiple alignment of conserved amino acid sequences of H-NS and StpA was performed using ClustalW2 (<http://www.ebi.ac.uk/Tools/clustalw2/>), and shading with BoxShade 3.21 ([http://www.isrec.isb-sib.ch/software/BOX\\_form\\_old.html](http://www.isrec.isb-sib.ch/software/BOX_form_old.html)). Black shading indicates residues that are completely conserved, while gray shading indicates conservative substitutions.

Biochemical analysis revealed that DNA binding preferences for H-NS and StpA are similar and that, like H-NS, StpA can also constrain DNA supercoils. Scanning force microscopy analysis demonstrated that StpA, like H-NS, also has the ability to bridge DNA helices held in close proximity (Figure 7) (Dame *et al.*, 2005). Furthermore, both H-NS and StpA can repress the expression of the *galU* promoter (Zhang *et al.*, 1996).

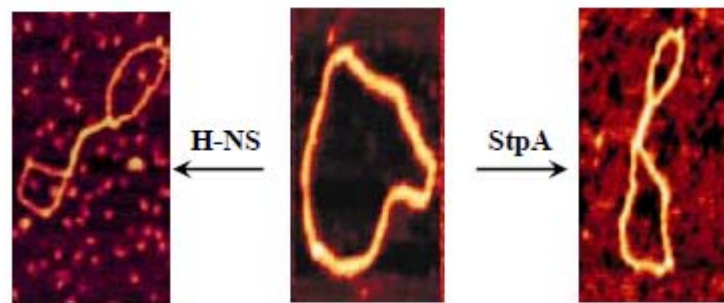


**Figure 7.** DNA bridging ability of H-NS and StpA. Incubation of pUC19 DNA molecules with *E. coli* H-NS (on the left) or StpA (on the right) leads to similar type of protein-DNA complexes (From Dame *et al.*, 2000; Dame *et al.*, 2005).

Considering above mentioned studies, it can be concluded that the H-NS and StpA proteins have similar properties. Nevertheless, there are some differences with respect to the function of StpA compared with H-NS. The basic difference between H-NS and StpA is that StpA can work as an RNA chaperone to facilitate the proper folding of the self-splicing intron (Zhang *et al.*, 1995; Zhang *et al.*, 1996). Furthermore, StpA binds to DNA with a greater affinity than H-NS (Sonnenfield *et al.*, 2001). Although StpA mimics H-NS-mediated transcriptional regulation, it is possible to see different mode of action of

StpA for regulation of some genes such as *ompF* (Deighan *et al.*, 2000). OmpF is an outer membrane porin protein whose expression is controlled at both transcriptional and post-transcriptional levels. H-NS indirectly involved in the transcriptional activation of *ompF* by repressing the *micF* transcription (Suzuki *et al.*, 1996), since *micF* RNA hybridizes to 5' end of *ompF* mRNA and cause destabilization, which in turn leads to reduction in OmpF level (Schmidt *et al.*, 1995). On the other hand, StpA contributes to OmpF expression occurs by reducing the stability of *micF* RNA (Deighan *et al.*, 2000), most probably because of its RNA binding ability.

Although there is no direct evidence to support this statement, StpA is supposed to form heterodimers with H-NS in wild type cells. Since it has been reported that StpA has low dimerization ability and most of the StpA monomers tend to form oligomers in the absence of H-NS. These oligomers are then digested by Lon-mediated proteolysis. Thus, StpA can protect itself through the dimerization with H-NS. However, low dimerization activity of StpA can be enhanced by Phe 21 Cys mutation to some extent and result in a partial improvement in cell growth.

As mentioned before, inactivation of *stpA* has no apparent effect on transcriptional repression and growth rate, which are both affected by the *hns* mutation. These findings support the proposal that StpA plays a supplementary role to H-NS. However, there are



obvious phenotypic differences between the *hns* and *stpA* double mutants and the respective single-gene mutants. The doubling time of the double mutant is markedly slower than that of the *hns* mutant, indicating an *in vivo* role for StpA that is not yet fully understood.

### 1.3. Basis and motivation of this work

H-NS is one of the major components of the bacterial nucleoid in Gram-negative bacteria, which compact massive DNA into so-called microdomains and acts as a transcriptional regulator at the same time to provide a dynamic genome to be responsive against environmental stresses such as temperature and osmotic shock. Interestingly, most of the bacteria bearing *hns* have at least another *hns*-related gene. For instance, StpA, a paralogue of H-NS, is considered as another architectural protein that takes place in the organization of the chromosomal DNA in *E. coli*. However, apart from RNA chaperone activity, its role has not been evaluated in details so far. Disruption of the *hns* gene results in derepression of many genes and coupled with growth impairment. In contrast, disruption of *stpA* has no effect on the cell growth. Thus, this observation suggests a differentiation in their function. Furthermore, the strain lacking both StpA and H-NS shows unstable phenotype and poor survival which is susceptible to point mutation.

The work presented herein concentrates on *in vivo* binding properties of StpA and elucidates the reason behind the differential phenotypes observed in *hns* and *stpA* single mutants.

## 2. MATERIALS AND METODS

### 2.1. Bacterial strains and plasmids

The *E. coli* strains and the plasmids used in this study are given in Table 2. The primer sequences used are listed in Table 3. The epitope tagging protocol (Uzzau *et al.*, 2001) was followed for the construction of the strain expressing C-terminally FLAG-tagged StpA (ZEU01), using the P650 and P651 primers. Removal of the kanamycin resistance cassette from the ZEU01 strain was achieved by introduction into cells of the pCP20 plasmid encoding FLP recombinase (Datsenko and Wanner, 2000). Using P1 transduction, the *hns::km* allele was introduced into kanamycin-sensitive strain expressing StpA-3xFLAG to generate the ZEU04 strain. Inactivation of the *stpA* gene (ZEU02) was accomplished with the primer pair P645 and P651 according to the procedure described by Datsenko and Wanner (Datsenko and Wanner, 2000) using the plasmids pKD3 and pKD46. The strains ZEU03 and ZEU06 were generated by P1 transduction of *stpA::cat* allele using TON1816 and RM539 as recipient strains, respectively. The strain ZEU07 was generated by introducing *stpA(F21C)-3xFLAG-cat* allele into wild type strain using P1 phage.

**Table 2.** Bacterial strains and plasmids used in this study.

Strains	Relevant characteristics	Reference
<b><i>E. coli</i> strains</b>		
W3110	Prototroph	Laboratory stock
TON1816	W3110 <i>hns-3xFLAG-km</i>	(Oshima <i>et al.</i> , 2006)
ZEU01	W3110 <i>stpA-3xFLAG-km</i>	This work
ZEU02	W3110 $\Delta$ <i>stpA::cat</i>	This work
ZEU03	W3110 $\Delta$ <i>stpA::cat hns-3xFLAG-km</i>	This work
RM539	W3110 $\Delta$ <i>hns::km</i>	(Ito <i>et al.</i> , 1994)
ZEU04	W3110 $\Delta$ <i>hns::km stpA-3xFLAG</i>	This work
ZEU05	W3110 $\Delta$ <i>hns::km stpA (F21C)-3xFLAG-cat</i>	This work
ZEU06	W3110 $\Delta$ <i>hns::km <math>\Delta</math>stpA::cat</i>	This work
ZEU07	W3110 <i>stpA (F21C)-3xFLAG-cat</i>	This work
	F <sup>-</sup> $\phi$ 80d <i>lacZ</i> $\Delta$ M15 $\Delta$ ( <i>lacZYA-argF</i> )U169	
DH5 $\alpha$	<i>endA1 recA1 hsdR17 (r<sub>K</sub><sup>-</sup>m<sub>K</sub><sup>+</sup>) deoR</i> <i>thi-1 phoA supE44 <math>\lambda</math><sup>-</sup> gyrA96 relA1</i>	Laboratory stock
pSUB11	Template plasmid carrying FRT- <i>cat</i> -FRT-3xFLAG	(Uzzau <i>et al.</i> , 2001)
pKD46	Helper plasmid encoding $\lambda$ Red genes	(Datsenko and Wanner, 2000)
pKD3	Template plasmid carrying FRT- <i>cat</i> -FRT cassette	(Datsenko and Wanner, 2000)
pCP20	Helper plasmid carrying FLP recombinase	(Datsenko and Wanner, 2000)
pMYH107	Template plasmid carrying FRT- <i>cat</i> -FRT cassette	This work

**Table 3.** PCR primers used in this study.

<b>Primers</b>	<b>DNA sequence (5' → 3')</b>
P645	TACGCGACGAAATACTTTTTTTGTTTTGGCGTTAAAAGGTTTTCTTTATTGTGTAGGCTG
P646	TTGAGAAGCGACGCCGGACGCGCCCTAGCAGCGACATCCGGCCTCAGTAACATATGAATA
P650	CAATTGCTCAGGCGCTGGCAGAAGGTAAATCTCTCGACGATTCCTGATCGACTACAAAG
P651	CAAGGTTGTTAGATAAGATGCCGTGGAACCAACGAGCTTGAGAAGCGACGCATATGAATA
P690	GCTCGCGAATgtTCCATTGACGTTCTTGAAGAAATGCTCG
P691	TCAATGGAacATTCGCGAGCCATCGCACGGAGGGTGCG
P1027	CGGCA <u>AAGCTT</u> <sup>a</sup> GCTGAAATAATCTCGCGCAGGACTGTAAATAG
P1028	CGGCGCATGC <sup>b</sup> TACTATTTATCGTCGTCATCTTTG
P1029	GCGACGCCGGACGCGCCCTAGCAGCGACATCCGGCCTCAGTAAGTGTAGGCTGGAGCTGC
PME0176	GCGGATCC <sup>c</sup> GTGTAGGCTGGAGCTGCTTC
PME0177	GCGAATTC <sup>d</sup> CATATGAATATCCTCCTTAG

\*Restriction recognition sequences introduced for cloning purpose are represented by underlined italic letters (a: *Hind*III, b: *Sph*I, c: *Bam*HI, d: *Eco*RI).

\*\*Mutated bases are shown in lowercase letters.

## 2.2. Construction of *hns* mutant strain expressing StpA(F21C)-3xFLAG

The strategy used for construction of *hns* mutant strain expressing StpA(F21C)-3xFLAG is illustrated in Figure 8. Using the genomic DNA of the strain ZEU01 as a template, two PCR amplifications were carried out with P690/P1028 and P691/P1027 primer pairs to amplify the DNA fragments encompassing the 3xFLAG-tagged *stpA* gene within the promoter region. Primer P690 and P691 contain substituted base pairs coding for cysteine at amino acid position 21 (A). Ligation PCR amplification was performed using the primer pair P1027/P1028 to create a DNA fragment with the F21C point mutation (solid rectangles) (B). The amplification product was double digested with *Hind*III and *Sph*I, and inserted into the pMYH107 plasmid, which harbors the *cat* fragment derived from pIT801 (27) (amplified with the PME0176/PME0177 primer pairs) at the *Bam*HI/*Eco*RI site of pSTV28 (C). The DNA fragment containing *stpA*(F21C)-3xFLAG-*cat* was amplified by the P1027/P1029 primer pair (D). The *stpA*(F21C)-3xFLAG-*cat* fragment was introduced into the chromosome of *E. coli* BW25113 by homologous recombination using  $\lambda$  Red recombinase encoded by the pKD46 plasmid (E). Then, the *stpA*(F21C)-3xFLAG-*cat* fragment was transferred into the genome of W3110  $\Delta$ *hns*::Km by P1 phage transduction, to create the strain ZEU05 (F).

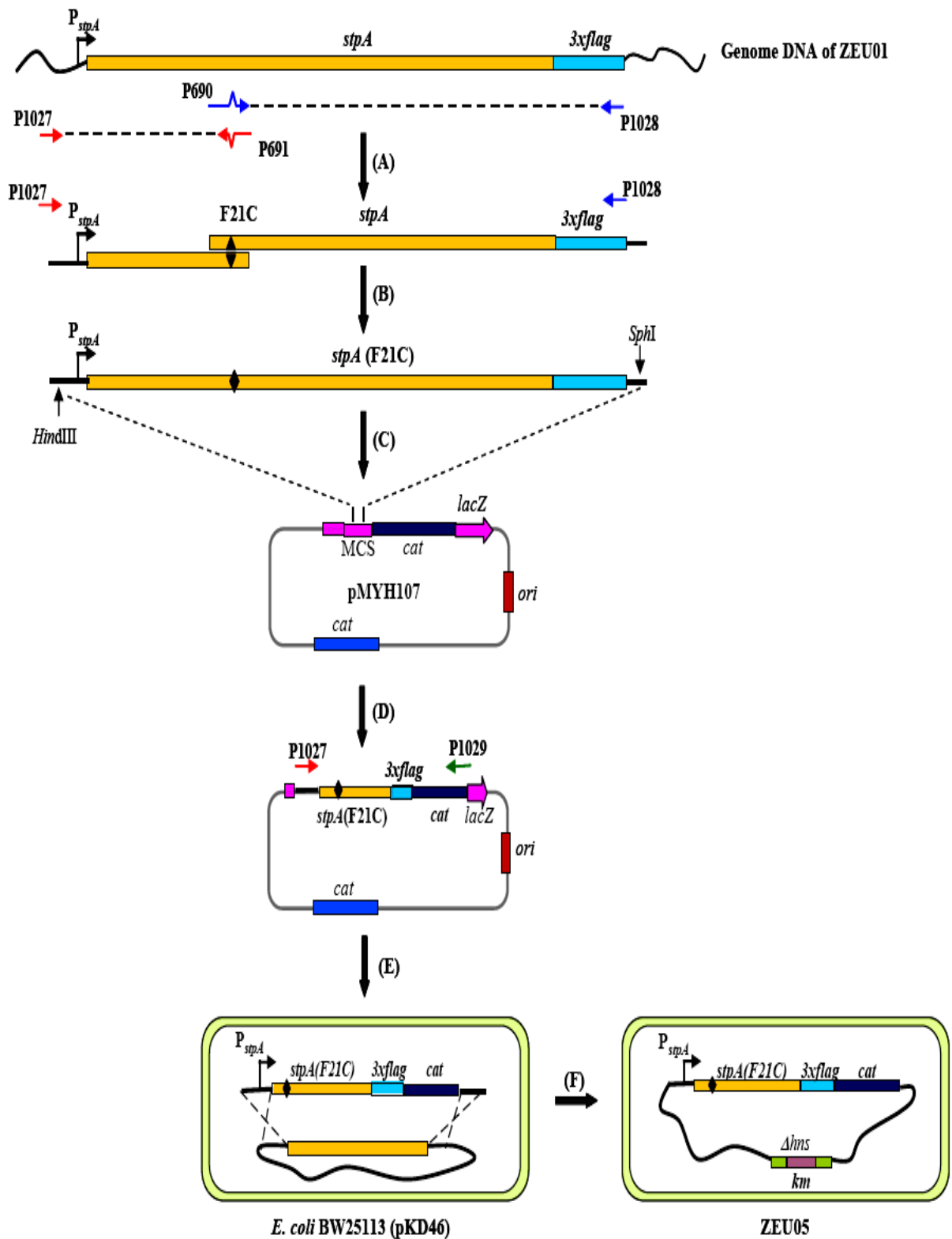


**Figure 8.** Strategy used for the construction of *hns* mutant strain expressing StpA(F21C)-3xFLAG

## **2.3. Materials, media and buffers**

### **2.3.1. Enzymes**

Most of the enzymes (DNA polymerases and restriction enzymes) used were purchased from Takara Shuzo Co Ltd. KOD plus DNA polymerase was used for cloning purpose due to its high processivity and proof reading activity (TOYOBO)

### **2.3.2. Growth media**

Bacterial strains were grown in Luria-Bertani (LB) medium (5 g of yeast extract, 10 g of tryptone and 10 g of NaCl per liter) supplemented with kanamycin (50 µg/ml) or chloramphenicol (10 µg/ml) as required, according to the strain. During construction of the strain expressing StpA(F21C)-3xFLAG, transformant colonies carrying *stpA*-3xFLAG on pMYH107 plasmid were selected based on the inactivation of *lacZ* on LB plate supplemented with X-gal ( 50mg/ml).

### **2.3.3. Buffers (for ChIP-chip experiment)**

#### **Lysis buffer**

Tris-HCl (pH: 8.0)	10 mM
Sucrose	20%
NaCl	50 mM
EDTA (pH: 8.0)	10 mM



**IP Buffer**

HEPES-KOH (pH: 7.5)	50 mM
NaCl	150 mM
EDTA	1 mM
Triton X-100	1%
Na:deoxycholate	0.1%
SDS	0.1%
Glycerol	5%

**IP Salt Buffer**

IP buffer containing 500 mM NaCl

**Wash Buffer**

Tris-HCl (pH: 8.0)	10 mM
LiCl	250 mM
EDTA (pH: 8.0)	1 mM
Nonidet P-40	0.5 %
Na-deoxycholate	0.5 %

**5X Elution Buffer**

Tris-HCl (pH: 7.5)	250 mM
EDTA (pH:8.0)	50 mM
SDS	5%

Prior to use, it was diluted to 1X.

**TE Buffer**

Tris-HCl (pH: 8.0)	10 mM
EDTA (pH:8.0)	1 mM

**Buffers (for *in vitro* analysis of homodimer formation)****Wash Buffer**

Tris-HCl (pH:8.0)	1 M
-------------------	-----

### **Cross-linking Buffer**

Triethanolamine-HCl (pH: 8.5)	1 M
NaCl	5 M
Dithiothreitol	5 mM

### **Other reagents**

Phenyl Methyl Sulfonyl Fluoride (PMSF) was dissolved in 1 ml methanol and kept at -20 C.

3 M Glycine was dissolved in appropriate volume of dH<sub>2</sub>O, sterilized by membrane filtration and kept at 55 °C prior to use.

#### **2.3.4. Antibodies**

H-NS antibody was kindly provided by Hirofumi Aiba (Nagoya Univ.)  
Costume-made StpA peptide-antibody and M2 anti-FLAG antibody were purchased from Sigma. Peptides corresponding to the residues 41-57 (REEEQQQRELAERQEK), 83-99 (APRAGKKRQPRPAKYKF), and 105-120 (ETKTWTGQGRTPKPIA) of StpA were synthesized and used to raise antiserum in rabbits. The StpA anti-peptide antibody was then purified from antiserum using peptide affinity column chromatography. Anti- $\sigma^{70}$  antibody and anti-MalE antibody were purchased from Neoclone and Abcam.

#### **2.4. SDS-PAGE analysis of cellular proteins**

Bacteria were cultured at 37°C in LB medium to an OD<sub>600</sub> of 0.4. Total cellular proteins of each strain were precipitated by the addition of 10% trichloroacetic acid (TCA) and collected by centrifugation. The precipitates were then washed with cold acetone and the dried pellet was dissolved in SDS-TBS sample buffer. The appropriate amount of total protein was separated by sodium dodecyl sulfate polyacrylamide gel electrophoresis (SDS-PAGE) on a 15% Tris-tricine gel and transferred to polyvinylidene fluoride (PVDF) membrane (Amersham Bioscience). The following antibody dilutions were used: anti-StpA (1:1500), anti-H-NS (1:2000) anti-FLAG (1:2000), and anti- $\sigma^{70}$  antibody (1:1000). HRP conjugated anti-rabbit IgG (for StpA, H-NS, and FLAG-tagged StpA/H-NS) and anti-mouse IgG (for  $\sigma^{70}$ ) were used as secondary antibody at a 1:5000 dilution. Chemiluminescent signals (ECL kit, Amersham) were detected using X-ray film (Fuji Film, Japan).  $\sigma^{70}$  was used as an internal control.

Expression levels of Male protein under normal (LB medium) and maltose-induced condition (LB medium supplemented with 0.2% maltose) were detected by anti-Male primary antibody (1:5000 dilution) and HRP-conjugated anti-mouse IgG. Internal control  $\sigma^{70}$  was detected by anti- $\sigma^{70}$  antibody.

## **2.5. In vitro analysis of StpA and H-NS homodimer formation**

In vitro chemical crosslinking was carried out according to the protocol described by Ueguchi et al. (1993). Briefly, cells were grown in LB medium at 37°C and harvested from 5 ml of each culture at an OD<sub>600</sub> of 0.4. Cells were washed with wash buffer followed by sequential freezing and thawing in the same buffer. After centrifugation, cells were resuspended in crosslinking buffer, disrupted by sonication and then ultracentrifuged at 100,000g for 30 min. The supernatants were incubated at room temperature for 30 to 60 min with and without 1 mg/ml dimethylsuberimidate (DMS). Subsequent to precipitation of total proteins with 10% TCA, the samples were subjected to 15% Tris-tricine SDS-PAGE and the protein bands were detected by immunoblotting with polyclonal anti-FLAG antibody.

## **2.6. ChIP-on-chip analysis**

### **2.6.1. ChIP-on-chip analysis using anti-FLAG antibody**

Basic steps of ChIP-on-chip procedure are illustrated in Figure 9. All strains used for ChIP-chip analysis were grown in 250 ml of LB with aeration at 37°C using a rotary shaker (200 rpm) until the culture reached an OD<sub>600</sub> of 0.4. 200 ml of each culture was fixed with formaldehyde at a final concentration of 1% for 30 min at room temperature. The excess formaldehyde was quenched with 6 ml of 3 M glycine for 10 min. Cultures were

harvested and subjected to successive washing steps with TBS and lysis buffer. Cells were suspended in lysis buffer containing 20 mg/ml lysozyme and incubated for 30 min at 37°C. 6 ml of IP buffer and PMSF (to give a final concentration of 1 mg/ml) were added to the samples. The cell samples were then sonicated (XL2020, Astrason, USA) on ice 10 times each for 1 min at 1-min intervals. Chromatin solution was clarified by centrifugation at 20,000g for 30 min at 4°C. The supernatant (whole cell extract) was mixed with anti-FLAG antibody coated-protein A Dynal Dynabeads (100.02, Invitrogen) that had been washed twice with cold TBS containing 5 mg/ml BSA and the mixture was further incubated at 4°C overnight with rotation. The beads were rinsed twice with IP buffer for 10 min with rotation at 4°C, once with IP salt buffer, three times with wash buffer and then once with TE. Protein bound DNA fragments were released from the beads by heating at 65°C for 20 min after addition of 100 µl elution buffer. Proteins in whole cell extract and immunoprecipitated DNA fractions were digested with 2mg/ml proteinase K at 42°C for 2 h, followed by incubation at 65°C for 6 h to inactivate the proteinase K. Free DNA fragments in the whole cell extract and immunoprecipitated DNA fractions were purified by the Qiaquick purification kit and eluted with 100 µl elution buffer provided by the kit. Recovered DNA fragments were amplified according to the random DNA amplification method described by Katou et al. (2006) using the primers, PF 43 and PF 44. The PCR reaction was performed

using 28 cycles for the H-NS analysis, using Phusion high-fidelity DNA polymerase. Terminal labeling and hybridization with the oligonucleotide chip was performed following the Affymetrix instruction manual. Briefly, PCR amplified DNA was digested with DNaseI and then terminally labeled with biotin-ddUTP using ENZO BioArray Terminal Labeling Kit. Hybridization with the oligonucleotide chip was performed for 16 h at 42°C, followed by washing, staining and scanning using the GeneChip Instrument System, according to the manufacturer's instructions (Affymetrix).

### **2.6.2. ChIP-on-chip analysis using anti-StpA peptide-antibody**

To map native StpA distribution in *hns* mutant by anti-StpA-peptide antibody, the protocol described by Grainger et al. (Grainger *et al.*, 2004) was applied, modifying the incubation time from 90 min to 12 h for immunoprecipitation. Using Ultralink protein A/G bead (Pierce) coated by the antibody (5 µg), DNA fragments bound by native StpA were recovered, PCR amplified using 32 cycles and hybridized to the custom oligonucleotide chip mentioned above.

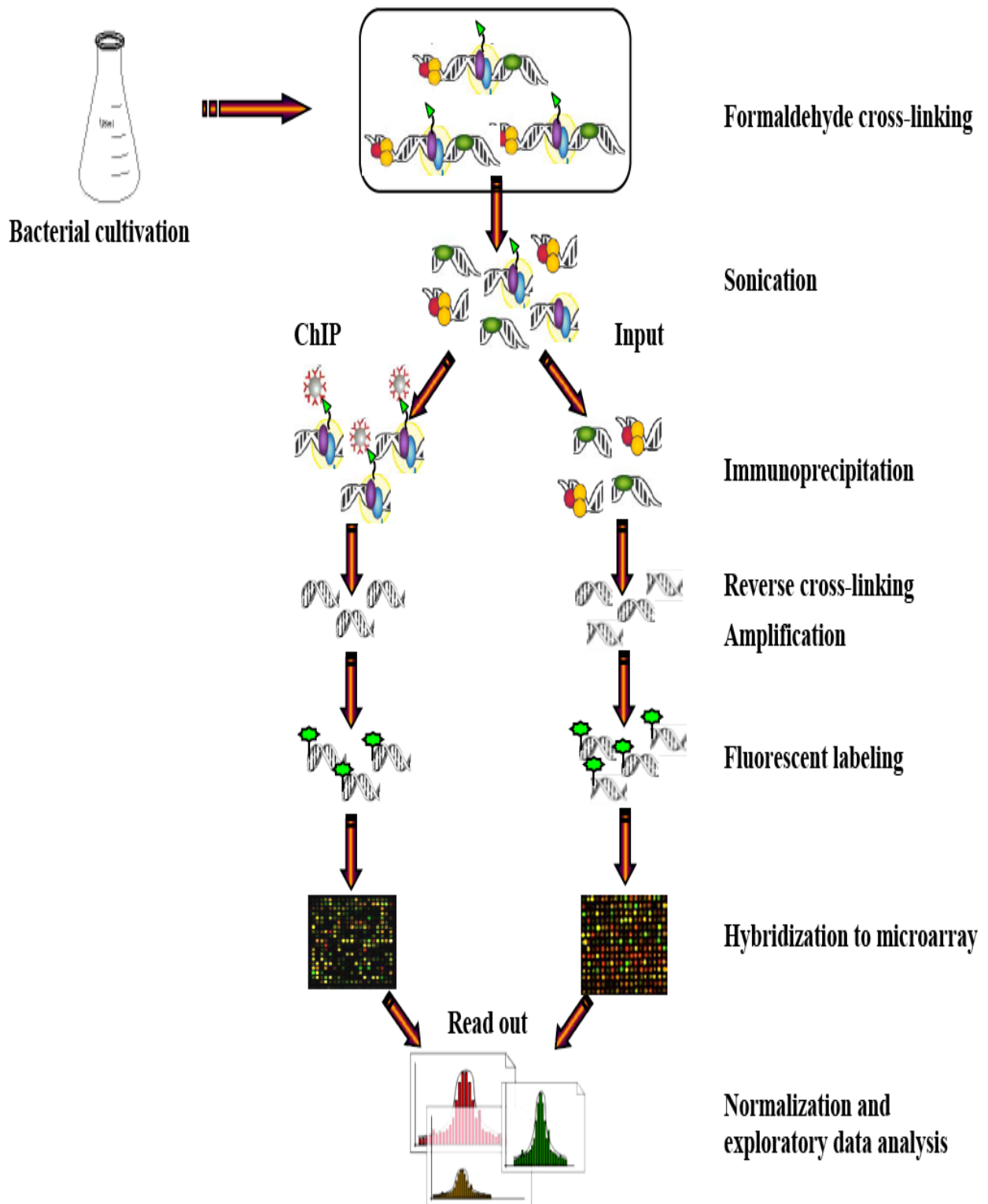


**Figure 9.** Basic steps of the protocol used for ChIP-chip analysis

## **2.7. Data assessment and quantitative analysis of the number of the StpA and H-NS binding sites**

Hybridization data are visualized by the Array edition of In Silico Molecular Cloning program (In Silico Biology, Japan) for the localization of protein binding regions. Signal intensities of mismatch probes were subtracted from those of perfect match probes. Probes with a negative value for signal intensity were excluded from further analysis. The signal intensities of DNA in the affinity-purified fraction and those of DNA isolated from the whole cell extract fraction before purification (control DNA) were adjusted to confer a signal average of 500. Then, the signal intensities of DNA in the immunoprecipitated fraction were divided by those of control DNA, to quantitatively estimate the enrichment of DNA fragments by immunoprecipitation (enrichment factor). All experiments were duplicated.

Quantitative analysis of the number of binding sites was achieved by setting a threshold for StpA and H-NS binding where probes with high enrichment factor above 3.5 clustered in a region greater than 150 bp.



### 3. RESULTS

#### 3.1. Confirmation of the FLAG-tagged StpA and H-NS expression levels

To analyze the genome-wide distribution of StpA and H-NS, we first considered to use the specific antibodies directed against StpA and H-NS. However, these antibodies frequently cross-react with each others' antigen because of the high homology in their amino acid sequence (Figure 10). Therefore, in order to eliminate crossreactivity between StpA and H-NS during CHIP-chip analysis, several strains were generated expressing either StpA or H-NS tagged with 3xFLAG epitope at the C-terminal end (Figure 10C).

In order to make sure that if the amounts of FLAG-tagged StpA or H-NS in genetically modified strains are the same with their parental strains expressing native StpA or H-NS, we monitored the expression level of StpA and H-NS by western blotting. All strains were grown aerobically in LB medium at 37 °C. When OD<sub>600</sub> of the culture reached the 0.4, 1 ml of each cultures were subjected to trichloroacetic acid (TCA) precipitation to precipitate total cellular proteins. Equal volume of samples was subjected to SDS-PAGE. As shown in Figure 10, the addition of a FLAG-tag to H-NS and StpA had no effect on the protein expression levels of H-NS or StpA (Figure 10 A-B), and no impairment in growth rate was observed for cells expressing either FLAG-tagged StpA or H-NS in otherwise wild type backgrounds (Figure 14).

Ali Azam et al. demonstrated that, although H-NS is constitutively expressed from the exponential to stationary phase of growth (20,000 molecules per cell), the *stpA* promoter is switched on during the exponential phase to maintain the number of StpA monomers within the range of 20,000 to 25,000 molecules per cell in W3110 cells (Free and Dorman, 1995; Azam and Ishihama, 1999). By comparison, StpA is not expressed during the exponential phase in the M182 strain, a K12 derivative, instead, a high level of StpA is observed only in the *hns* mutant (Zhang *et al.*, 1996). These observations suggest that the expression level of StpA is flexible and dependent on genetic background. Our western blotting results indicate that a high level of StpA is expressed during the exponential phase of growth of the W3110-derived strains used in the present study.

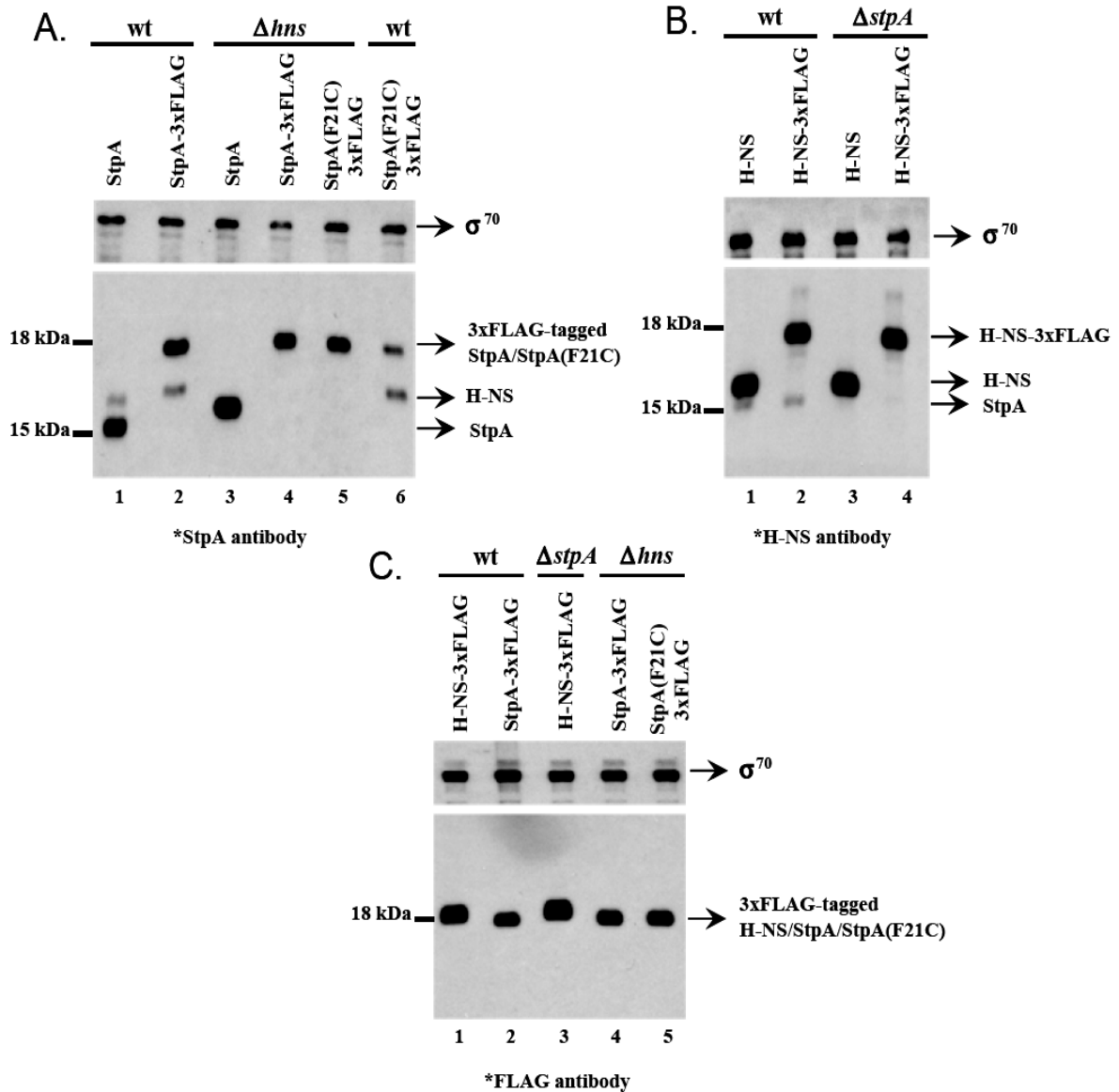


**Figure 10.** The effect of FLAG tagging on StpA and H-NS expression. Total cellular proteins of each strain were prepared by TCA precipitation and separated on Tris-tricine SDS PAGE. Expression levels of native StpA in wild type (lane 1) and  $\Delta hns$  (lane 3) cells, FLAG-tagged StpA in wild type (lane 2) and  $\Delta hns$  (lane 4) cells, and FLAG-tagged StpA(F21C) in  $\Delta hns$  (lane 5) and wild type (lane 6) cells were detected by the StpA anti-peptide antibody (A). Expression levels of native H-NS in wild type (lane 1) and  $\Delta stpA$  (lane 3) cells, FLAG-tagged H-NS in wild type (lane 2) and  $\Delta stpA$  (lane 4) cells were detected by the H-NS antibody (B). Expression levels of FLAG-tagged H-NS in wild type (lane 1) and  $\Delta stpA$  (lane 3) cells, FLAG-tagged StpA in wild type (lane 2) and  $\Delta hns$  (lane 4) cells, and FLAG-tagged StpA(F21C) in  $\Delta hns$  cells were detected by anti-FLAG antibody.  $\sigma^{70}$  was used as an internal control and detected by anti- $\sigma^{70}$  antibody.

### **3.2. The genome-wide StpA binding profile overlaps with the H-NS binding profile**

Using the FLAG-tagged strains, we first examined the genome-wide distribution of StpA and H-NS in wild type cells. To achieve this, exponential cultures at an OD600 of 0.4 growing aerobically in LB medium were treated with formaldehyde to crosslink proteins to DNA. Subsequent sonication of chromatin yielded DNA fragments approximately 500 bp in length and the DNA-protein complexes were immunoprecipitated with Protein A magnetic beads coated with the anti-FLAG antibody. After de-crosslinking by heat treatment, immunoprecipitated DNA was amplified by PCR and terminally labeled for hybridization with a high-density oligonucleotide chip. Array edition of In Silico Molecular Cloning program was used for visualization of the protein binding regions across the *E. coli* genome. The enrichment factors for each 25-mer probe, calculated by dividing the signal intensities of the DNA in the immunoprecipitated fraction by those of the DNA in the supernatant

Typical distribution of H-NS and StpA in wild type cells are shown Figure 11. Figure 11A and B represent the genes such as *gadB*, *hdeAB*, and *gadAX* involved in acid fitness island (AFI). It has been demonstrated that many genes of this island are repressed by H-NS (Hommais *et al.*, 2001; Oshima *et al.*, 2006). Distribution of StpA and H-NS around *fim* locus, which is responsible for type1 fimbriae production, is shown in Figure 11C.

Transcription of type1 fimbriae genes is decided by the *fim* switch that is extremely sensitive to DNA topological changes and negatively affected by H-NS (Dove and Dorman, 1994).

Visualization of hybridization intensities for each probe along the genome coordinates revealed no significant differences between the distribution profiles of StpA and H-NS across the *E.coli* genome. Thus, we came to the conclusion that, StpA and H-NS bind to the same regions in wild type cells in order to compact genomic DNA. The full data set for H-NS and StpA obtained from two independent experiments is shown in Supplementary Figure S1.

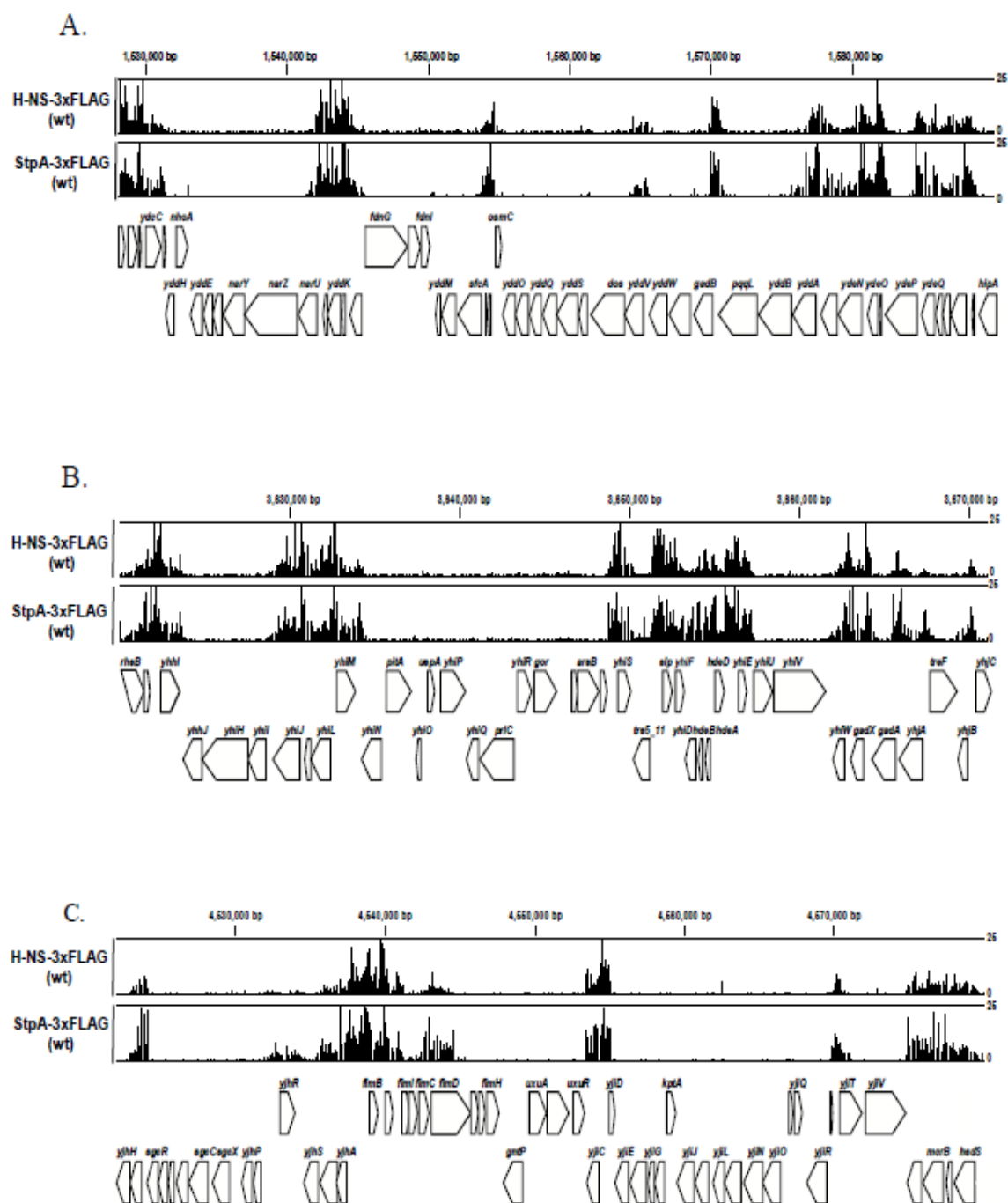


**Figure 11.** Genome-wide distribution of H-NS and StpA in exponential-phase *E. coli* cells. Typical overlapping profiles of H-NS (lane 1) and StpA (lane 2) binding signals in wild type cells are shown around AFI island (A-B) and *fim* operon (C). The relative hybridization intensity of each 25-mer probe on the chip was calculated by dividing the signal intensities of the DNA in the immunoprecipitated fraction by those of the DNA in the supernatant. These results are shown by vertical bars at their corresponding positions on the genome. Arrangement and direction of the ORFs are indicated at the bottom.

To confirm the correlation between H-NS and StpA binding sites, we generated scatter plots of the signal intensity of StpA and H-NS for each probe, from two independent hybridizations. The comparison of the signals reveal that the binding intensities of H-NS and StpA have a very high correlation coefficient (Figure 12), further supporting the genome-wide overlapping profile of H-NS and StpA binding signals.

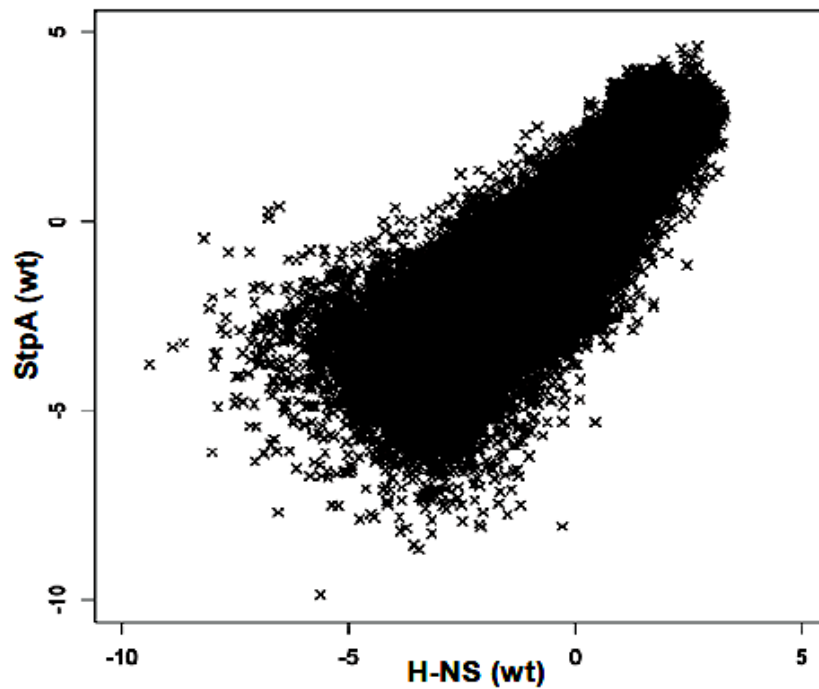


**Figure 12.** Scatter plot of StpA signals versus H-NS signals in wild type cells. The correlation between H-NS and StpA binding signals for each probe on the chip are plotted for two independent experiments in wild type cells and found reproducible.

### **3.3. StpA binding regions are reduced in the absence of H-NS**

In wild type cells, the binding sites of H-NS and StpA essentially overlap. However, the inactivation of *hns* resulted in a reduction of the growth rate, whereas the inactivation of *stpA* had no apparent effect. To gain insight into the molecular events underlying this difference, we mapped the localization of H-NS and StpA in *stpA* and *hns* single mutants, respectively (Figure 13 lane 3 and Figure S1). We found that the inactivation of *stpA* had no effect on the distribution profile of H-NS. This data implied that H-NS has an ability to bind to the regions observed in wild type cells without StpA. Thus, loss of StpA has no change on cellular growth.

By comparison, there was a marked reduction in the number of StpA binding regions in the *hns* mutant cells (Figure 13 lane 4 and Figure S1). However, in these experiments, we observed impairment of growth of the *hns* mutant when the FLAG-tag was fused to StpA (Figure 14). Therefore, we confirmed the biological activity of FLAG-tagged StpA, as described below.



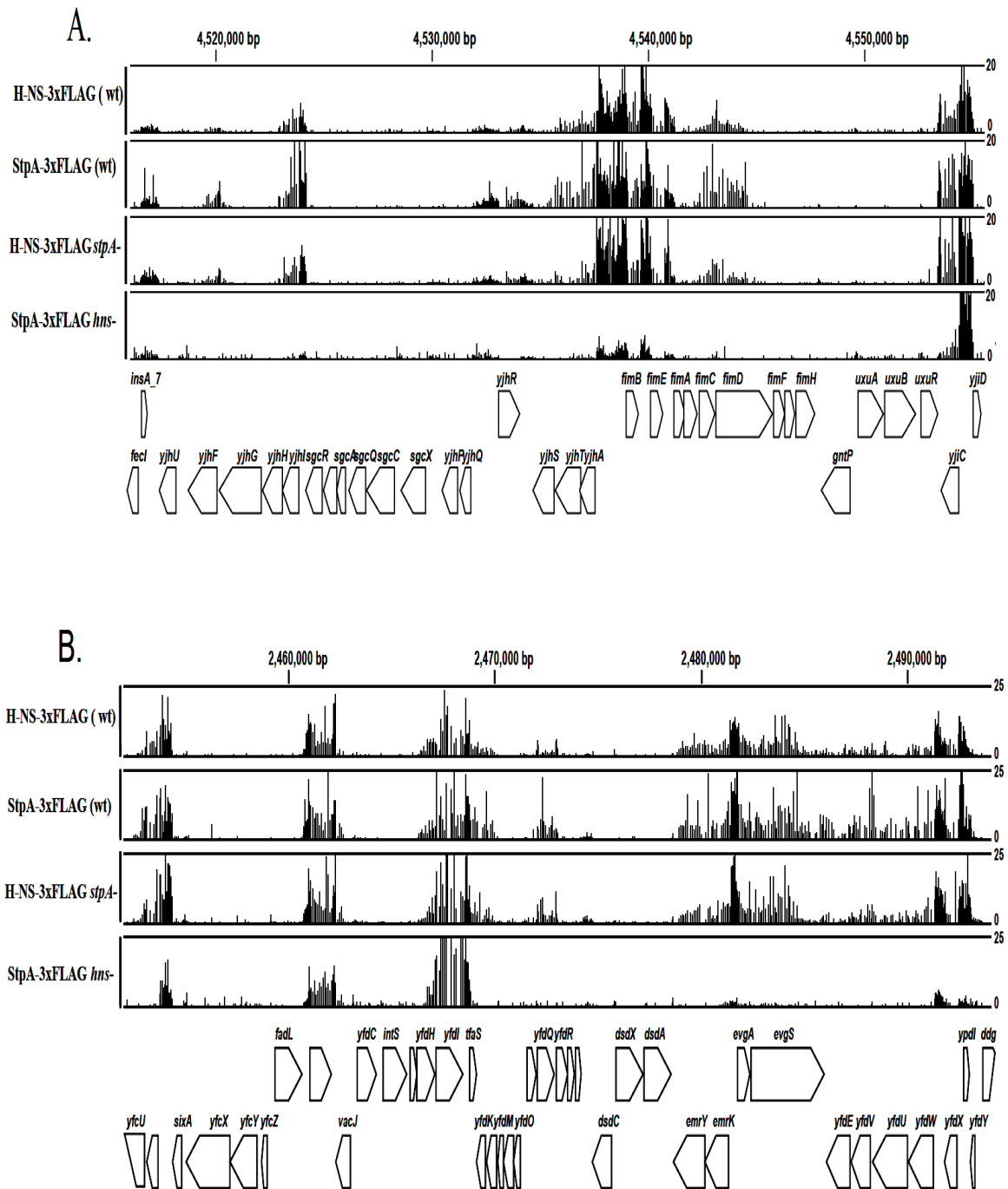


**Figure 13.** Comparison of H-NS and StpA distribution in wild type and single mutants of *stpA*. While H-NS restores its distribution around *fim* (A) and *evg* (B) loci in *stpA* mutant cells (lane 3), StpA lost its interaction with these loci in the *hms* mutant (lane 4). Lane 1 and lane 2 represent H-NS and StpA distribution in wild type cells, respectively. The relative hybridization intensity is given on the right. Arrangement and direction of the ORFs are indicated at the bottom.

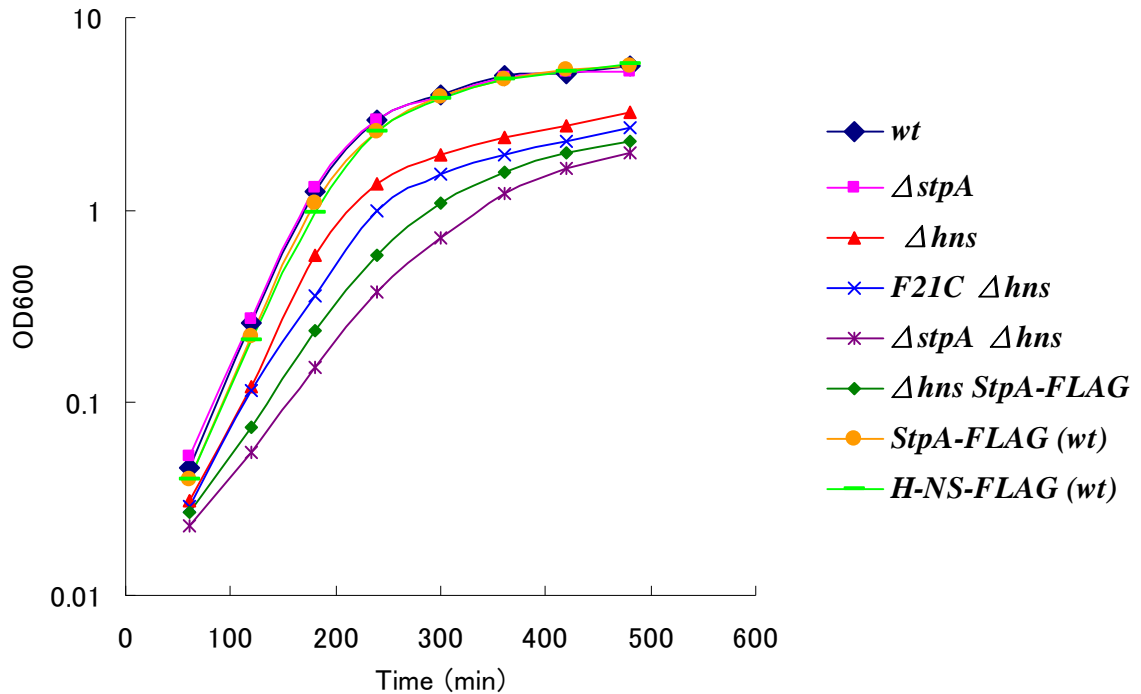


**Figure 14.** Growth curve of the strains used in ChIP-on-chip analysis.

### 3.4. Confirmation of biological activity of FLAG-tagged StpA

To prove whether StpA retained its native biological activity after FLAG-tagging, we checked the expression level of MalE (Maltose-binding protein-MBP) protein which has been demonstrated to be positively regulated by both StpA and H-NS indirectly through the transcriptional activator MalT (Johansson *et al.*, 1998). To this end, the strains expressing native or FLAG-tagged StpA and double mutant of *stpA* and *hns* were grown to an OD<sub>600</sub> of 0.4 in LB medium with and without 0.2 % maltose to induce the MalE expression. Total

cellular proteins of 1ml of each culture were precipitated by TCA and separated on SDS-PAGE (Figure 15). The results indicate that, in comparison with MalE level in double mutant of *stpA* and *hns* genes, FLAG-tagged StpA has the same ability with native StpA to induce the MalE expression wild type cells. However, partial reduction in MalE expression was observed when compared with *hns* mutant expressing native StpA. Therefore, we concluded that FLAG tagging result in partial loss of StpA activity. Next, we wanted to asses the activity of StpA-3xFLAG using a promoter which is directly bound by StpA. *stpA* promoter is one of the candidate for such purpose. Using W3110 and MC4100 as host strains, we attempted to construct *stpA-lacZ* translational fusion. Although we achieved to obtain wild type and *hns* mutant cells expressing either native StpA or StpA-3xFLAG (ZEU09), we could not succeed to get *stpA*, *hns* double mutant.

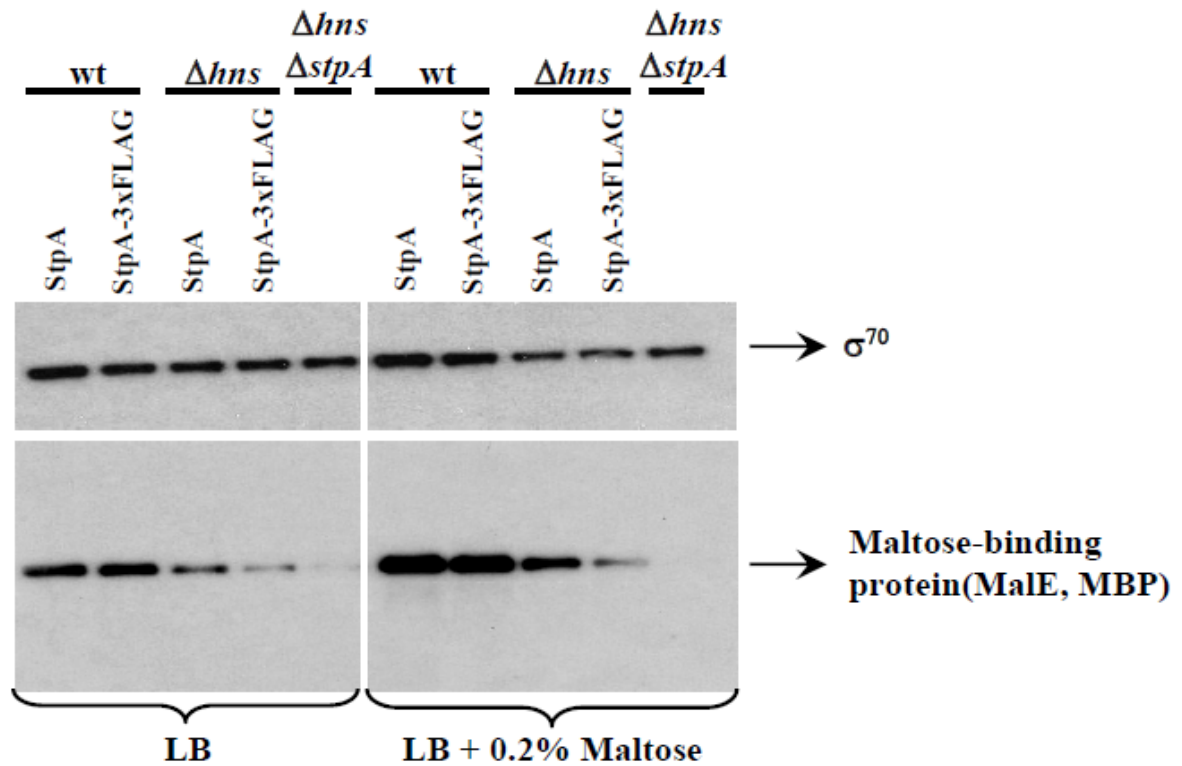


**Figure 15.** Western blot analysis of MalE expression level. Total cellular proteins of each strain were prepared by TCA precipitation; equal volume of each sample was loaded on a SDS-PAGE and transferred to PVDF membrane. Expression levels of MalE induced by native StpA (lane 1 and 6) and FLAG-tagged StpA (lane 2 and 7) in wild type, by native StpA (3 and 8) and FLAG-tagged StpA (lane 4 and 9) in *hns* mutant cells, and in *hns*, *stpA* double mutant cells (lane 5 and 10) in LB medium (lane 1-5) or LB medium supplemented with 0.2% maltose (lane 6-10). MalE protein and  $\sigma^{70}$  (internal control) were detected by Mal E antibody and anti- $\sigma^{70}$  antibody, respectively.

### **3.5. Distribution analysis of native StpA in the *hns* mutant using anti-StpA antibody**

To further evaluate that the reduction in the number of StpA binding sites in the *hns* mutant is not an artifact arising from the FLAG-tag fusion, we repeated the ChIP-chip experiment using anti-StpA antibody. The result revealed that distribution of native and FLAG-tagged StpA are the same in *hns* mutant cells (Figure 16A). Differential regulation of gene expression by StpA has been previously demonstrated. In that work, Wolf et al proved that (Wolf *et al.*, 2006) StpA can bind to its own promoter and represses the transcription, even in the *hns* mutant. However, in the absence of H-NS, StpA has no effect on supercoiling-sensitive *bgl* promoter. Consistent with these findings, our ChIP-chip results show that StpA localizes to its own promoter in the presence and absence of H-NS (Figure 16B), whereas StpA can bind to the *bgl* promoter region only in wild type cells (Figure 16C). Therefore, we concluded that despite the reduction in growth rate, the data for FLAG-tagged StpA reflects the natural distribution of StpA in the *hns* mutant. In addition to this, we observed a low correlation between the binding intensities of StpA in wild type and *hns* mutant cells (Figure 17) reflecting the apparent loss of StpA binding (Figure 16A, compare lane 2 and lane 4).

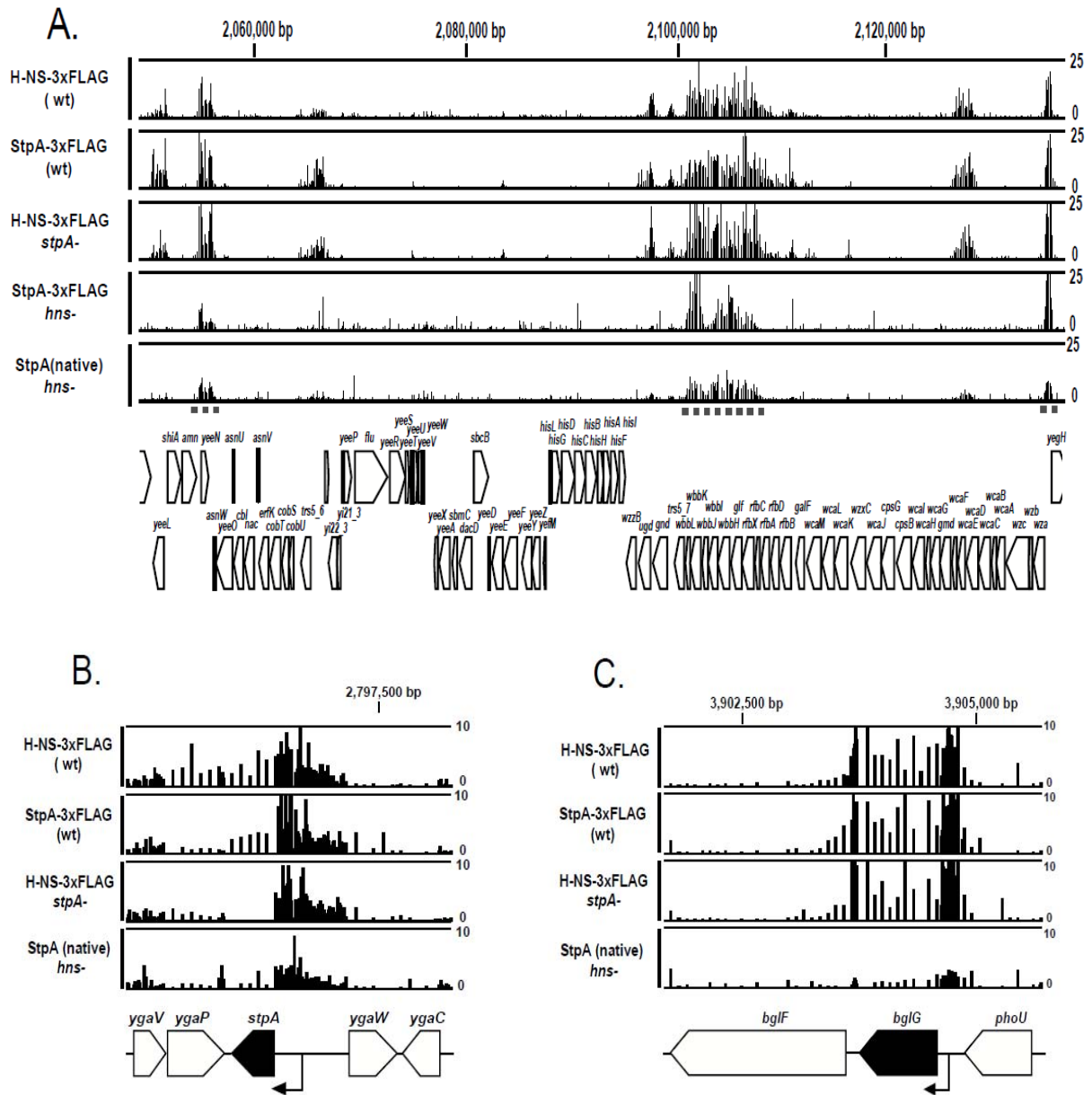


**Figure 16.** Consistency between distribution profile of FLAG-tagged StpA and that of native StpA in *hns* mutant cells. Typical profile of reduction of FLAG-tagged and native StpA binding sites (lane 4 and lane 5) in the *hns* mutant (A) Autonomous binding of StpA around the *stpA* promoter (B), and H-NS-dependent binding of StpA at the *bglG* promoter (C) are shown. H-NS binding signals in wild type (lane 1) and *stpA* mutant (lane 3) cells, and StpA binding signals in wild type cells (lane 2) are also presented. Bent arrows and dashed lines below the distribution map represent the transcriptional start sites and H-NS-independent StpA binding regions in the *hns* mutant, respectively. Relative hybridization intensity is given on the right-side of the distribution map.

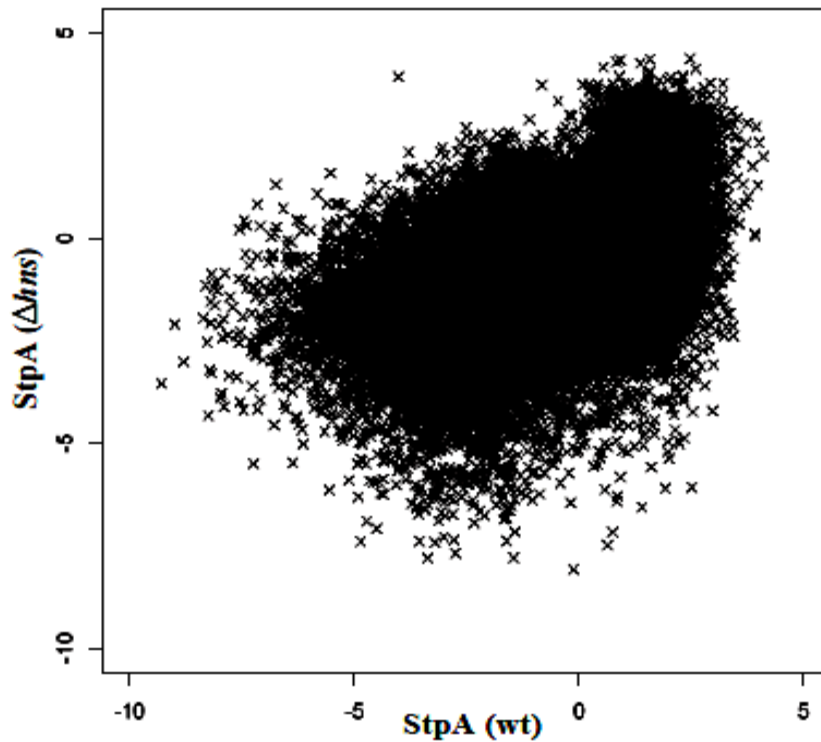


**Figure 17.** Scatter plot of StpA signals in wild type versus *hns* mutant cells. The correlation between the binding signals of each probe on the chip are plotted for two independent experiments and found reproducible.

We classified the genes bound by StpA homodimers according to their function (Supplementary Table). However, we could not observe a particular classification for the genes.

### 3.6. Quantitative analysis of the number of the StpA binding regions in *hns*

#### mutant verified the reduction of StpA distribution in *hns* mutant strain

We quantitatively estimated the dependency of the number of StpA and H-NS binding on their respective binding sites. This was achieved by setting a threshold for StpA and H-NS binding where the probes with high signal intensity above 3.5 clustered in a region greater than 150 bp (Table 4).

	H-NS		StpA		
	wt	$\Delta stpA$	wt	$\Delta hns$	F21C $\Delta hns$
Number of reproducible binding sites	375	329	474	160	239
Number of overlapping binding sites	375	326	474	161	226
Relative ratio	100%	87%	100%	34%	48%

**Table 4.** Quantitative analysis of the number of the StpA and H-NS binding sites. Number of reproducible the binding sites (obtained from two independent experiments over the threshold value of 3.5), overlapping binding sites against reproducible H-NS and StpA binding sites, and their relative ratio are given.

We counted 375 H-NS binding sites for H-NS in wild type cells and 85% of these were also recognized as H-NS binding sites in the *stpA* mutant. By comparison, only 34% of binding sites among 474 binding sites for StpA in wild type cells were recognized in the *hns* mutant. The difference in the number of estimated H-NS and StpA binding sites appears to



result from the general tendency for StpA binding signals to spread along the genome compared with those of H-NS, for unknown reasons. Thus, there is a tendency for H-NS binding signals to localize within regions less than 150 bp and for StpA signals to localize within regions that extend over more than 150 bp.

In conclusion, the result obtained from quantitative measurement of the number of binding sites approved the reduction of StpA homodimer binding sites in *hns* mutant which is represented by approximately one-third of the total StpA binding sites observed in wild type cell. Due to this restricted occupancy of common binding site, StpA is able to function as a molecular back up of H-NS.

### **3.7. StpA(F21C) mutant shows H-NS-like dimerization activity**

In the *hns* mutant, a large proportion of the StpA monomers (>60%) form Lon-sensitive oligomers, with the small proportion remaining in either the monomeric (~20 %) or homodimeric form (~20 %) (Johansson and Uhlin, 1999). Furthermore, effective dimerization of StpA occurs via substitution of Phe 21 with Cys (F21C mutation) and the mutant protein is resistant to Lon protease through enhanced dimerization (Johansson *et al.*, 2001). If insufficient dimerization of StpA in the absence of H-NS is the main reason for the

restricted binding of StpA in the *hns* mutant, it is possible that the F21C mutation would restore the binding profiles of StpA comparable to that in the wild type cell.

To assess this possibility, we constructed *hns* mutant expressing StpA(F21C)-3xFLAG. The F21C point mutation was generated by PCR-directed mutagenesis and the mutated gene was integrated into the *E. coli* genome by double crossover recombination. Homodimer formation efficiencies for the H-NS-FLAG, StpA-FLAG and StpA(F21C)-FLAG constructs were examined by *in vitro* DMS crosslinking analysis to confirm if the characteristic dimerization was maintained after the addition of the FLAG epitope. The chemical crosslinking assay revealed a high level of homodimer formation for H-NS-FLAG (Figure 18). In contrast, the efficiency of homodimer formation for StpA-FLAG was markedly lower than that of H-NS-FLAG. This observation is consistent with previous report for StpA. We then revealed that the F21C mutation in FLAG tagged-StpA increases the dimerization ability of StpA to a level comparable with H-NS.

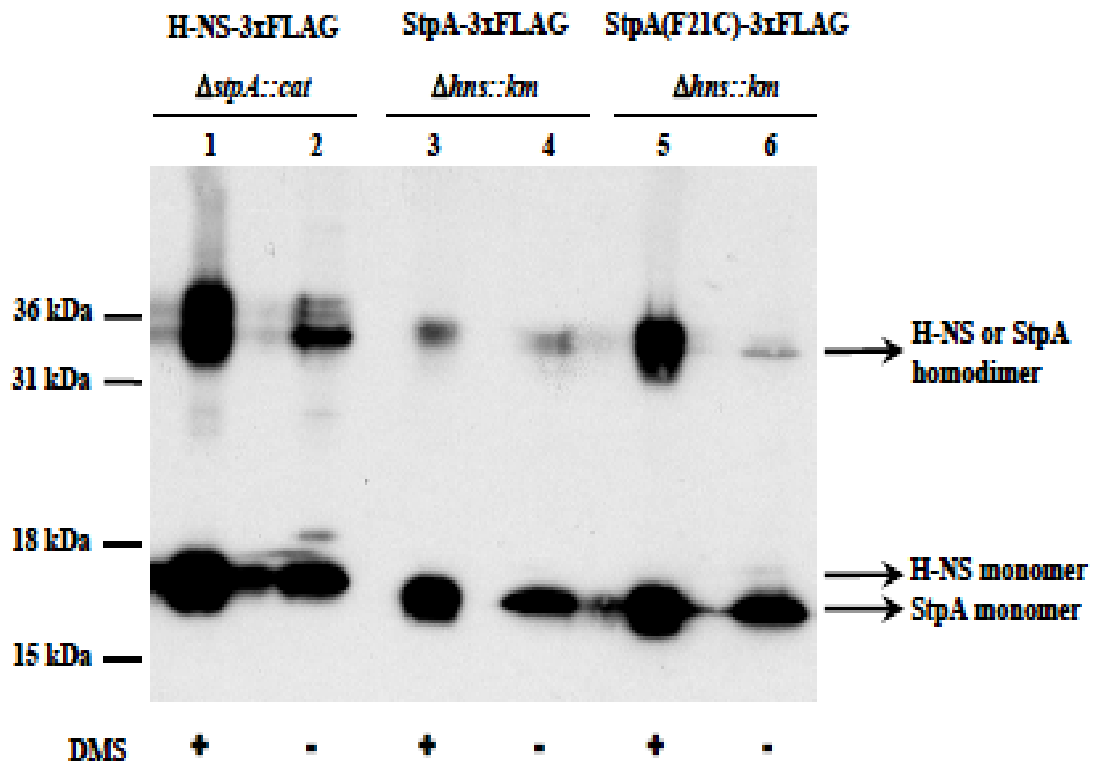


**Figure 18.** Dimerization proficiency of H-NS and StpA. Cultures expressing either H-NS-3xFLAG or StpA/StpA (F21C)-3 x FLAG were subjected to DMS crosslinking and crude extracts were separated by SDS-PAGE. Lane 1-2, *hns-3xFLAG*,  $\Delta stpA::cat$ ; lane 3-4, *stpA-3xFLAG*,  $\Delta hns::km$ ; lane 5-6, *stpA (F21C)-3xFLAG*,  $\Delta hns::km$ . The protein bands were detected by immunoblotting with anti-FLAG antibodies. Sizes of protein standards are indicated on the left in kDa, together with presumed positions correspond to H-NS or StpA dimers on the right.

**3.8. Reduction of StpA binding in the *hns* mutant reflects the difference in the intrinsic DNA binding properties between the StpA dimer and H-NS dimer**

ChIP-chip analysis of StpA(F21C) indicated that stabilization of the StpA dimer does not dramatically change the StpA binding profile of the *hns* mutant (Figure 19 and Fig. S1). The F21C mutation restores several binding regions of StpA in the *hns* mutant, increasing the relative ratio of StpA binding sites within these regions from 34% to 50% of the level in wild type cells (Table 4). However, the restorative effect of the mutation is limited to approximately 75 StpA binding regions, which is only 16% of all StpA binding regions in wild type cells. Consistent with these findings, the F21C mutation partially improved the growth impairment induced by *hns* inactivation in StpA-FLAG expressing cells (Figure 14). These results strongly suggest that the reduction in the number of StpA binding sites in the *hns* mutant is not due to the limited amount of the StpA dimer, but most likely resulted from differences in intrinsic DNA binding properties between the StpA dimer and the H-NS dimer.

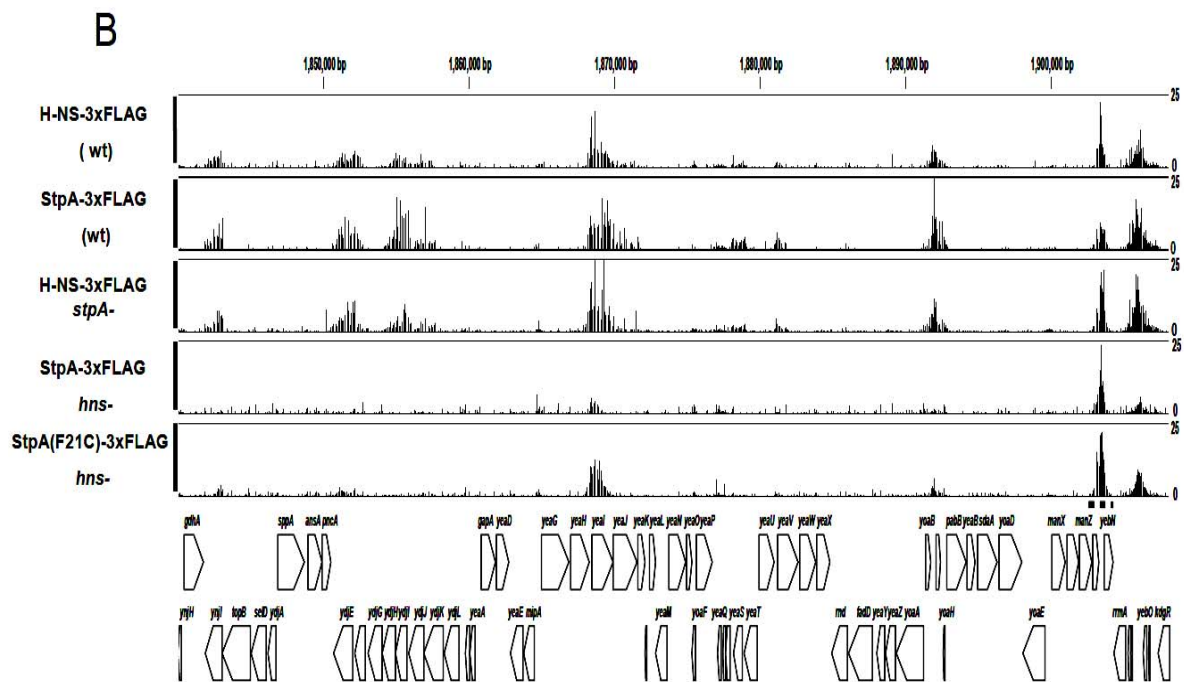
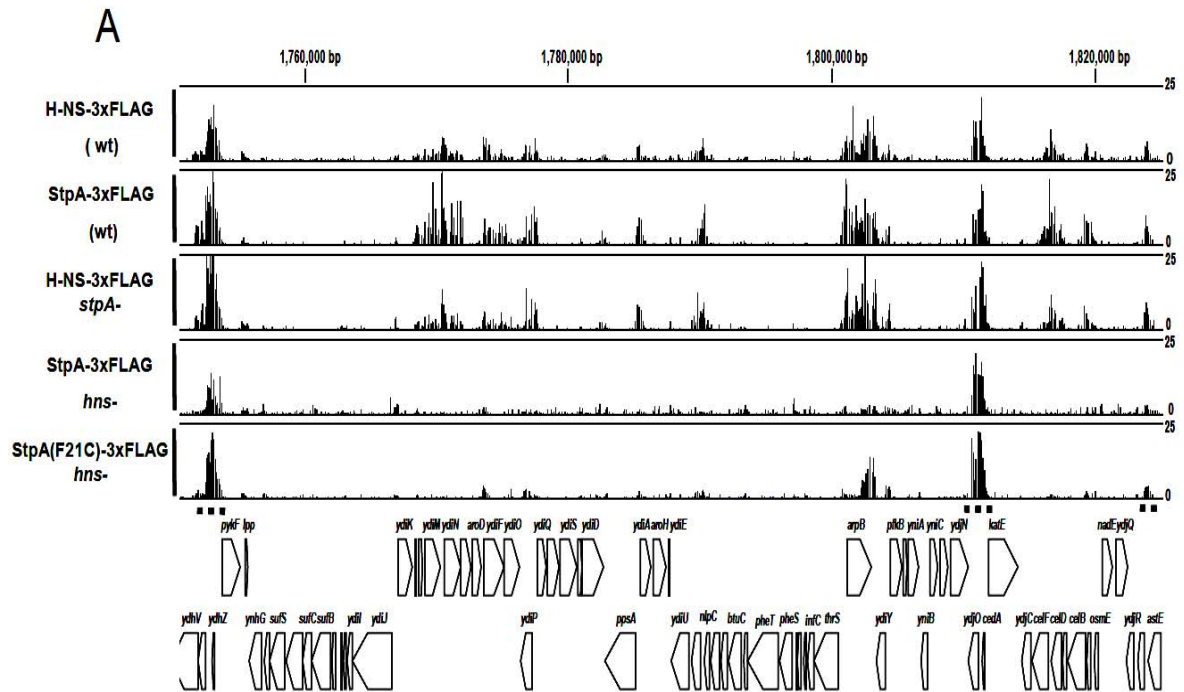


**Figure 19.** Distribution of StpA(F21C) in the *hns* mutant. H-NS binding signals in wild type (lane 1) and *stpA* mutant (lane 3) cells, StpA binding signals in wild type (lane 2) and *hns* mutant (lane 4) cells, and StpA(F21C) binding signals in *hns* mutant cells (lane 5) are shown. H-NS-independent binding sites are indicated by dashed lines.

On the basis of our findings, we also attempted to identify the sequence characteristics that differentiate the StpA dimer binding sites from the H-NS dimer binding sites. Using DNA footprinting results of H-NS regulated promoters in combination with ChIP-chip data, Lang and co-workers recently proposed a 10 bp DNA binding motif (5'-TCGATATATT-3') that may facilitate H-NS binding and spreading for the formation of higher order protein complexes (Lang *et al.*, 2007). We found no correlation between this proposed DNA binding motif and StpA dimer binding sites. Another possibility that may differentiate the StpA dimer and H-NS dimer binding sites is the A + T content of the binding sequences. We found that the H-NS-independent StpA binding sites have an average A + T content of 67% compared with an average of 65% for the H-NS binding sites.

To further analyze if limited interaction between StpA and DNA is resulted from its intrinsic DNA binding property or not, we attempted to construct *hns* and *stpA* double mutant expressing extrachromosomal StpA(F21C)-3xFLAG under the arabinose-inducible promoter. However, we fail to construct a stable strain, most likely due to the suppressor mutation frequently occurs in *spoT* (Johansson et al., 2000). For the same reason, we could not provide transcriptome profile for double mutant of *hns* and *stpA* genes. Thus, it should be emphasized that the inactivation of *stpA* in the *hns* mutant resulted in further growth

impairment in our strain, indicating the importance of the remaining StpA binding in the *hns* mutant for cell growth.

#### 4. DISCUSSION

Inspired by the phenotypical variations between the single mutants of *hns* and *stpA*, we sought to investigate the genome-wide distribution of H-NS and StpA using the ChIP-chip approach. Western blot analysis demonstrated that StpA and H-NS are expressed at high levels in the exponential growth phase of the strains used in the present study. ChIP-chip analysis using FLAG-tagged H-NS and StpA revealed that distributions of both proteins on the genome are essentially the same in wild type cells. Furthermore, the distribution of H-NS was similar in *stpA* mutant cells and in wild type cells, indicating that the fundamental DNA binding activity of H-NS does not require the presence of StpA, at least under our experimental conditions. This feature of H-NS explains the lack of a discriminative phenotype for the *stpA* mutant; it has a normal growth rate (Sonden and Uhlin, 1996; Zhang *et al.*, 1996) and its transcriptome retains a similar profile to wild type cells (Muller *et al.*, 2006).

Heteromeric interaction between StpA and H-NS has been shown *in vitro* and *in vivo* (Williams *et al.*, 1996). Although both StpA and H-NS proteins can form homodimers, StpA is considered to prefer to interact with H-NS to form heterodimeric units in wild type cells (Johansson and Uhlin, 1999; Johansson *et al.*, 2001). Furthermore, direct and indirect involvement of StpA in the transcriptional regulation of some H-NS-repressed promoters



has been demonstrated. For instance, overexpression of StpA can repress the transcription at the H-NS-repressed *proU* and *galU* promoters (Zhang et al., 1996; Williams et al., 1996). Conversely, StpA promotes the transcription of *mal* operon which is also up-regulated by H-NS. Taken together, StpA has been suggested as a molecular back-up of H-NS in transcriptional regulation. In the present study, this proposal has been proven by the fact that StpA and H-NS distributions overlap in wild type cells. It is clear that StpA binding spreads to regions covered by H-NS in wild type cells even if its loss has no meaning for the cell. This spreading may be through H-NS/StpA heterodimer formation and/or interaction between H-NS and StpA homodimer.

In the *hns* mutant cells, the StpA binding sites were reduced dramatically in comparison with those observed in wild type cells. Wolf et al. reported that StpA has the ability to repress its own expression, even in the *hns* mutant, but does not repress the *bgl* operon in the *hns* mutant (Wolf et al., 2006). Our findings are consistent with these observations and revealed that StpA binding sites can be classified into two groups; H-NS-dependent, and H-NS-independent binding sites. Our transcriptome analysis reported previously (Oshima et al., 2006) indicates that the reduction of the StpA binding sites in *hns* mutant cells results in the de-silencing of many genes that are covered by H-NS and StpA in wild type cells, and this would lead to the impairment of growth rate of the *hns* mutant. On

the other hand, expression of genes covered by StpA remained repressed or silent in the *hns* mutant, although it is unknown if derepression of genes covered by StpA in *hns* mutant cells is induced by further inactivation of *stpA*. As double mutant of *hns* and *stpA* is unstable, we were unable to provide its transcriptome data. functional classification of the genes bound by StpA homodimers represents no particular

Introduction of the F21C point mutation in StpA increased the stability of the StpA dimer to a level comparable with the H-NS dimer. However, restoration of StpA binding and growth rate by the F21C mutation was very limited. These observations strongly suggest that the difference in phenotype between the *stpA* and *hns* mutations results from differences in the DNA binding properties of the StpA and H-NS homodimers *in vivo*, although the sequence characteristics that differentiate the StpA binding sites from the H-NS binding sites remain to be elucidated. In addition to this, it has been reported that with a similar preference for curved DNA, StpA binds to the *yghJ* promoter and downstream regulatory element (DRE) of *proU* promoter with approximately four-fold higher affinity than H-NS (Sonnenfield *et al.*, 2001; Yang *et al.*, 2007). Furthermore, the same level of H-NS-mediated constraining of negative supercoils can be obtained by lower amount of StpA (Zhang *et al.*, 1996). In agreement with these reports, we found a slight difference between the DNA sequences occupied by either StpA or H-NS homodimers since the average AT content of

the StpA-bound genomic DNA in *hns* mutant (~67%) is higher than that of H-NS homodimers in *stpA* mutant (~65%). It is also possible that the restriction of StpA interaction with DNA may result from a secondary effect of H-NS absence that generates unfavorable DNA structures for StpA binding.

Recently, Noom et al. proposed that most H-NS in the cell is bound to DNA, based on the calculation of molecular number of H-NS necessary to cover the binding sites identified by CHIP-chip experiments (Noom *et al.*, 2007). During the exponential phase, rapid DNA replication in bacterial cells may cause a temporal shortage of H-NS. The compensation by StpA might function to maintain the nucleoid structure, even when the cell has the maximal DNA content. Conversely, excess StpA can be degraded by Lon protease. The introduction of Lon-resistant StpA(F21C) allele into wild type cells did not give a distinctive phenotype. Examination of the protein expression level pointed out a strict control of H-NS and StpA over *stpA* promoter, since the amount of StpA(F21C) is diminished in comparison with that of wild type strain expressing native StpA. Therefore, without any negative effects from the presence of excess amounts of H-NS homolog, StpA can temporally support H-NS by means of its protease-sensitive character.

Inactivation of *stpA* in the *hns* mutant resulted in further impairment of cell growth, indicating the importance of the remaining StpA binding in the *hns* mutant. In prokaryotic

cells, DNA molecules longer than the size of the cell undergo a complex packing procedure to form a well-organized nucleoid structure through the formation of independent domains. H-NS is one of the pivotal proteins involved in this process (Noom *et al.*, 2007). Interestingly, a stringent response has been observed in the *hns* and *stpA* double mutant, even under nonstringent conditions, probably due to the reduction of negative supercoiling of genomic DNA (Johansson *et al.*, 2000). Although FLAG-tag fusion to StpA did not affect the DNA binding profile, growth impairment resulting from the FLAG-tag fusion to StpA was observed in the *hns* mutant background. It is possible that the FLAG-tag affects the formation of the higher order nucleoid structure normally achieved by StpA. While the main role of H-NS is considered the repression of unfavorable gene expression of horizontally acquired genes, it is possible that H-NS and StpA play a more fundamental role in cell growth.

In summary, we have demonstrated, for the first time, the distribution of StpA on the *E. coli* genome. Our results revealed that there are two types of StpA binding sites in the bacterial genome. About two-thirds of the StpA binding sites in wild type cells are dependent on H-NS, while the remaining one-third is recognized by the StpA dimer in the absence of H-NS. The remaining level of StpA binding in the *hns* mutant might ensure minimal activity to maintain the genome DNA topology to ensure continued cell viability,

although it is also possible desilencing of StpA bound genes causes deleterious effects on cell growth.

## REFERENCES

Almiron, M., Link, A.J., Furlong, D., and Kolter, R. (1992). A novel DNA-binding protein with regulatory and protective roles in starved *Escherichia coli*. *Genes Dev* 6, 2646-2654.

Azam, T.A., and Ishihama, A. (1999). Twelve species of the nucleoid-associated protein from *Escherichia coli*. Sequence recognition specificity and DNA binding affinity. *J Biol Chem* 274, 33105-33113.

Ball, C.A., Osuna, R., Ferguson, K.C., and Johnson, R.C. (1992). Dramatic changes in Fis levels upon nutrient upshift in *Escherichia coli*. *J Bacteriol* 174, 8043-8056.

Barba, J., Bustamante, V.H., Flores-Valdez, M.A., Deng, W., Finlay, B.B., and Puente, J.L. (2005). A positive regulatory loop controls expression of the locus of enterocyte effacement-encoded regulators Ler and GrlA. *J Bacteriol* 187, 7918-7930.

Beloin, C., Deighan, P., Doyle, M., and Dorman, C.J. (2003). *Shigella flexneri* 2a strain 2457T expresses three members of the H-NS-like protein family: characterization of the Sfh protein. *Mol Genet Genomics* 270, 66-77.

Bertin, P., Hommais, F., Krin, E., Soutourina, O., Tendeng, C., Derzelle, S., and Danchin, A. (2001). H-NS and H-NS-like proteins in Gram-negative bacteria and their multiple role in the regulation of bacterial metabolism. *Biochimie* 83, 235-241.

Boles, T.C., White, J.H., and Cozzarelli, N.R. (1990). Structure of plectonemically supercoiled DNA. *J Mol Biol* 213, 931-951.

Bouffartigues, E., Buckle, M., Badaut, C., Travers, A., and Rimsky, S. (2007). H-NS cooperative binding to high-affinity sites in a regulatory element results in transcriptional silencing. *Nat Struct Mol Biol* 14, 441-448.

Castang, S., McManus, H.R., Turner, K.H., and Dove, S.L. (2008). H-NS family members function coordinately in an opportunistic pathogen. *Proc Natl Acad Sci USA* 105, 18947-18952.

Choi, S.H., Baumler, D.J., and Kaspar, C.W. (2000). Contribution of *dps* to acid stress tolerance and oxidative stress tolerance in *Escherichia coli* O157:H7. *Appl Environ Microbiol* 66, 3911-3916.

Craig, N.L., and Nash, H.A. (1984). *E. coli* integration host factor binds to specific sites in DNA. *Cell* 39, 707-716.

Dame, R.T. (2005). The role of nucleoid-associated proteins in the organization and compaction of bacterial chromatin. *Mol Microbiol* 56, 858-870.

Dame, R.T., Luijsterburg, M.S., Krin, E., Bertin, P.N., Wagner, R., and Wuite, G.J. (2005). DNA bridging: a property shared among H-NS-like proteins. *J Bacteriol* 187, 1845-1848.

Dame, R.T., Noom, M.C., and Wuite, G.J. (2006). Bacterial chromatin organization by H-NS protein unravelled using dual DNA manipulation. *Nature* 444, 387-390.

Dame, R.T., Wyman, C., Wurm, R., Wagner, R., and Goosen, N. (2002). Structural basis for H-NS-mediated trapping of RNA polymerase in the open initiation complex at the *rrnB* P1. *J Biol Chem* 277, 2146-2150.

Datsenko, K.A., and Wanner, B.L. (2000). One-step inactivation of chromosomal genes in *Escherichia coli* K-12 using PCR products. *Proc Natl Acad Sci USA* 97, 6640-6645.

Deighan, P., Beloin, C., and Dorman, C.J. (2003). Three-way interactions among the Sfh, StpA and H-NS nucleoid-structuring proteins of *Shigella flexneri* 2a strain 2457T. *Mol Microbiol* 48, 1401-1416.

Deighan, P., Free, A., and Dorman, C.J. (2000). A role for the *Escherichia coli* H-NS-like protein StpA in OmpF porin expression through modulation of *micF* RNA stability. *Mol Microbiol* 38, 126-139.

Ditto, M.D., Roberts, D., and Weisberg, R.A. (1994). Growth phase variation of integration host factor level in *Escherichia coli*. *J Bacteriol* 176, 3738-3748.

Dorman, C.J. (2004). H-NS: a universal regulator for a dynamic genome. *Nat Rev Microbiol* 2, 391-400.



Dorman, C.J., Hinton, J.C., and Free, A. (1999). Domain organization and oligomerization among H-NS-like nucleoid-associated proteins in bacteria. *Trends Microbiol* 7, 124-128.

Dove, S.L., and Dorman, C.J. (1994). The site-specific recombination system regulating expression of the type 1 fimbrial subunit gene of *Escherichia coli* is sensitive to changes in DNA supercoiling. *Mol Microbiol* 14, 975-988.

Drlica, K., and Rouviere-Yaniv, J. (1987). Histone-like proteins of bacteria. *Microbiol Rev* 51, 301-319.

Elliott, S.J., Sperandio, V., Giron, J.A., Shin, S., Mellies, J.L., Wainwright, L., Hutcheson, S.W., McDaniel, T.K., and Kaper, J.B. (2000). The locus of enterocyte effacement (LEE)-encoded regulator controls expression of both LEE- and non-LEE-encoded virulence factors in enteropathogenic and enterohemorrhagic *Escherichia coli*. *Infect Immun* 68, 6115-6126.

Ellison, D.W., and Miller, V.L. (2006). H-NS represses *inv* transcription in *Yersinia enterocolitica* through competition with RovA and interaction with YmoA. *J Bacteriol* 188, 5101-5112.

Ellison, D.W., Young, B., Nelson, K., and Miller, V.L. (2003). YmoA negatively regulates expression of invasins from *Yersinia enterocolitica*. *J Bacteriol* 185, 7153-7159.

Engelhorn, M., Boccard, F., Murtin, C., Prentki, P., and Geiselman, J. (1995). In vivo interaction of the *Escherichia coli* integration host factor with its specific binding sites. *Nucleic Acids Res* 23, 2959-2965.

Falconi, M., Brandi, A., La Teana, A., Gualerzi, C.O., and Pon, C.L. (1996). Antagonistic involvement of FIS and H-NS proteins in the transcriptional control of *hns* expression. *Mol Microbiol* 19, 965-975.

Free, A., and Dorman, C.J. (1995). Coupling of *Escherichia coli* *hns* mRNA levels to DNA synthesis by autoregulation: implications for growth phase control. *Mol Microbiol* 18, 101-113.

Frenkiel-Krispin, D., Ben-Avraham, I., Englander, J., Shimoni, E., Wolf, S.G., and Minsky, A. (2004). Nucleoid restructuring in stationary-state bacteria. *Mol Microbiol* 51, 395-405.

Grainger, D.C., Goldberg, M.D., Lee, D.J., and Busby, S.J. (2008). Selective repression by Fis and H-NS at the *Escherichia coli* *dps* promoter. *Mol Microbiol* 68, 1366-1377.

Grainger, D.C., Hurd, D., Goldberg, M.D., and Busby, S.J. (2006). Association of nucleoid proteins with coding and non-coding segments of the *Escherichia coli* genome. *Nucleic Acids Res* 34, 4642-4652.

Grainger, D.C., Overton, T.W., Reppas, N., Wade, J.T., Tamai, E., Hobman, J.L., Constantinidou, C., Struhl, K., Church, G., and Busby, S.J. (2004). Genomic studies with

*Escherichia coli* MelR protein: applications of chromatin immunoprecipitation and microarrays. *J Bacteriol* *186*, 6938-6943.,

Grant, R.A., Filman, D.J., Finkel, S.E., Kolter, R., and Hogle, J.M. (1998). The crystal structure of Dps, a ferritin homolog that binds and protects DNA. *Nat Struct Biol* *5*, 294-303.

Hardy, C.D., and Cozzarelli, N.R. (2005). A genetic selection for supercoiling mutants of *Escherichia coli* reveals proteins implicated in chromosome structure. *Mol Microbiol* *57*, 1636-1652.

Hommais, F., Krin, E., Laurent-Winter, C., Soutourina, O., Malpertuy, A., Le Caer, J.P., Danchin, A., and Bertin, P. (2001). Large-scale monitoring of pleiotropic regulation of gene expression by the prokaryotic nucleoid-associated protein, H-NS. *Mol Microbiol* *40*, 20-36.

Ito, K., Oshima, T., Mizuno, T., and Nakamura, Y. (1994). Regulation of lysyl-tRNA synthetase expression by histone-like protein H-NS of *Escherichia coli*. *J Bacteriol* *176*, 7383-7386.

Johansson, J., Balsalobre, C., Wang, S.Y., Urbonaviciene, J., Jin, D.J., Sonden, B., and Uhlin, B.E. (2000). Nucleoid proteins stimulate stringently controlled bacterial promoters: a link between the cAMP-CRP and the (p)ppGpp regulons in *Escherichia coli*. *Cell* *102*, 475-485.

Johansson, J., Dagberg, B., Richet, E., and Uhlin, B.E. (1998). H-NS and StpA proteins stimulate expression of the maltose regulon in *Escherichia coli*. *J Bacteriol* *180*, 6117-6125.

Johansson, J., Eriksson, S., Sonden, B., Wai, S.N., and Uhlin, B.E. (2001). Heteromeric interactions among nucleoid-associated bacterial proteins: localization of StpA-stabilizing regions in H-NS of *Escherichia coli*. *J Bacteriol* *183*, 2343-2347.

Johansson, J., and Uhlin, B.E. (1999). Differential protease-mediated turnover of H-NS and StpA revealed by a mutation altering protein stability and stationary-phase survival of *Escherichia coli*. *Proc Natl Acad Sci USA* *96*, 10776-10781.

Kaidow, A., Wachi, M., Nakamura, J., Magae, J., and Nagai, K. (1995). Anucleate cell production by *Escherichia coli* delta *hns* mutant lacking a histone-like protein, H-NS. *J Bacteriol* *177*, 3589-3592.

Katou, Y., Kaneshiro, K., Aburatani, H., and Shirahige, K. (2006). Genomic approach for the understanding of dynamic aspect of chromosome behavior. *Methods Enzymol* *409*, 389-410.

La Teana, A., Brandi, A., Falconi, M., Spurio, R., Pon, C.L., and Gualerzi, C.O. (1991). Identification of a cold shock transcriptional enhancer of the *Escherichia coli* gene encoding nucleoid protein H-NS. *Proc Natl Acad Sci USA* *88*, 10907-10911.

Lang, B., Blot, N., Bouffartigues, E., Buckle, M., Geertz, M., Gualerzi, C.O., Mavathur, R., Muskhelishvili, G., Pon, C.L., Rimsky, S., Stella, S., Babu, M.M., and Travers, A. (2007).

High-affinity DNA binding sites for H-NS provide a molecular basis for selective silencing within proteobacterial genomes. *Nucleic Acids Res* 35, 6330-6337.

Luijsterburg, M.S., Noom, M.C., Wuite, G.J., and Dame, R.T. (2006). The architectural role of nucleoid-associated proteins in the organization of bacterial chromatin: a molecular perspective. *J Struct Biol* 156, 262-272.

Madrid, C., Balsalobre, C., Garcia, J., and Juarez, A. (2007a). The novel Hha/YmoA family of nucleoid-associated proteins: use of structural mimicry to modulate the activity of the H-NS family of proteins. *Mol Microbiol* 63, 7-14.

Madrid, C., Garcia, J., Pons, M., and Juarez, A. (2007b). Molecular evolution of the H-NS protein: interaction with Hha-like proteins is restricted to *Enterobacteriaceae*. *J Bacteriol* 189, 265-268.

Martinez, A., and Kolter, R. (1997). Protection of DNA during oxidative stress by the nonspecific DNA-binding protein Dps. *J Bacteriol* 179, 5188-5194.

Megraw, T.L., and Chae, C.B. (1993). Functional complementarity between the HMG1-like yeast mitochondrial histone HM and the bacterial histone-like protein HU. *J Biol Chem* 268, 12758-12763.

Mellies, J.L., Barron, A.M., and Carmona, A.M. (2007). Enteropathogenic and enterohemorrhagic *Escherichia coli* virulence gene regulation. *Infect Immun* 75, 4199-4210.

Mellies, J.L., Larabee, F.J., Zarr, M.A., Horback, K.L., Lorenzen, E., and Mavor, D. (2008). Ler interdomain linker is essential for anti-silencing activity in enteropathogenic *Escherichia coli*. *Microbiology* 154, 3624-3638.

Menzel, R., and Gellert, M. (1983). Regulation of the genes for *E. coli* DNA gyrase: homeostatic control of DNA supercoiling. *Cell* 34, 105-113.

Miyoshi, D., and Sugimoto, N. (2008). Molecular crowding effects on structure and stability of DNA. *Biochimie* 90, 1040-1051.

Muller, C.M., Dobrindt, U., Nagy, G., Emody, L., Uhlin, B.E., and Hacker, J. (2006). Role of histone-like proteins H-NS and StpA in expression of virulence determinants of uropathogenic *Escherichia coli*. *J Bacteriol* 188, 5428-5438.

Nair, S., and Finkel, S.E. (2004). Dps protects cells against multiple stresses during stationary phase. *J Bacteriol* 186, 4192-4198.

Nash, H.A., and Robertson, C.A. (1981). Purification and properties of the *Escherichia coli* protein factor required for lambda integrative recombination. *J Biol Chem* 256, 9246-9253.

Navarre, W.W., McClelland, M., Libby, S.J., and Fang, F.C. (2007). Silencing of xenogeneic DNA by H-NS-facilitation of lateral gene transfer in bacteria by a defense system that recognizes foreign DNA. *Genes Dev* 21, 1456-1471.

Navarre, W.W., Porwollik, S., Wang, Y., McClelland, M., Rosen, H., Libby, S.J., and Fang, F.C. (2006). Selective silencing of foreign DNA with low GC content by the H-NS protein in *Salmonella*. *Science* 313, 236-238.

Nieto, J.M., Madrid, C., Miquelay, E., Parra, J.L., Rodriguez, S., and Juarez, A. (2002). Evidence for direct protein-protein interaction between members of the enterobacterial Hha/YmoA and H-NS families of proteins. *J Bacteriol* 184, 629-635.

Noom, M.C., Navarre, W.W., Oshima, T., Wuite, G.J., and Dame, R.T. (2007). H-NS promotes looped domain formation in the bacterial chromosome. *Curr Biol* 17, R913-914.

Oshima, T., Ishikawa, S., Kurokawa, K., Aiba, H., and Ogasawara, N. (2006). *Escherichia coli* histone-like protein H-NS preferentially binds to horizontally acquired DNA in association with RNA polymerase. *DNA Res* 13, 141-153.

Owen-Hughes, T.A., Pavitt, G.D., Santos, D.S., Sidebotham, J.M., Hulton, C.S., Hinton, J.C., and Higgins, C.F. (1992). The chromatin-associated protein H-NS interacts with curved DNA to influence DNA topology and gene expression. *Cell* 71, 255-265.

Pan, C.Q., Finkel, S.E., Cramton, S.E., Feng, J.A., Sigman, D.S., and Johnson, R.C. (1996). Variable structures of Fis-DNA complexes determined by flanking DNA-protein contacts. *J Mol Biol* 264, 675-695.

Paytubi, S., Madrid, C., Forns, N., Nieto, J.M., Balsalobre, C., Uhlin, B.E., and Juarez, A. (2004). YdgT, the Hha paralogue in *Escherichia coli*, forms heteromeric complexes with H-NS and StpA. *Mol Microbiol* 54, 251-263.

Postow, L., Hardy, C.D., Arsuaga, J., and Cozzarelli, N.R. (2004). Topological domain structure of the *Escherichia coli* chromosome. *Genes Dev* 18, 1766-1779.

Prosseda, G., Falconi, M., Giangrossi, M., Gualerzi, C.O., Micheli, G., and Colonna, B. (2004). The *virF* promoter in *Shigella*: more than just a curved DNA stretch. *Mol Microbiol* 51, 523-537.

Renzoni, D., Esposito, D., Pfuhl, M., Hinton, J.C., Higgins, C.F., Driscoll, P.C., and Ladbury, J.E. (2001). Structural characterization of the N-terminal oligomerization domain of the bacterial chromatin-structuring protein, H-NS. *J Mol Biol* 306, 1127-1137.

Rice, P.A., Yang, S., Mizuuchi, K., and Nash, H.A. (1996). Crystal structure of an IHF-DNA complex: a protein-induced DNA U-turn. *Cell* 87, 1295-1306.

Robinow, C., and Kellenberger, E. (1994). The bacterial nucleoid revisited. *Microbiol Rev* 58, 211-232.



Rui, S., and Tse-Dinh, Y.C. (2003). Topoisomerase function during bacterial responses to environmental challenge. *Front Biosci* 8, d256-263.

Schmidt, M., Zheng, P., and Delihias, N. (1995). Secondary structures of *Escherichia coli* antisense *micF* RNA, the 5'-end of the target *ompF* mRNA, and the RNA/RNA duplex. *Biochemistry* 34, 3621-3631.

Schneider, R., Lurz, R., Luder, G., Tolksdorf, C., Travers, A., and Muskhelishvili, G. (2001). An architectural role of the *Escherichia coli* chromatin protein FIS in organising DNA. *Nucleic Acids Res* 29, 5107-5114.

Schnell, S., and Turner, T.E. (2004). Reaction kinetics in intracellular environments with macromolecular crowding: simulations and rate laws. *Prog Biophys Mol Biol* 85, 235-260.

Shi, X., and Bennett, G.N. (1994). Plasmids bearing *hfq* and the *hns*-like gene *stpA* complement *hns* mutants in modulating arginine decarboxylase gene expression in *Escherichia coli*. *J Bacteriol* 176, 6769-6775.

Shin, M., Song, M., Rhee, J.H., Hong, Y., Kim, Y.J., Seok, Y.J., Ha, K.S., Jung, S.H., and Choy, H.E. (2005). DNA looping-mediated repression by histone-like protein H-NS: specific requirement of Esigma70 as a cofactor for looping. *Genes Dev* 19, 2388-2398.

Sledjeski, D., and Gottesman, S. (1995). A small RNA acts as an antisilencer of the H-NS-silenced *rcaA* gene of *Escherichia coli*. *Proc Natl Acad Sci USA* 92, 2003-2007.

Sonden, B., and Uhlin, B.E. (1996). Coordinated and differential expression of histone-like proteins in *Escherichia coli*: regulation and function of the H-NS analog StpA. *EMBO J* 15, 4970-4980.

Sonnenfield, J.M., Burns, C.M., Higgins, C.F., and Hinton, J.C. (2001). The nucleoid-associated protein StpA binds curved DNA, has a greater DNA-binding affinity than H-NS and is present in significant levels in *hns* mutants. *Biochimie* 83, 243-249.

Soutourina, O., Kolb, A., Krin, E., Laurent-Winter, C., Rimsky, S., Danchin, A., and Bertin, P. (1999). Multiple control of flagellum biosynthesis in *Escherichia coli*: role of H-NS protein and the cyclic AMP-catabolite activator protein complex in transcription of the *flhDC* master operon. *J Bacteriol* 181, 7500-7508.

Spassky, A., Rimsky, S., Garreau, H., and Buc, H. (1984). H1a, an *E. coli* DNA-binding protein which accumulates in stationary phase, strongly compacts DNA in vitro. *Nucleic Acids Res* 12, 5321-5340.

Spurio, R., Durrenberger, M., Falconi, M., La Teana, A., Pon, C.L., and Gualerzi, C.O. (1992). Lethal overproduction of the *Escherichia coli* nucleoid protein H-NS: ultramicroscopic and molecular autopsy. *Mol Gen Genet* 231, 201-211.

Stavans, J., and Oppenheim, A. (2006). DNA-protein interactions and bacterial chromosome architecture. *Phys Biol* 3, R1-10.

- Stella, S., Spurio, R., Falconi, M., Pon, C.L., and Gualerzi, C.(2005). Nature and mechanism of the in vivo oligomerization of nucleoid protein H-NS. *EMBO J* 24, 2896-2905.
- Stoebel, D.M., Free, A., and Dorman, C.J. (2008). Anti-silencing: overcoming H-NS-mediated repression of transcription in Gram-negative enteric bacteria. *Microbiology* 154, 2533-2545.
- Suzuki, T., Ueguchi, C., and Mizuno, T. (1996). H-NS regulates OmpF expression through *micF* antisense RNA in *Escherichia coli*. *J Bacteriol* 178, 3650-3653.
- Tendeng, C., and Bertin, P.N. (2003). H-NS in Gram-negative bacteria: a family of multifaceted proteins. *Trends Microbiol* 11, 511-518.
- Thanbichler, M., and Shapiro, L. (2008). Getting organized-how bacterial cells move proteins and DNA. *Nat Rev Microbiol* 6, 28-40.
- Tolstorukov, M.Y., Virnik, K.M., Adhya, S., and Zhurkin, V.B. (2005). A-tract clusters may facilitate DNA packaging in bacterial nucleoid. *Nucleic Acids Res* 33, 3907-3918.
- Torres, A.G., Lopez-Sanchez, G.N., Milflores-Flores, L., Patel, S.D., Rojas-Lopez, M., Martinez de la Pena, C.F., Arenas-Hernandez, M.M., and Martinez-Laguna, Y. (2007). Ler and H-NS, regulators controlling expression of the long polar fimbriae of *Escherichia coli* O157:H7. *J Bacteriol* 189, 5916-5928.
- Travers, A., and Muskhelishvili, G. (2005). Bacterial chromatin. *Curr Opin Genet Dev* 15, 507-514.

Travers, A., Schneider, R., and Muskhelishvili, G. (2001). DNA supercoiling and transcription in *Escherichia coli*: The FIS connection. *Biochimie* 83, 213-217.

Tupper, A.E., Owen-Hughes, T.A., Ussery, D.W., Santos, D.S., Ferguson, D.J., Sidebotham, J.M., Hinton, J.C., and Higgins, C.F. (1994). The chromatin-associated protein H-NS alters DNA topology in vitro. *EMBO J* 13, 258-268.

Ueguchi, C., Kakeda, M., and Mizuno, T. (1993). Autoregulatory expression of the *Escherichia coli hns* gene encoding a nucleoid protein: H-NS functions as a repressor of its own transcription. *Mol Gen Genet* 236, 171-178.

Umanski, T., Rosenshine, I., and Friedberg, D. (2002). Thermoregulated expression of virulence genes in enteropathogenic *Escherichia coli*. *Microbiology* 148, 2735-2744.

Uzzau, S., Figueroa-Bossi, N., Rubino, S., and Bossi, L. (2001). Epitope tagging of chromosomal genes in *Salmonella*. *Proc Natl Acad Sci USA* 98, 15264-15269.

Vallet-Gely, I., Donovan, K.E., Fang, R., Joung, J.K., and Dove, S.L. (2005). Repression of phase-variable *cup* gene expression by H-NS-like proteins in *Pseudomonas aeruginosa*. *Proc Natl Acad Sci USA* 102, 11082-11087.

Vallet, I., Diggle, S.P., Stacey, R.E., Camara, M., Ventre, I., Lory, S., Lazdunski, A., Williams, P., and Filloux, A. (2004). Biofilm formation in *Pseudomonas aeruginosa*:

fimbrial *cup* gene clusters are controlled by the transcriptional regulator MvaT. *J Bacteriol* *186*, 2880-2890.

van Noort, J., Verbrugge, S., Goosen, N., Dekker, C., and Dame, R.T. (2004). Dual architectural roles of HU: formation of flexible hinges and rigid filaments. *Proc Natl Acad Sci USA* *101*, 6969-6974.

Varshavsky, A.J., Nedospasov, S.A., Bakayev, V.V., Bakayeva, T.G., and Georgiev, G.P. (1977). Histone-like proteins in the purified *Escherichia coli* deoxyribonucleoprotein. *Nucleic Acids Res* *4*, 2725-2745.

Wang, J.C. (1996). DNA topoisomerases. *Annu Rev Biochem* *65*, 635-692.

Westfall, L.W., Carty, N.L., Layland, N., Kuan, P., Colmer-Hamood, J.A., and Hamood, A.N. (2006). *mvaT* mutation modifies the expression of the *Pseudomonas aeruginosa* multidrug efflux operon *mexEF-oprN*. *FEMS Microbiol Lett* *255*, 247-254.

Wolf, S.G., Frenkiel, D., Arad, T., Finkel, S.E., Kolter, R., and Minsky, A. (1999). DNA protection by stress-induced biocrystallization. *Nature* *400*, 83-85.

Wolf, T., Janzen, W., Blum, C., and Schnetz, K. (2006). Differential dependence of StpA on H-NS in autoregulation of *stpA* and in regulation of *bgl*. *J Bacteriol* *188*, 6728-6738.

Worcel, A., and Burgi, E. (1972). On the structure of the folded chromosome of *Escherichia coli*. *J Mol Biol* *71*, 127-147.

Yang, J., Baldi, D.L., Tauschek, M., Strugnell, R.A., and Robins-Browne, R.M. (2007). Transcriptional regulation of the *yghJ-pppA-yghG-gspCDEFGHIJKLM* cluster, encoding the type II secretion pathway in enterotoxigenic *Escherichia coli*. *J Bacteriol* 189, 142-150.

Yang, S.W., and Nash, H.A. (1995). Comparison of protein binding to DNA in vivo and in vitro: defining an effective intracellular target. *EMBO J* 14, 6292-6300.

Zechiedrich, E.L., Khodursky, A.B., Bachellier, S., Schneider, R., Chen, D., Lilley, D.M., and Cozzarelli, N.R. (2000). Roles of topoisomerases in maintaining steady-state DNA supercoiling in *Escherichia coli*. *J Biol Chem* 275, 8103-8113.

Zhang, A., and Belfort, M. (1992). Nucleotide sequence of a newly-identified *Escherichia coli* gene, *stpA*, encoding an H-NS-like protein. *Nucleic Acids Res* 20, 6735.

Zhang, A., Derbyshire, V., Salvo, J.L., and Belfort, M. (1995). *Escherichia coli* protein StpA stimulates self-splicing by promoting RNA assembly in vitro. *RNA* 1, 783-793.

Zhang, A., Rimsky, S., Reaban, M.E., Buc, H., and Belfort, M. (1996). *Escherichia coli* protein analogs StpA and H-NS: regulatory loops, similar and disparate effects on nucleic acid dynamics. *EMBO J* 15, 1340-1349.

Zimmerman, S.B., and Trach, S.O. (1991). Estimation of macromolecule concentrations and excluded volume effects for the cytoplasm of *Escherichia coli*. *J Mol Biol* 222, 599-620.

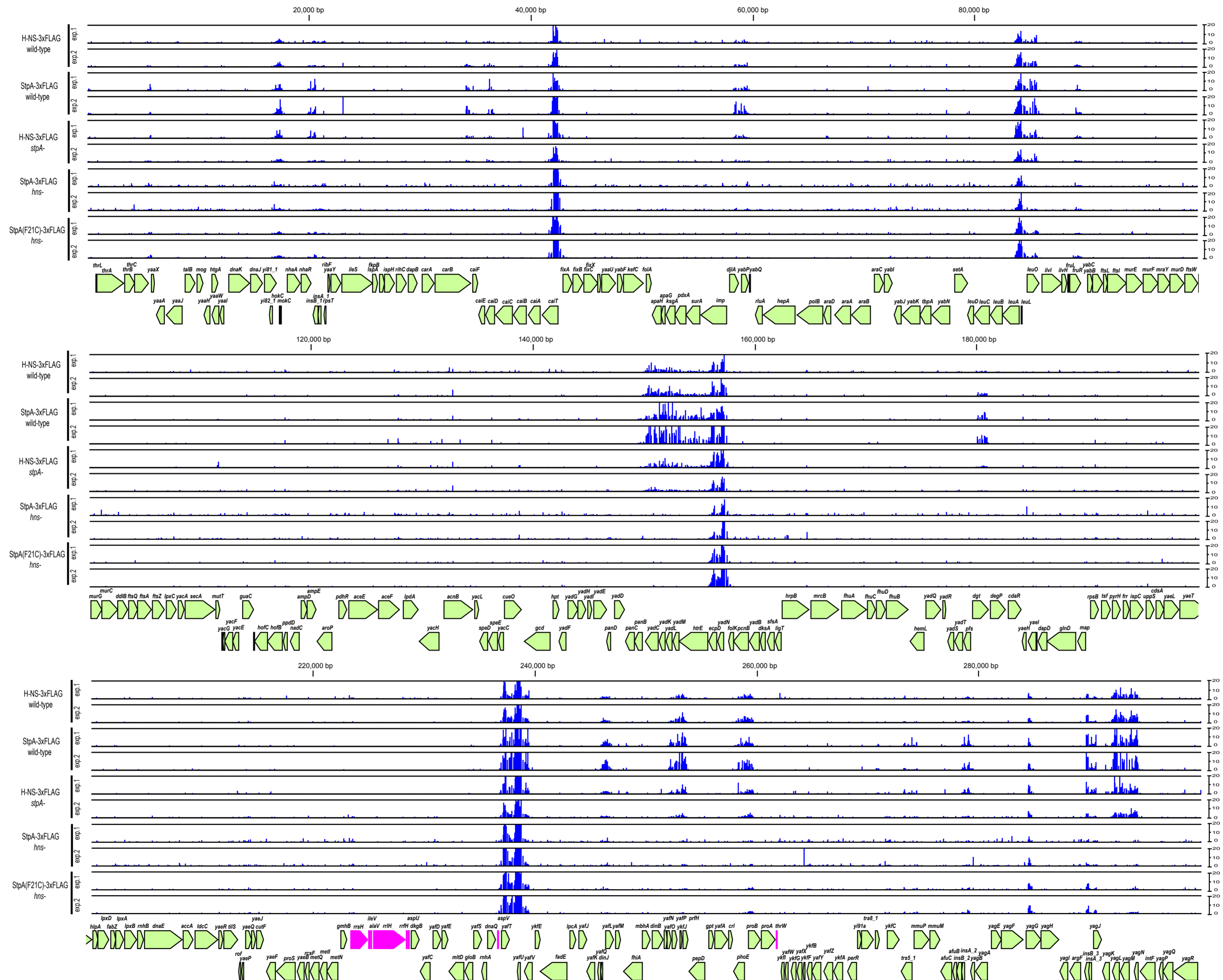


Fig. S1-1





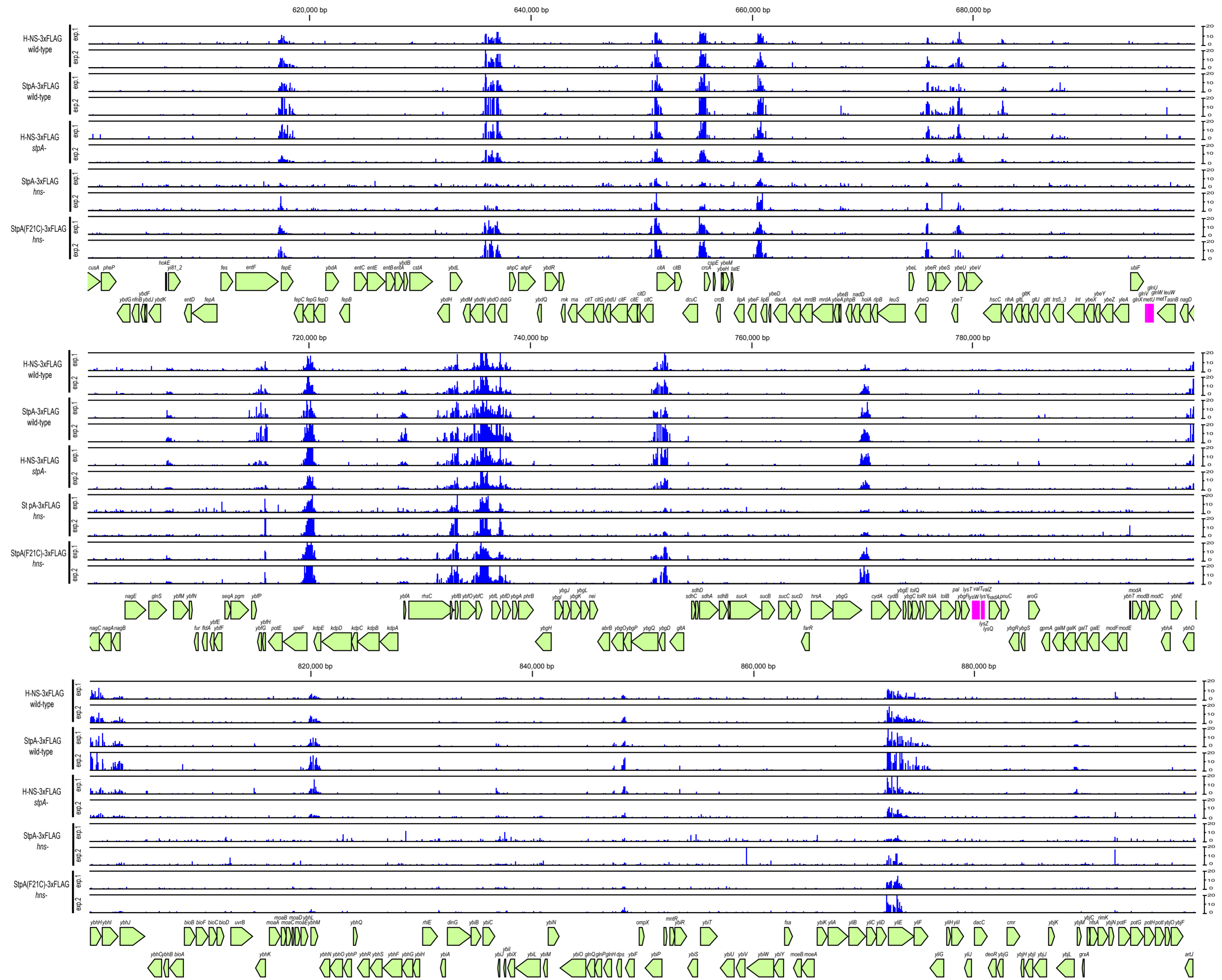


Fig. S1-3

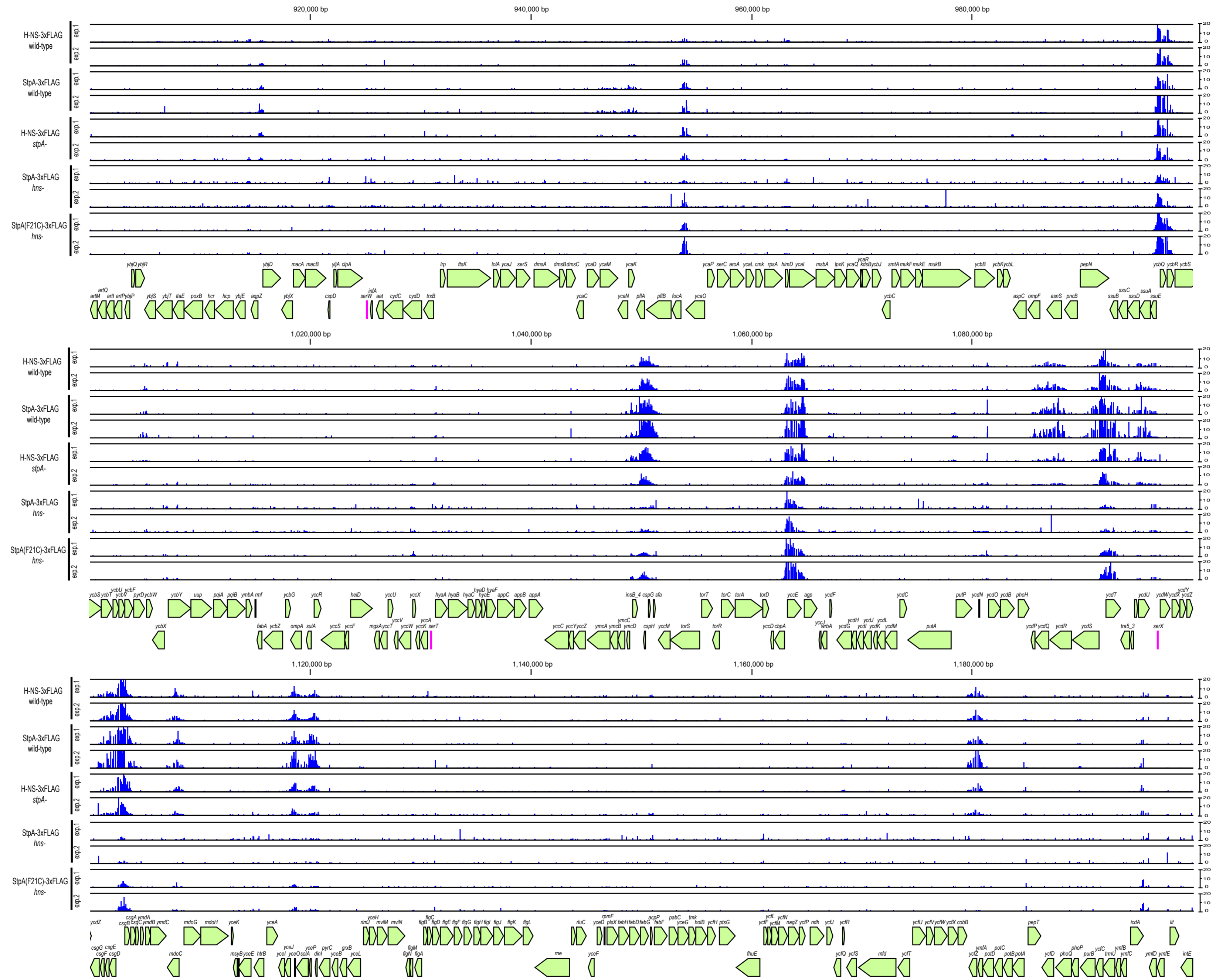


Fig. S1-4



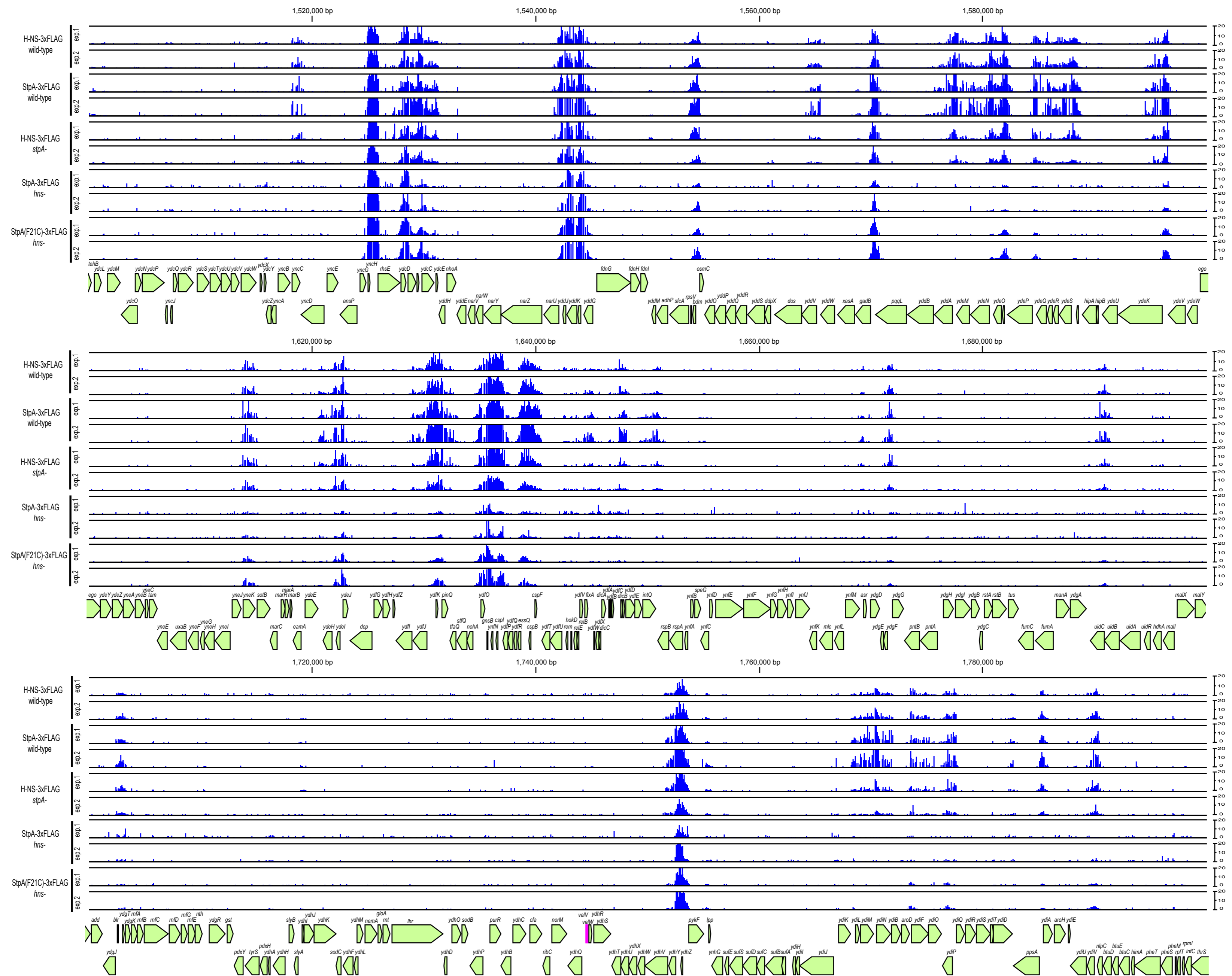


Fig. S1-6

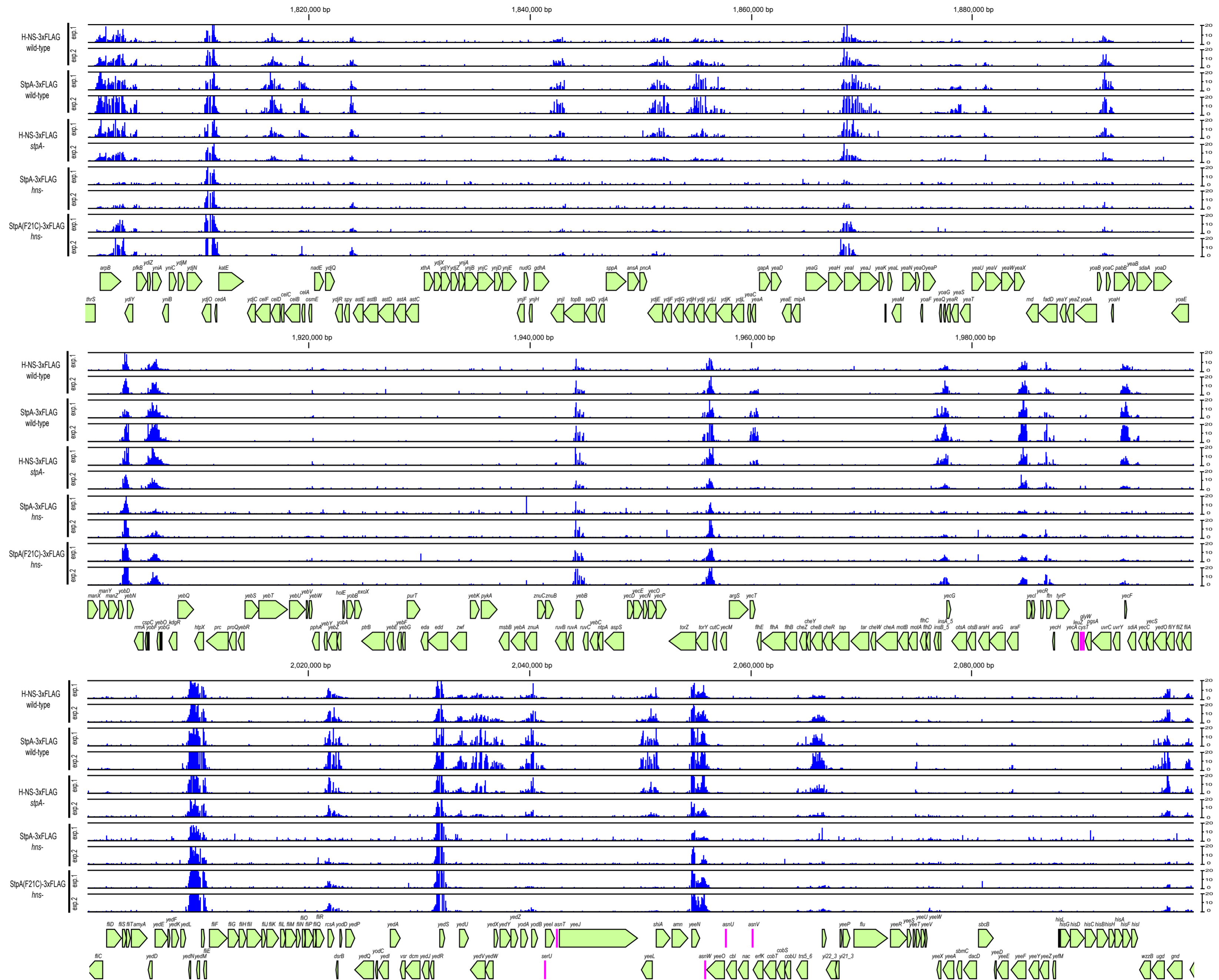


Fig. S1-7

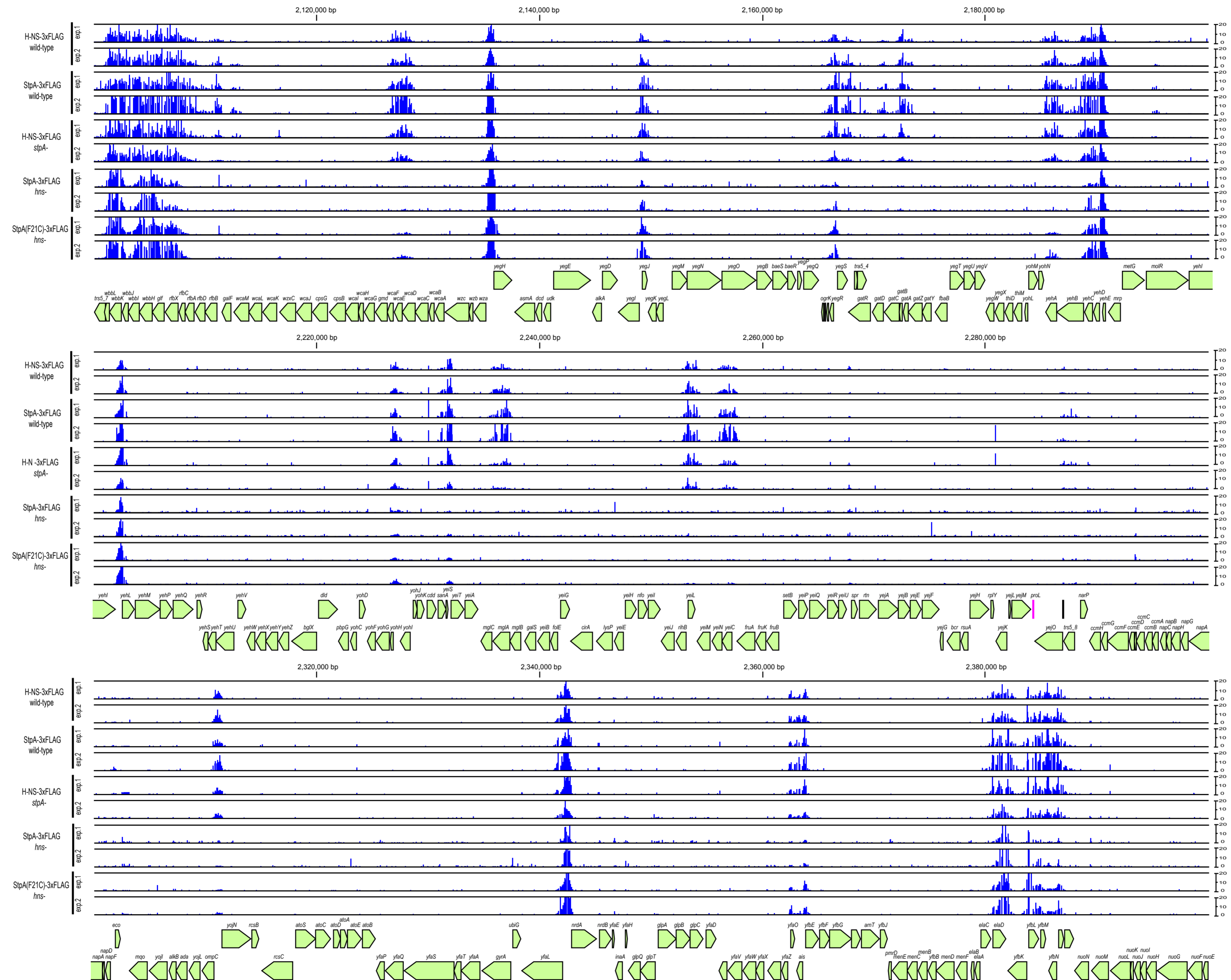


Fig. S1-8

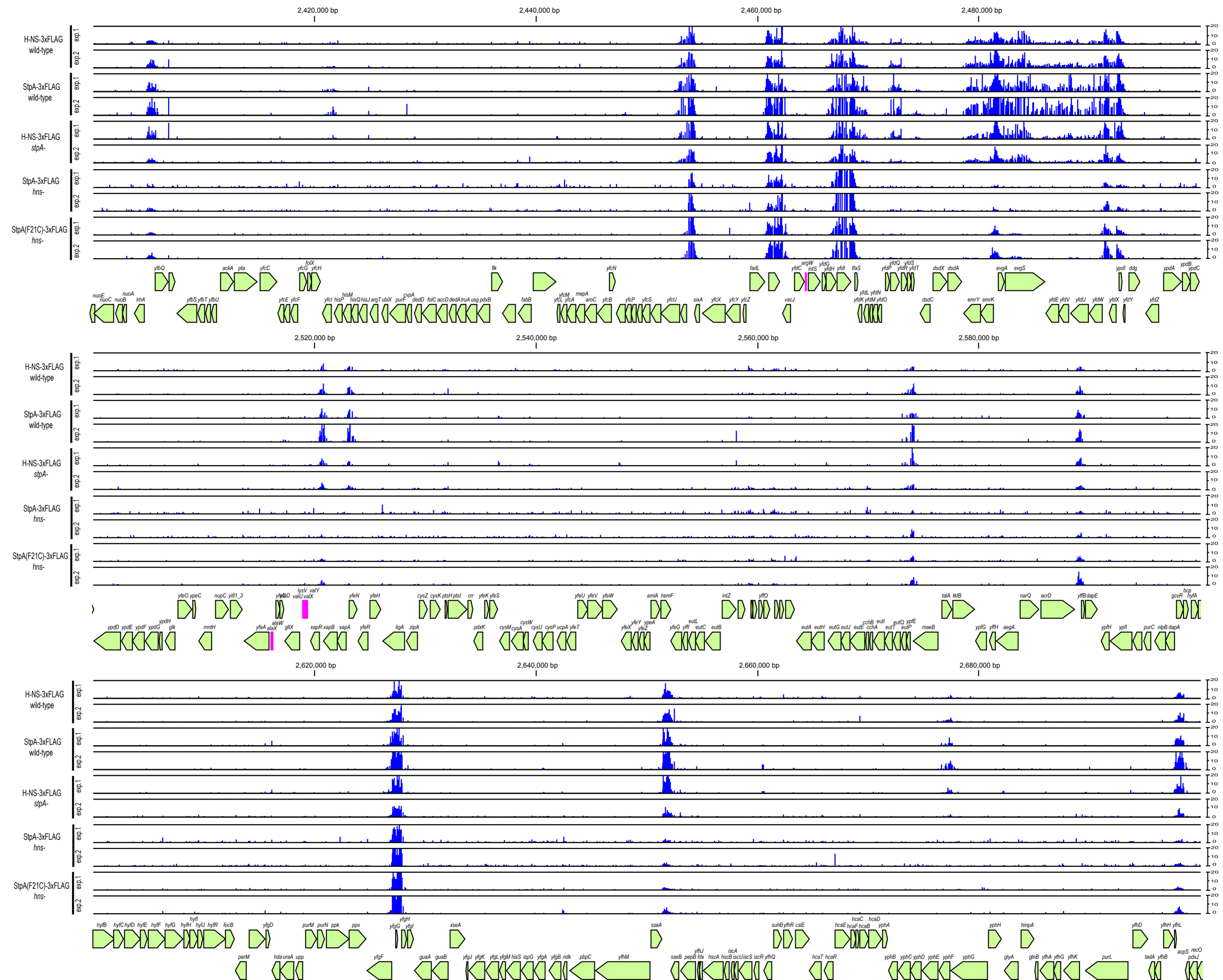


Fig. S1-9  
95

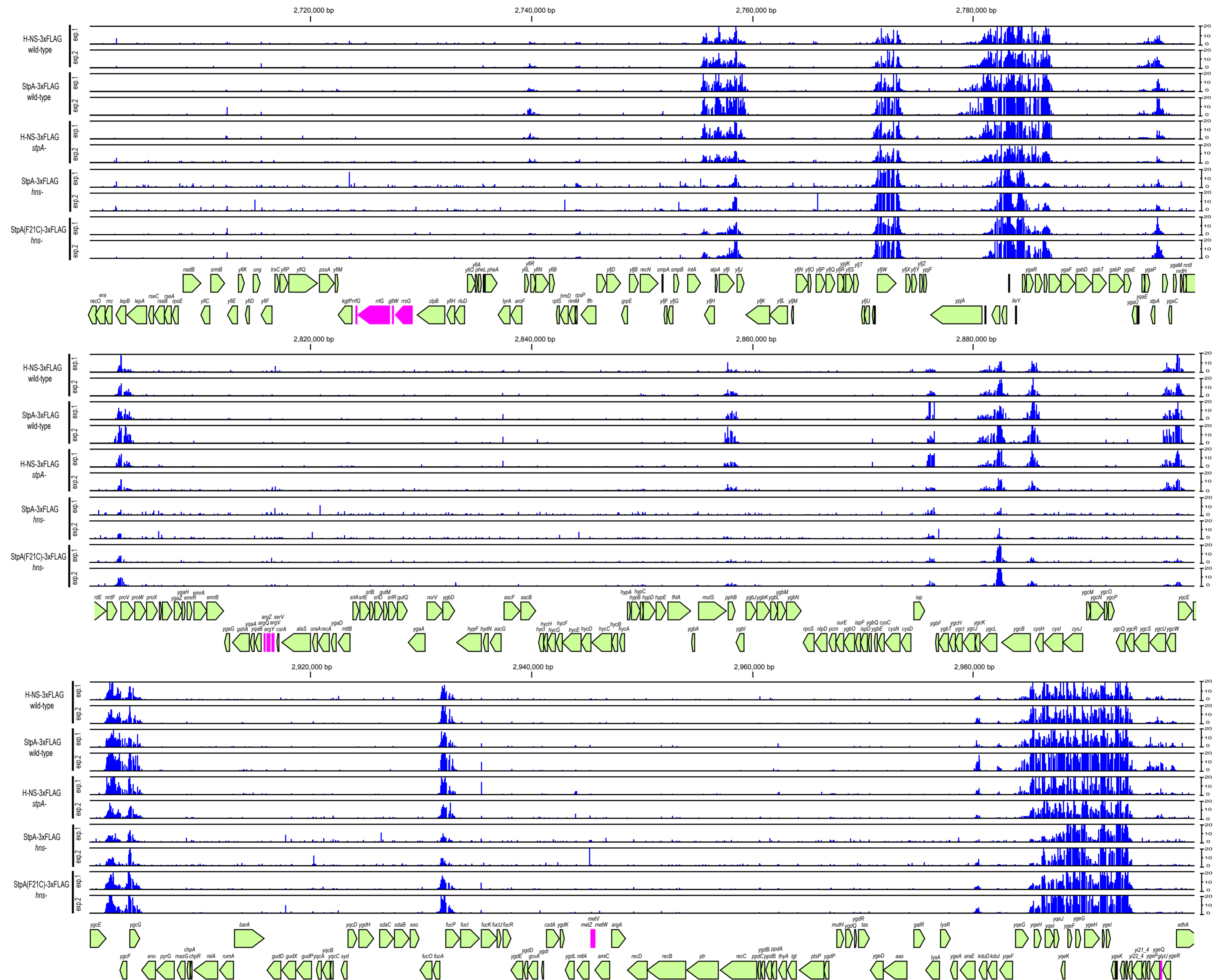


Fig. S1-10





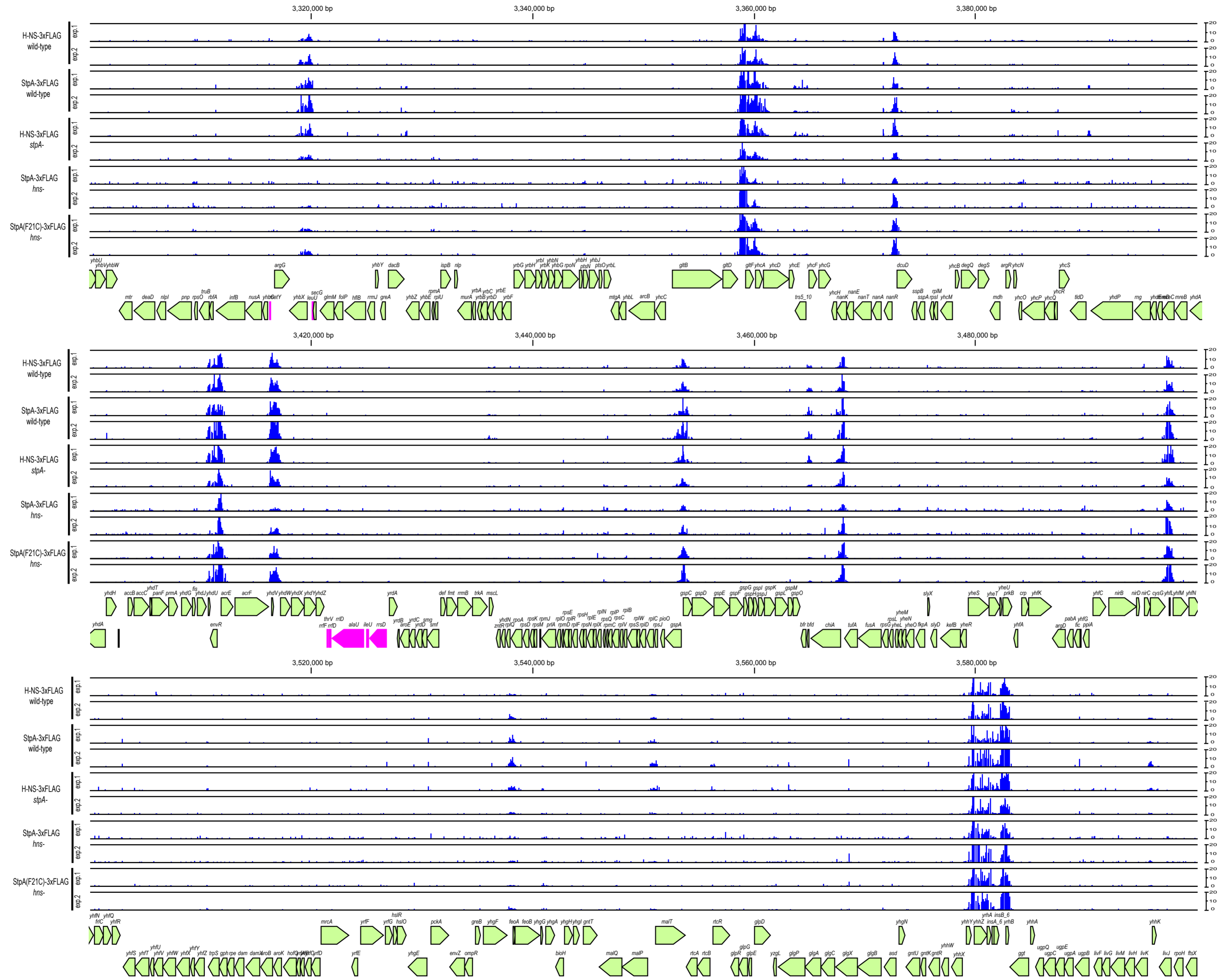


Fig. S1-12

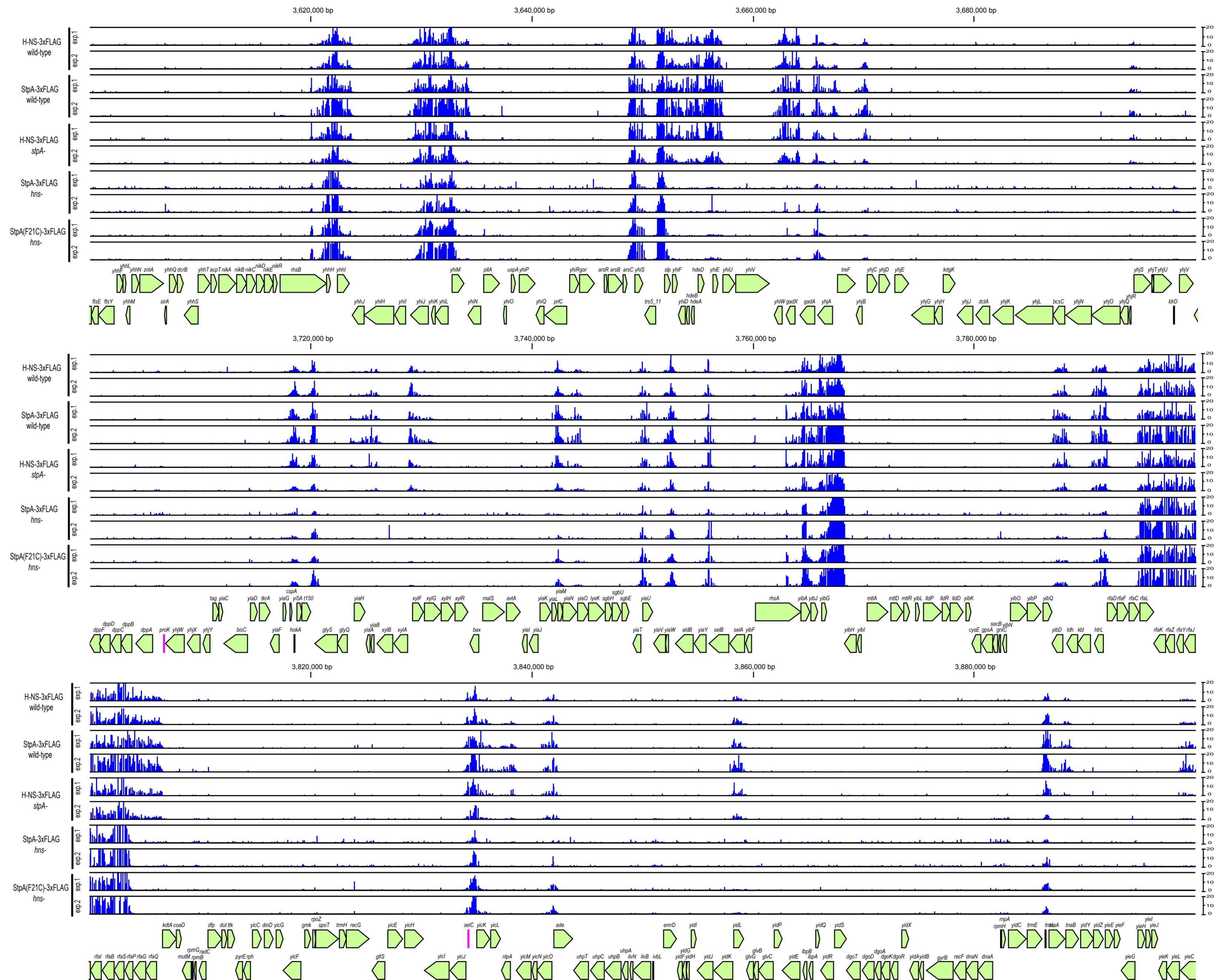


Fig. S1-13

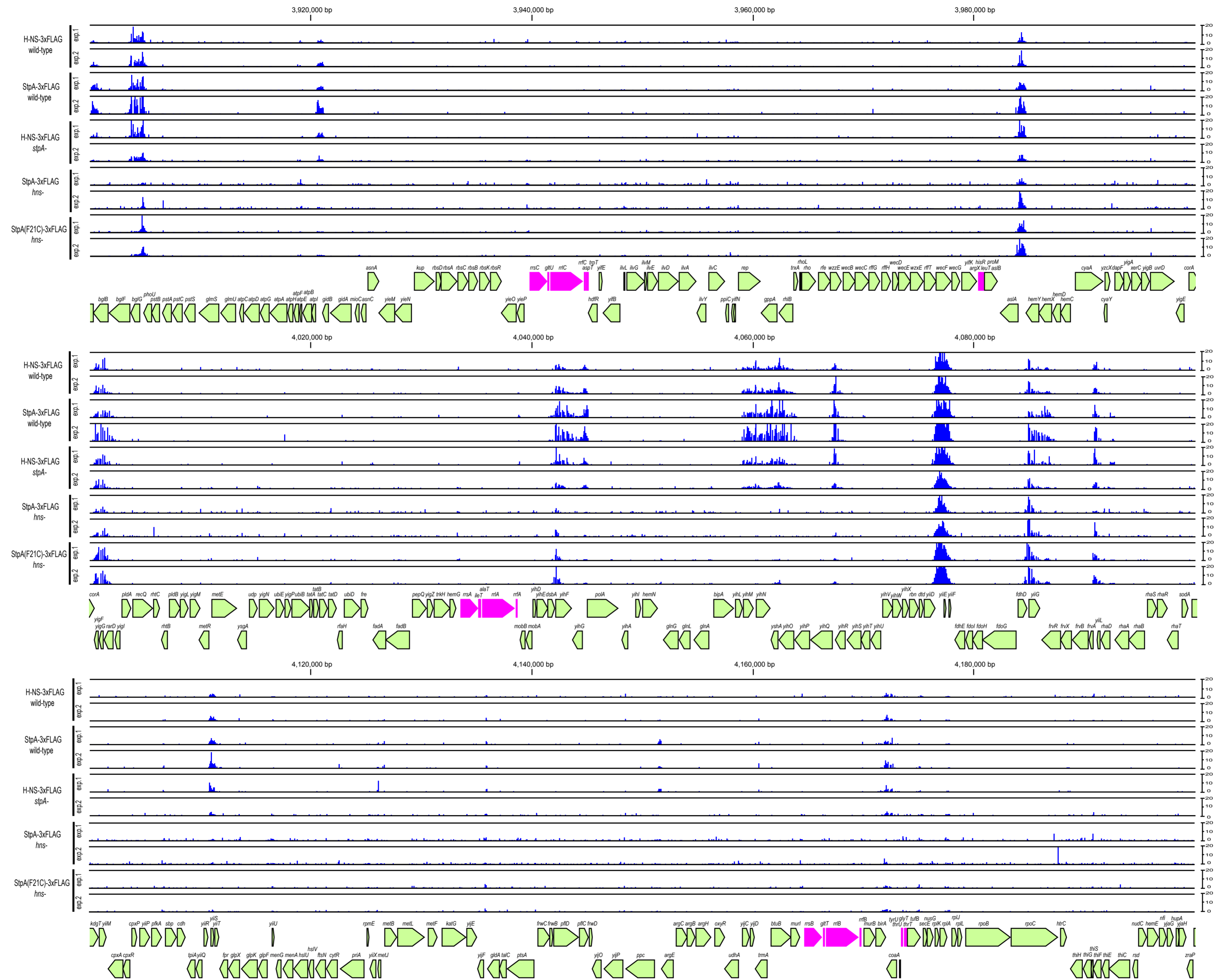


Fig. S1-14

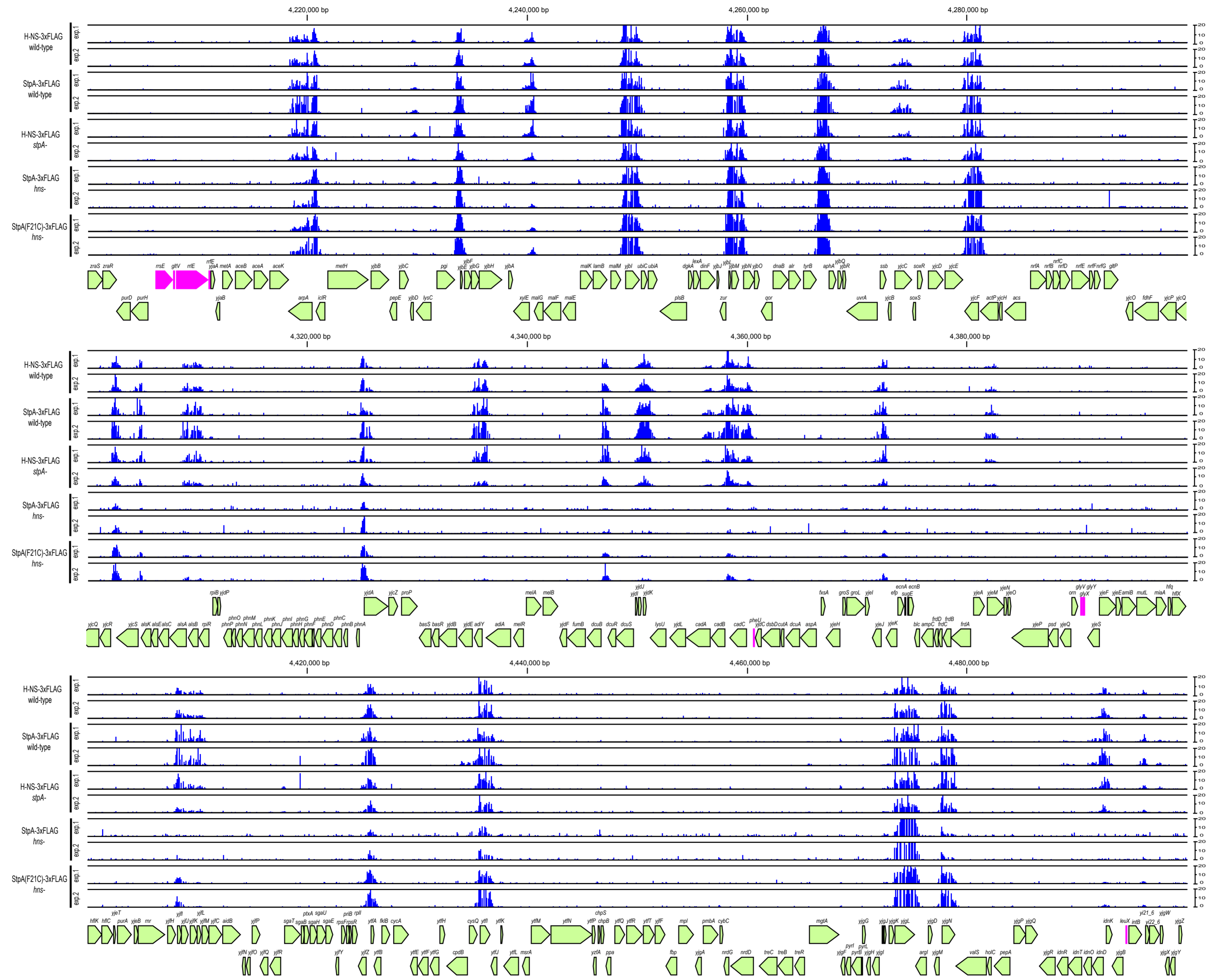


Fig. S1-15

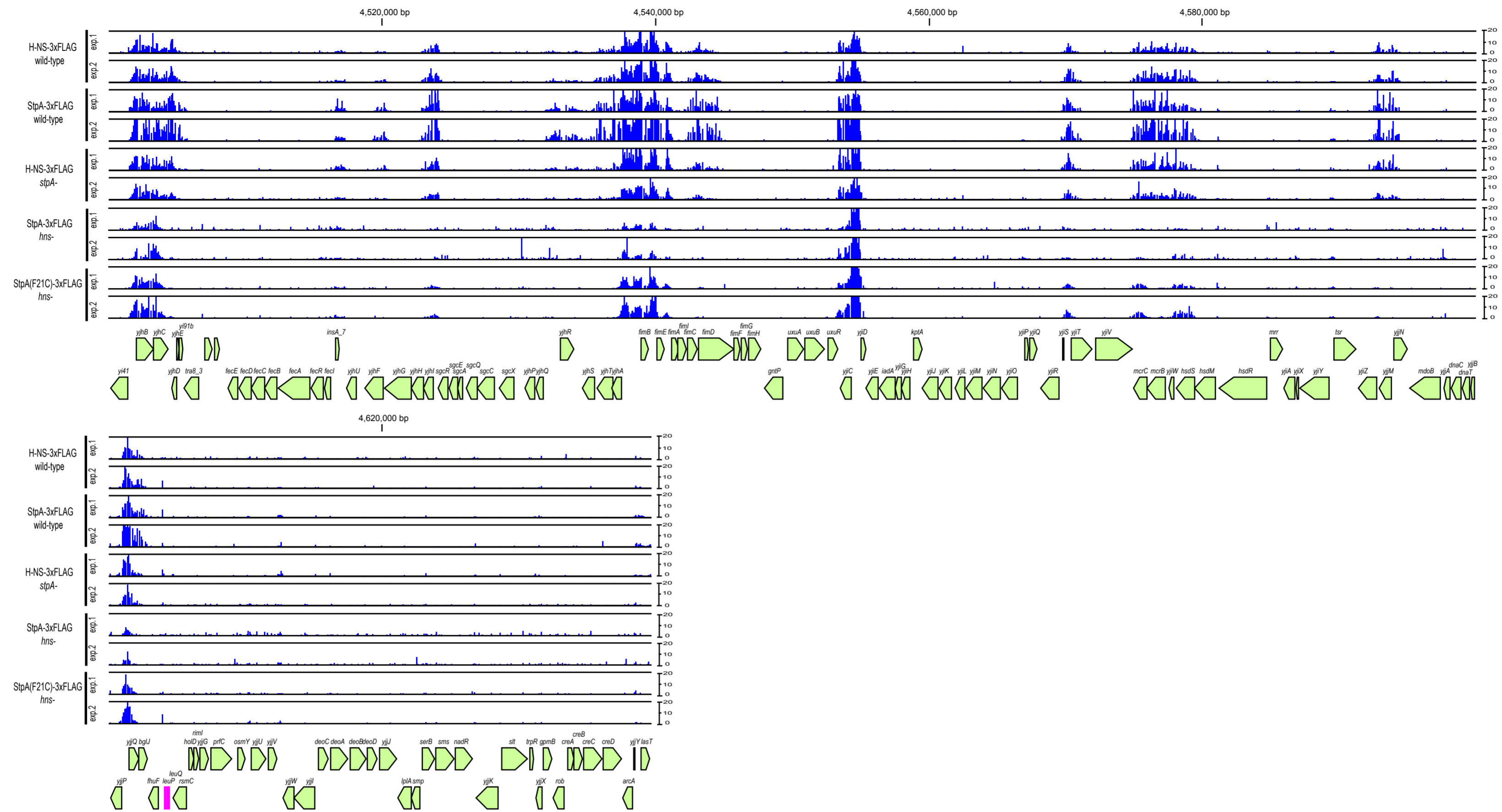


Fig. S1-16









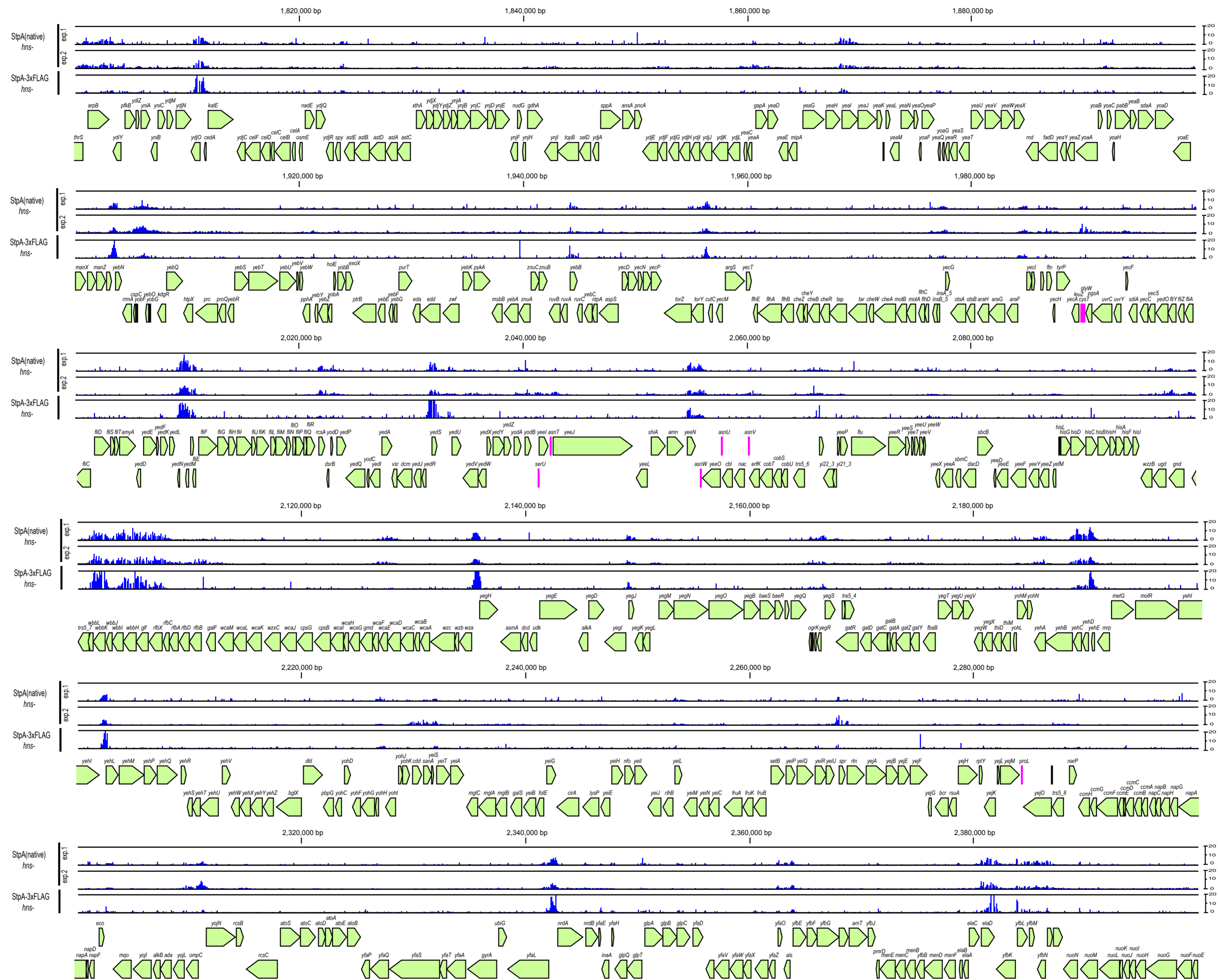


Fig. S2-4

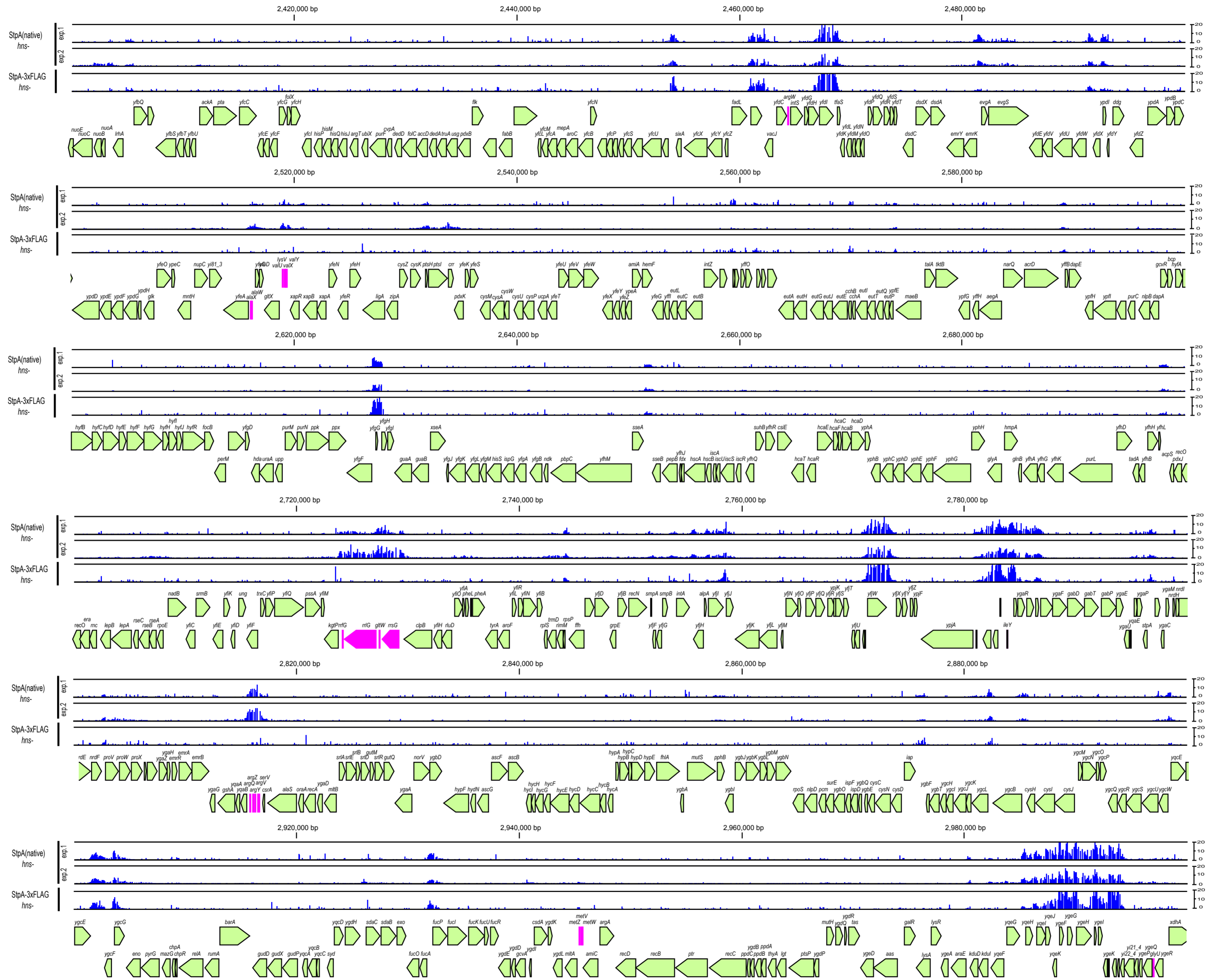


Fig. S2-5





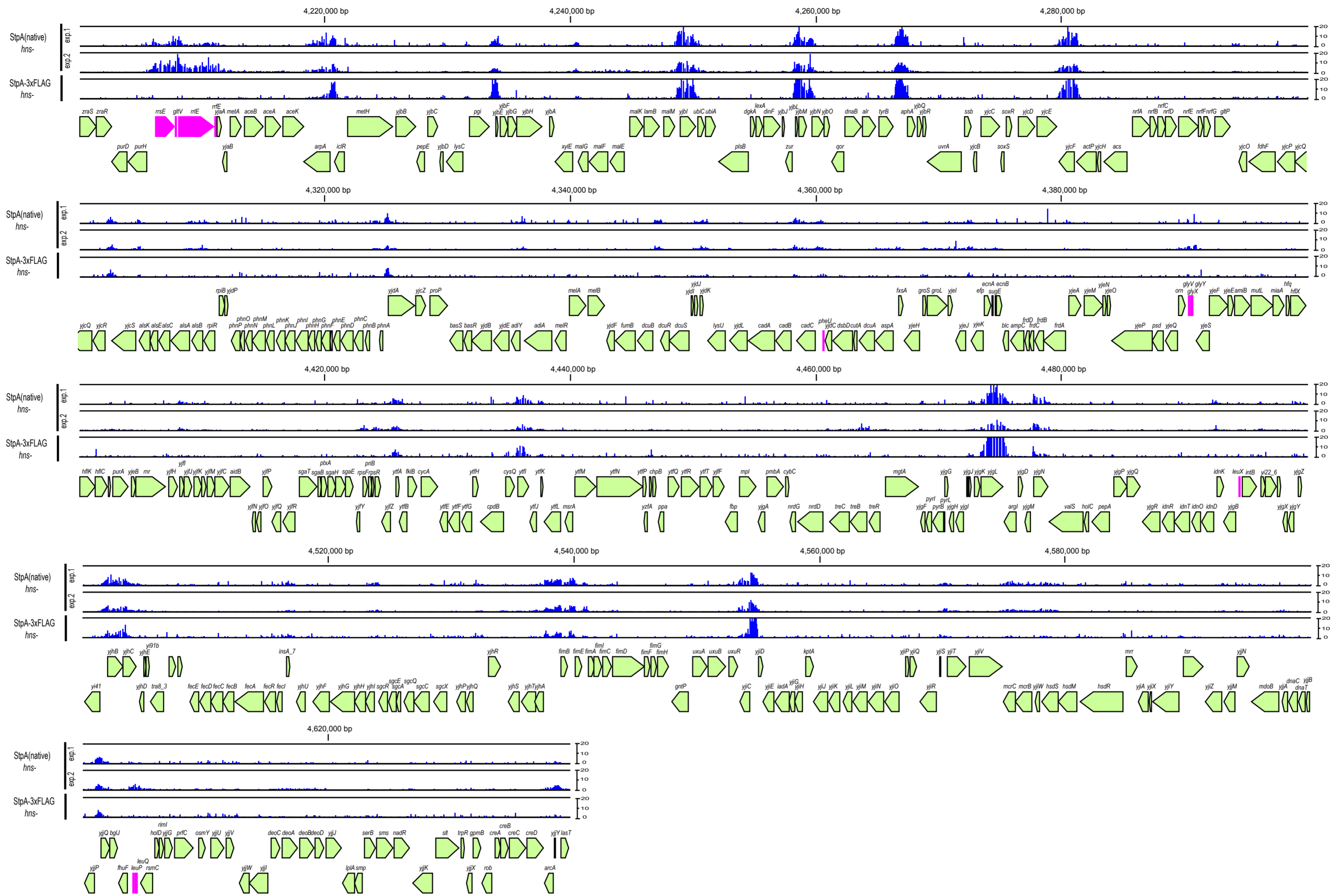


Fig. S2-8  
110

## Supplementary Table. Functional classification of the genes bound by StpA homodimers

Gene	Product	Clusters of Orthologous Groups of Proteins(COGs)
<i>caiT</i>	predicted transporter	Cell wall/membrane biogenesis
<i>fixA</i>	predicted electron transfer flavoprotein subunit, ETFP adenine nucleotide-binding domain	Function unknown
<i>leuA</i>	2-isopropylmalate synthase	Amino acid transport and metabolism
<i>leuL</i>	leu operon leader peptide	Function unknown
<i>leuO</i>	DNA-binding transcriptional activator	Transcription
<i>ecpD</i>	predicted periplasmic pilin chaperone	Cell motility/Intracellular trafficking and secretion
<i>yadN</i>	predicted fimbrial-like adhesin protein	Cell motility/Intracellular trafficking and secretion
<i>folK</i>	2-amino-4-hydroxy-6- hydroxymethylidihydropteridine pyrophosphokinase	Coenzyme transport and metabolism
<i>yaJ</i>	predicted aminopeptidase	Function unknown
<i>yaJ</i>	predicted inner membrane protein	Function unknown
<i>yaJ</i>	predicted C-N hydrolase family amidase, NAD(P)-binding	General function prediction only
<i>ykgM</i>	predicted ribosomal protein	Translation
<i>eaeH</i>	attaching and effacing protein, pathogenesis factor	Function unknown
<i>ykgB</i>	conserved inner membrane protein	Function unknown
<i>ykgI</i>	hypothetical protein	Function unknown
<i>ykgD</i>	predicted DNA-binding transcriptional regulator	Transcription
<i>ykgE</i>	predicted oxidoreductase	Energy production and conversion
<i>yaiP</i>	predicted glucosyltransferase	Cell wall/membrane biogenesis
<i>yaiS</i>	hypothetical protein	Function unknown
<i>tauA</i>	taurine transporter subunit	Inorganic ion transport and metabolism
<i>hemB</i>	porphobilinogen synthase	Coenzyme transport and metabolism
<i>b0370</i>	hypothetical protein	Function unknown
<i>yaiT</i>	hypothetical protein	Function unknown
<i>ybbP</i>	predicted inner membrane protein	Secondary metabolites biosynthesis, transport and catabolism
<i>rhsD</i>	rhsD element protein	Cell wall/membrane biogenesis
<i>ybbC</i>	hypothetical protein	Function unknown
<i>b0499</i>	conserved hypothetical protein, rhs-like	Cell wall/membrane biogenesis
<i>ybbD</i>	hypothetical protein	Function unknown
<i>b0501</i>	predicted DNA-binding transcriptional regulator	Function unknown
<i>b0502</i>	predicted DNA-binding transcriptional regulator	Function unknown
<i>allD</i>	ureidoglycolate dehydrogenase	Energy production and conversion
<i>fdxA</i>	predicted acyl-CoA synthetase with NAD(P)-binding Rossmann-fold domain	Energy production and conversion
<i>folD</i>	bifunctional 5,10-methylene-tetrahydrofolate dehydrogenase and 5,10-methylene-tetrahydrofolate cyclohydrolase	Coenzyme transport and metabolism
<i>sfmA</i>	predicted fimbrial-like adhesin protein	Cell motility/Intracellular trafficking and secretion
<i>sfmC</i>	pilin chaperone, periplasmic	Cell motility/Intracellular trafficking and secretion
<i>emrE</i>	multidrug resistance protein	Inorganic ion transport and metabolism
<i>ybcK</i>	predicted recombinase	Replication, recombination and repair
<i>ybcL</i>	predicted kinase inhibitor	General function prediction only
<i>nmpC</i>	outer membrane porin protein	Function unknown
<i>ybcR</i>	hypothetical protein	Function unknown
<i>ybcS</i>	predicted lysozyme	General function prediction only
<i>ybcY</i>	predicted SAM-dependent methyltransferase	Secondary metabolites biosynthesis, transport and catabolism/General function prediction only
<i>ylcE</i>	hypothetical protein	Function unknown
<i>appY</i>	DNA-binding transcriptional activator	Transcription
<i>ompT</i>	outer membrane protease VII	Cell wall/membrane biogenesis
<i>entF</i>	enterobactin synthase multienzyme complex component, ATP-dependent	Secondary metabolites biosynthesis, transport and catabolism
<i>fepE</i>	regulator of length of O-antigen component of lipopolysaccharide chains	Cell wall/membrane biogenesis
<i>citC</i>	citrate:succinate antiporter	Inorganic ion transport and metabolism
<i>citA</i>	sensory histidine kinase in two-component regulatory system with citB	Signal transduction mechanisms
<i>ybeF</i>	predicted DNA-binding transcriptional regulator	Transcription
<i>lipB</i>	lipoyl-protein ligase	Coenzyme transport and metabolism
<i>ybfH</i>	hypothetical protein	Function unknown
<i>potE</i>	putrescine/proton symporter	Amino acid transport and metabolism
<i>speF</i>	ornithine decarboxylase isozyme, inducible	Amino acid transport and metabolism
<i>kdpE</i>	DNA-binding response regulator in two-component regulatory system with KdpD	Signal transduction mechanisms/Transcription
<i>rhcC</i>	rhcC element core protein RshC	Cell wall/membrane biogenesis
<i>ybfB</i>	predicted inner membrane protein	Function unknown
<i>ybfO</i>	conserved hypothetical protein, rhs-like	Cell wall/membrane biogenesis
<i>ybfC</i>	hypothetical protein	Function unknown
<i>ybfL</i>	putative receptor	Function unknown
<i>ybfD</i>	hypothetical protein	Lipid transport and metabolism
<i>yliD</i>	predicted peptide transporter subunit	Amino acid transport and metabolism/Inorganic ion transport and metabolism
<i>yltE</i>	conserved inner membrane protein	Signal transduction mechanisms
<i>ssuE</i>	NAD(P)H-dependent FMN reductase	General function prediction only
<i>ybcQ</i>	predicted fimbrial-like adhesin protein	Cell motility/Intracellular trafficking and secretion

<i>ycbR</i>	predicted periplasmic pilin chaperone	Cell motility/Intracellular trafficking and secretion
<i>cbpA</i>	curved DNA-binding protein, DnaJ homologue that functions as a co-chaperone of DnaK	Posttranslational modification, protein turnover, chaperones
<i>yccE</i>	hypothetical protein	Function unknown
<i>mcrA</i>	5-methylcytosine-specific restriction endonuclease B	Defense mechanisms
<i>ycgW</i>	hypothetical protein	Function unknown
<i>ycgX</i>	hypothetical protein	General function prediction only
<i>yciG</i>	hypothetical protein	General function prediction only
<i>trpA</i>	tryptophan synthase, alpha subunit	Amino acid transport and metabolism
<i>ompN</i>	outer membrane pore protein N, non-specific	Cell wall/membrane biogenesis
<i>ydbK</i>	fused predicted Fe-S subunit of pyruvate-flavodoxin oxidoreductase	Energy production and conversion
<i>paaY</i>	predicted hexapeptide repeat acetyltransferase	General function prediction only
<i>ydbA</i>	—	Function unknown
<i>yncG</i>	hypothetical protein	Posttranslational modification, protein turnover, chaperones
<i>yncH</i>	hypothetical protein	Function unknown
<i>rhsE</i>	rhsE element core protein RshE	Cell wall/membrane biogenesis
<i>ydcD</i>	hypothetical protein	Function unknown
<i>b1458</i>	hypothetical protein	Function unknown
<i>b1459</i>	hypothetical protein	Function unknown
<i>ydcC</i>	hypothetical protein	Function unknown
<i>narU</i>	nitrate/nitrite transporter	Inorganic ion transport and metabolism
<i>yddJ</i>	hypothetical protein	Function unknown
<i>yddK</i>	hypothetical protein	Function unknown
<i>b1472</i>	predicted lipoprotein	Cell wall/membrane biogenesis
<i>yddG</i>	predicted methyl viologen efflux pump	Carbohydrate transport and metabolism/General function prediction only/Amino acid transport and metabolism
<i>bdm</i>	biofilm-dependent modulation protein	Function unknown
<i>osmC</i>	osmotically inducible, stress-inducible membrane protein	Posttranslational modification, protein turnover, chaperones
<i>gadB</i>	glutamate decarboxylase B, PLP-dependent	Amino acid transport and metabolism
<i>pqqL</i>	predicted peptidase	General function prediction only
<i>ydeI</i>	hypothetical protein	Function unknown
<i>ydeJ</i>	hypothetical protein	General function prediction only
<i>nohA</i>	predicted packaging protein	Replication, recombination and repair
<i>ydfO</i>	hypothetical protein	Function unknown
<i>gnsB</i>	hypothetical protein	Function unknown
<i>ynfN</i>	hypothetical protein	Function unknown
<i>ydhY</i>	predicted 4Fe-4S ferridoxin-type protein	Energy production and conversion
<i>ydhZ</i>	hypothetical protein	Function unknown
<i>pykF</i>	pyruvate kinase I	Carbohydrate transport and metabolism
<i>ydfN</i>	predicted transporter	General function prediction only
<i>ydfO</i>	hypothetical protein	Function unknown
<i>cedA</i>	cell division modulator	Function unknown
<i>katE</i>	hydroperoxidase HPII(III)	Inorganic ion transport and metabolism
<i>yobD</i>	conserved inner membrane protein	Function unknown
<i>yebN</i>	conserved inner membrane protein	Function unknown
<i>yobF</i>	hypothetical protein	Function unknown
<i>yebO</i>	hypothetical protein	Function unknown
<i>ruvA</i>	component of RuvABC resolvosome, regulatory subunit	Replication, recombination and repair
<i>yebB</i>	hypothetical protein	Function unknown
<i>ruvC</i>	component of RuvABC resolvosome, endonuclease	Replication, recombination and repair
<i>torY</i>	TMAO reductase III (TorYZ), cytochrome c-type subunit	Energy production and conversion
<i>cutC</i>	copper homeostasis protein	Inorganic ion transport and metabolism
<i>yecR</i>	hypothetical protein	Function unknown
<i>fn</i>	cytoplasmic ferritin iron storage protein	Inorganic ion transport and metabolism
<i>yedL</i>	predicted acyltransferase	Transcription/General function prediction only
<i>b4495</i>	—	Function unknown
<i>yedM</i>	hypothetical protein	Function unknown
<i>b1936</i>	hypothetical protein	Function unknown
<i>fljE</i>	flagellar basal-body component	Cell motility/Intracellular trafficking and secretion
<i>yedR</i>	predicted inner membrane protein	Carbohydrate transport and metabolism/General function prediction only/Amino acid transport and metabolism
<i>yedS</i>	—	Function unknown
<i>amn</i>	AMP nucleosidase	Nucleotide transport and metabolism
<i>yeeN</i>	hypothetical protein	Function unknown
<i>yeeO</i>	predicted multidrug efflux system	Defense mechanisms
<i>trs_5_7</i>	IS5 transposase and trans-activator	Replication, recombination and repair
<i>wbbL</i>	putative lipopolysaccharide biosynthesis glycosyl transferase	Function unknown
<i>wbbK</i>	lipopolysaccharide biosynthesis protein	Cell wall/membrane biogenesis
<i>wbbJ</i>	predicted acyl transferase	General function prediction only
<i>wbbI</i>	hypothetical protein	Function unknown

Sup.Table 1/2



<i>wbbH</i>	O-antigen polymerase	Function unknown
<i>glf</i>	UDP-galactopyranose mutase, FAD/NAD(P)-binding	Cell wall/membrane biogenesis
<i>wza</i>	lipoprotein required for capsular polysaccharide translocation through the outer membrane	Cell wall/membrane biogenesis
<i>yegH</i>	fused predicted membrane proteins	Inorganic ion transport and metabolism/General function prediction only
<i>yegI</i>	hypothetical protein	General function prediction only
<i>yegJ</i>	hypothetical protein	Function unknown
<i>yehC</i>	predicted outer membrane protein	Cell motility/Intracellular trafficking and secretion
<i>yehD</i>	predicted fimbrial-like adhesin protein	Cell motility/Intracellular trafficking and secretion
<i>yehE</i>	hypothetical protein	Function unknown
<i>yehI</i>	hypothetical protein	Function unknown
<i>yehL</i>	predicted transporter subunit	General function prediction only
<i>yfaL</i>	adhesin	Cell wall/membrane biogenesis/Intracellular trafficking and secretion
<i>nrdA</i>	ribonucleoside diphosphate reductase 1, alpha subunit	Nucleotide transport and metabolism
<i>elaD</i>	hypothetical protein	Function unknown
<i>yfbK</i>	hypothetical protein	General function prediction only
<i>yfbL</i>	predicted peptidase	General function prediction only
<i>yfbM</i>	hypothetical protein	Function unknown
<i>b2339</i>	predicted fimbrial-like adhesin protein	Function unknown
<i>sixA</i>	phosphohistidine phosphatase	Signal transduction mechanisms
<i>fadL</i>	long-chain fatty acid outer membrane transporter	Lipid transport and metabolism
<i>b2345</i>	hypothetical protein	Function unknown
<i>vacJ</i>	predicted lipoprotein	Cell wall/membrane biogenesis
<i>yfdH</i>	bactoprenol glucosyl transferase	Cell wall/membrane biogenesis
<i>yfdI</i>	predicted inner membrane protein	Function unknown
<i>tfaS</i>	tail fiber assembly protein homolog from profage CSP-53	Function unknown
<i>yfdW</i>	putative enzyme	Function unknown
<i>yfdX</i>	hypothetical protein	Function unknown
<i>yfgF</i>	predicted inner membrane protein	Signal transduction mechanisms
<i>yfgG</i>	hypothetical protein	Function unknown
<i>yfgH</i>	predicted outer membrane lipoprotein	Function unknown
<i>yfiI</i>	hypothetical protein	Function unknown
<i>yfiJ</i>	hypothetical protein	Function unknown
<i>b2640</i>	hypothetical protein	Function unknown
<i>b2641</i>	hypothetical protein	Function unk33wn
<i>yfiW</i>	predicted inner membrane protein	Function unknown
<i>b2649</i>	hypothetical protein	Function unknown
<i>b2650</i>	hypothetical protein	Function unknown
<i>b2651</i>	hypothetical protein	Function unknown
<i>b2653</i>	hypothetical protein	Function unknown
<i>b2654</i>	hypothetical protein	Function unknown
<i>ygaR</i>	hypothetical protein	Carbohydrate transport and metabolism
<i>b2657</i>	putative enzyme	Function unknown
<i>b2658</i>	hypothetical protein	Function unknown
<i>b2659</i>	hypothetical protein	Function unknown
<i>stpA</i>	DNA binding protein, nucleoid-associated	General function prediction only
<i>b2670</i>	hypothetical protein	Function unknown
<i>ygcL</i>	hypothetical protein	Function unknown
<i>ygcB</i>	conserved hypothetical protein, member of DEAD box family	General function prediction only
<i>ygcE</i>	predicted DNA-binding transcriptional regulator	Transcription
<i>ycgF</i>	predicted FAD-binding phosphodiesterase	Signal transduction mechanisms
<i>ycgG</i>	conserved inner membrane protein	Signal transduction mechanisms
<i>fucA</i>	L-fucose-1-phosphate aldolase	Carbohydrate transport and metabolism
<i>fucP</i>	L-fucose transporter	Carbohydrate transport and metabolism
<i>yqeH</i>	conserved hypothetical protein with bipartite regulator domain	Transcription/Signal transduction mechanisms
<i>yqeI</i>	predicted transcriptional regulator	Coenzyme transport and metabolism/Transcription
<i>yqeJ</i>	hypothetical protein	Function unknown
<i>yqeK</i>	hypothetical protein	Function unknown
<i>yqeF</i>	predicted acyltransferase	Lipid transport and metabolism
<i>ygeG</i>	predicted transporter	Amino acid transport and metabolism
<i>ygeH</i>	predicted transcriptional regulator	General function prediction only/Transcription
<i>ygeI</i>	hypothetical protein	Function unknown
<i>b2854</i>	hypothetical protein	Function unknown
<i>ygeK</i>	predicted DNA-binding transcriptional regulator	Transcription/Signal transduction mechanisms
<i>b2856</i>	hypothetical protein	Function unknown
<i>b2857</i>	hypothetical protein	Function unknown
<i>b2858</i>	IS2 insertion element transposase InsAB'	Replication, recombination and repair
<i>b2859</i>	IS2 insertion element repressor InsA	Replication, recombination and repair

Sup.Table 1/3

<i>tktA</i>	transketolase 1, thiamin-binding	Carbohydrate transport and metabolism
<i>yghJ</i>	predicted inner membrane lipoprotein	Function unknown
<i>yghK</i>	glycolate transporter	Energy production and conversion
<i>yghS</i>	hypothetical protein with nucleoside triphosphate hydrolase domain	Nucleotide transport and metabolism
<i>yghT</i>	hypothetical protein with nucleoside triphosphate hydrolase domain	Nucleotide transport and metabolism
<i>pitB</i>	phosphate transporter	Inorganic ion transport and metabolism
<i>gss</i>	fused glutathionylspermidine amidase and glutathionylspermidine synthetase	Amino acid transport and metabolism
<i>ygiY</i>	sensory histidine kinase in two-component regulatory system with QseB	Signal transduction mechanisms
<i>ygiZ</i>	conserved inner membrane protein	Function unknown
<i>ndaB</i>	NADPH quinone reductase	General function prediction only
<i>yqiC</i>	hypothetical protein	Function unknown
<i>yqiL</i>	predicted fimbrial-like adhesin protein	Cell motility/Intracellular trafficking and secretion
<i>yhaH</i>	predicted inner membrane protein	Function unknown
<i>yhaI</i>	predicted inner membrane protein	Function unknown
<i>tdcB</i>	catabolic threonine dehydratase, PLP-dependent	Amino acid transport and metabolism
<i>tdcA</i>	DNA-binding transcriptional activator	Transcription
<i>tdcR</i>	DNA-binding transcriptional activator	Function unknown
<i>yhaB</i>	hypothetical protein	Function unknown
<i>yhaC</i>	hypothetical protein	Signal transduction mechanisms
<i>garK</i>	glycerate kinase I	Carbohydrate transport and metabolism
<i>garP</i>	predicted (D)-galactarate transporter	Carbohydrate transport and metabolism/General function prediction only/Amino acid transport and metabolism/Inorganic ion transport and metabolism
<i>garD</i>	(D)-galactarate dehydrogenase	Carbohydrate transport and metabolism
<i>agaY</i>	tagatose-6-phosphate ketose/aldose isomerase	Carbohydrate transport and metabolism
<i>agaB</i>	tagatose 6-phosphate aldolase 1, kbaY subunit	Carbohydrate transport and metabolism
<i>agal</i>	galactosamine-6-phosphate isomerase	Carbohydrate transport and metabolism
<i>yraH</i>	predicted fimbrial-like adhesin protein	Cell motility/Intracellular trafficking and secretion
<i>gltD</i>	glutamate synthase, 4Fe-4S protein, small subunit	Amino acid transport and metabolism/General function prediction only
<i>gltF</i>	periplasmic protein	Function unknown
<i>yhcA</i>	predicted periplasmic chaperone protein	Cell motility/Intracellular trafficking and secretion
<i>nanR</i>	DNA-binding transcriptional dual regulator	Transcription
<i>ducD</i>	predicted transporter	Energy production and conversion
<i>envR</i>	DNA-binding transcriptional regulator	Transcription
<i>acrE</i>	cytoplasmic membrane lipoprotein	Cell wall/membrane biogenesis
<i>yhdV</i>	predicted outer membrane protein	Function unknown
<i>yhdW</i>	predicted amino-acid transporter subunit	Amino acid transport and metabolism/Signal transduction mechanisms
<i>gspA</i>	general secretory pathway component, cryptic	Cell wall/membrane biogenesis
<i>gspC</i>	general secretory pathway component, cryptic	Intracellular trafficking and secretion
<i>chiA</i>	periplasmic endochitinase	General function prediction only
<i>tufA</i>	protein chain elongation factor EF-Tu	Translation
<i>cysG</i>	fused siroheme synthase 1,3-dimethyluroporphyriongen III dehydrogenase/siroheme ferredoxinase and uroporphyrinogen methyltransferase	Coenzyme transport and metabolism
<i>yhfL</i>	conserved secreted peptide	Function unknown
<i>yhfM</i>	predicted fructoselysine transporter	Amino acid transport and metabolism
<i>yhhY</i>	predicted acetyltransferase	Transcription/General function prediction only
<i>yhhZ</i>	hypothetical protein	Function unknown
<i>yrhA</i>	hypothetical protein	Function unknown
<i>insA_6</i>	IS1 repressor protein InsA	Replication, recombination and repair
<i>insB_6</i>	IS1 transposase InsAB'	Replication, recombination and repair
<i>yrhB</i>	hypothetical protein	Function unknown
<i>rhsB</i>	rhsB element core protein RshB	Cell wall/membrane biogenesis
<i>yhhH</i>	hypothetical protein	Function unknown
<i>yhhI</i>	predicted transposase	Replication, recombination and repair
<i>yhiJ</i>	hypothetical protein	Function unknown
<i>yhiK</i>	hypothetical protein	Function unknown
<i>yhiL</i>	hypothetical protein	Function unknown
<i>yhiM</i>	conserved inner membrane protein	Function unknown
<i>arsC</i>	arsenate reductase	Inorganic ion transport and metabolism
<i>yhiS</i>	hypothetical protein	Function unknown
<i>trs5_11</i>	IS5 transposase and trans-activator	Replication, recombination and repair
<i>slp</i>	outer membrane lipoprotein	Cell wall/membrane biogenesis
<i>gadA</i>	glutamate decarboxylase A, PLP-dependent	Amino acid transport and metabolism
<i>yhjA</i>	predicted cytochrome C peroxidase	Inorganic ion transport and metabolism
<i>tl50</i>	IS150 conserved protein InsB	Replication, recombination and repair
<i>glyS</i>	glycine tRNA synthetase, beta subunit	Translation
<i>yiaT</i>	hypothetical protein	Cell wall/membrane biogenesis
<i>yiaU</i>	predicted DNA-binding transcriptional regulator	Transcription
<i>yiaW</i>	conserved inner membrane protein	Function unknown
<i>aldB</i>	aldehyde dehydrogenase B	Energy production and conversion

Sup.Table 1/4

<i>yaiY</i>	predicted Fe-containing alcohol dehydrogenase	Energy production and conversion
<i>selB</i>	selenocysteinyl-tRNA-specific translation factor	Translation
<i>yibA</i>	lyase containing HEAT-repeat	Energy production and conversion
<i>yibJ</i>	predicted Rhs-family protein	Cell wall/membrane biogenesis
<i>yibG</i>	hypothetical protein	General function prediction only
<i>yibH</i>	hypothetical protein	Defense mechanisms
<i>htrI</i>	hypothetical protein	Function unknown
<i>rfaD</i>	ADP-L-glycero-D-mannoheptose-6-epimerase, NAD(P)-binding	Cell wall/membrane biogenesis/Carbohydrate transport and metabolism
<i>rfaC</i>	ADP-heptose:LPS heptosyl transferase I	Cell wall/membrane biogenesis
<i>rfaL</i>	O-antigen ligase	Cell wall/membrane biogenesis
<i>rfaK</i>	lipopolysaccharide core biosynthesis	Cell wall/membrane biogenesis
<i>rfaZ</i>	lipopolysaccharide core biosynthesis protein	Function unknown
<i>rfaY</i>	lipopolysaccharide core biosynthesis protein	General function prediction only/Signal transduction mechanisms
<i>rfaJ</i>	UDP-D-glucose:(galactosyl)lipopolysaccharide glucosyltransferase	Cell wall/membrane biogenesis
<i>rfaI</i>	UDP-D-galactose:(glucosyl)lipopolysaccharide- $\alpha$ -1,3-D-galactosyltransferase	Cell wall/membrane biogenesis
<i>rfaB</i>	UDP-D-galactose:(glucosyl)lipopolysaccharide-1, 6-D-galactosyltransferase	Cell wall/membrane biogenesis
<i>rfaS</i>	lipopolysaccharide core biosynthesis protein	Function unknown
<i>rfaP</i>	kinase that phosphorylates core heptose of lipopolysaccharide	General function prediction only/Signal transduction mechanisms/Transcription/Replication, recombination and repair
<i>yicJ</i>	putative permease	Function unknown
<i>yicK</i>	predicted sugar efflux system	Carbohydrate transport and metabolism/General function prediction only/Amino acid transport and metabolism/Inorganic ion transport and metabolism
<i>aslA</i>	acrylsulfatase-like enzyme	Inorganic ion transport and metabolism
<i>hemY</i>	predicted protoheme IX synthesis protein	Coenzyme transport and metabolism
<i>yigG</i>	predicted inner membrane protein	Function unknown
<i>rarD</i>	predicted chloramphenicol resistance permease	General function prediction only
<i>dsbA</i>	periplasmic protein disulfide isomerase I	Posttranslational modification, protein turnover, chaperones/Energy production and conversion
<i>yihF</i>	hypothetical protein	Function unknown
<i>yiiD</i>	predicted acetyltransferase	Transcription/General function prediction only
<i>yiiE</i>	predicted transcriptional regulator	Transcription
<i>yiiF</i>	hypothetical protein	Function unknown
<i>fdhD</i>	formate dehydrogenase formation protein	Energy production and conversion
<i>yiiG</i>	hypothetical protein	Function unknown
<i>arpA</i>	regulator of acetyl CoA synthetase	General function prediction only
<i>iclR</i>	DNA-binding transcriptional repressor	Transcription
<i>pgi</i>	glucosephosphate isomerase	Carbohydrate transport and metabolism
<i>yjbE</i>	hypothetical protein	Function unknown
<i>yjbF</i>	predicted lipoprotein	Function unknown
<i>malM</i>	maltose regulon periplasmic protein	Function unknown
<i>yjbI</i>	hypothetical protein	Function unknown
<i>ubiC</i>	chorismate pyruvate lyase	Coenzyme transport and metabolism
<i>zur</i>	DNA-binding transcriptional activator, Zn(II)-binding	Inorganic ion transport and metabolism
<i>yjbL</i>	hypothetical protein	Function unknown
<i>yjbM</i>	hypothetical protein	Function unknown
<i>yjbN</i>	tRNA-dihydrouridine synthase A	Translation
<i>tyrB</i>	tyrosine aminotransferase, tyrosine-repressible, PLP-dependent	Amino acid transport and metabolism
<i>aphA</i>	acid phosphatase/phosphotransferase, class B, non-specific	General function prediction only
<i>yjcE</i>	predicted cation/proton antiporter	Inorganic ion transport and metabolism
<i>yjcF</i>	hypothetical protein	Function unknown
<i>actP</i>	acetate transporter	General function prediction only
<i>yjcR</i>	predicted membrane fusion protein of efflux pump	Defense mechanisms
<i>yjcS</i>	predicted alkyl sulfatase	Secondary metabolites biosynthesis, transport and catabolism
<i>phnA</i>	predicted phosphonate metabolizing protein	Inorganic ion transport and metabolism
<i>yjdA</i>	conserved hypothetical protein with nucleoside triphosphate hydrolase domain	General function prediction only
<i>yjfZ</i>	hypothetical protein	Function unknown
<i>yjfA</i>	predicted transcriptional regulator	Transcription
<i>yjfB</i>	predicted cell envelope opacity-associated protein	Cell wall/membrane biogenesis
<i>cysQ</i>	PAPS (adenosine 3'-phosphate 5'-phosphosulfate) 3'(2'),5'-bisphosphate nucleotidase	Inorganic ion transport and metabolism
<i>yjfI</i>	hypothetical protein	Function unknown
<i>yjfJ</i>	predicted transcriptional regulator	General function prediction only
<i>yjgK</i>	hypothetical protein	Carbohydrate transport and metabolism
<i>yjgL</i>	hypothetical protein	Function unknown
<i>argI</i>	ornithine carbamoyltransferase 1	Amino acid transport and metabolism
<i>yjgM</i>	predicted acetyltransferase	Transcription/General function prediction only
<i>yjgN</i>	conserved inner membrane protein	Function unknown
<i>yjhB</i>	predicted transporter	Carbohydrate transport and metabolism/General function prediction only/Amino acid transport and metabolism/Inorganic ion transport and metabolism
<i>yjhC</i>	predicted oxidoreductase	General function prediction only
<i>yjHA</i>	N-acetylnuraminic acid outer membrane channel protein	Function unknown
<i>fimB</i>	tyrosine recombinase/inversion of on/off regulator of fimA	Replication, recombination and repair

*fimE* tyrosine recombinase/inversion of on/off regulator of fimA  
*uxuR* DNA-binding transcriptional repressor  
*yjiC* hypothetical protein  
*yjiD* DNA replication/recombination/repair protein  
*yjiP* predicted inner membrane protein  
*yjiQ* predicted DNA-binding transcriptional regulator

Replication, recombination and repair  
Transcription  
Function unknown  
Function unknown  
Function unknown  
Signal transduction mechanisms/Transcription

Functional classification of the genes was performed using the NCBI COGs ( Clusters of Orthologous Groups of proteins) database  
( <http://www.ncbi.nlm.nih.gov/sites/entrez?Db=genome&Cmd=ShowDetailView&TermToSearch=19221>)